Large-Scale Demand Management in Smart Grid

by

Fadi Elghitani

A thesis
presented to the University of Waterloo
in fulfillment of the
thesis requirement for the degree of
Doctor of Philosophy
in
Electrical and Computer Engineering

Waterloo, Ontario, Canada, 2018

Examining Committee Membership

The following served on the Examining Committee for this thesis. The decision of the Examining Committee is by majority vote.

External Examiner:	Amr Youssef
	Professor, Concordia Institute for Information Systems Engineering,
	Concordia University, Montreal, Canada

Supervisor:	Ehab El-Saadany
	Professor, Dept. of Electrical and Computer Engineering,
	University of Waterloo

Internal Member:	Kankar Bhattacharya
	Professor, Dept. of Electrical and Computer Engineering,
	University of Waterloo

Internal Member:	Liang-Liang Xie
	Professor, Dept. of Electrical and Computer Engineering,
	University of Waterloo

Internal-External Member:	Xianguo Li
	Professor, Dept. of Mechanical and Mechatronics Engineering,
	University of Waterloo

I hereby declare that I am the sole author of this thesis. This is a true copy of the thesis, including any required final revisions, as accepted by my examiners.

I understand that my thesis may be made electronically available to the public.

Abstract

Future energy grids are expected to rely extensively on controlling consumers' demands to achieve an efficient system operation. The demand-side of the power network is usually constituted of a large number of low power loads, unlike energy production which is concentrated in a few numbers of high power generators. This research is concerned with supporting the management of numerous loads, which can be challenging from a computational point-of-view. A common approach to facilitate the management of a large number of resources is through resource aggregation (clustering). Therefore, the main objective of our research is to develop efficient load aggregation methodologies for two categories of demands: residential appliances and electric vehicles. The proposed methodologies are based on queueing theory, where each queue represents a certain category (class) of demand.

Residential appliances are considered in the context of two demand management problems, where the first aims to minimize the energy consumption cost, while the second aims to reduce the magnitude of fluctuations in net demand, as a result of a large-scale integration of renewable energy sources (RESs). Existing models for residential demand aggregation suffer from two limitations:first, demand models ignore the inter-temporal demand dependence that is induced by scheduling deferrable appliances; Second, aggregated demand models for thermostatically-controlled loads are computationally inefficient to be used in DR problems that require optimization over multiple time intervals. Although the same aggregation methodology is applied to both problems, each one of them requires a different demand scheduling algorithm, due to the stochastic nature of RESs which is introduced in the second problem.

The second part of our research focuses on minimizing the expected system time needed for charging electric vehicles (EVs). This target can be achieved by two types of decisions, the assignment of EVs to charging stations and the charging of EVs' batteries. While there exist aggregation models for batteries' charging, aggregation models for EVs' assignment are almost non-existent. In addition, aggregation models for batteries' charging assume that information about EVs' arrival times, departure times and their required charging energies are given in advance. Such assumption is non-realistic for a charging station, where vehicles arrive randomly. Hence, the third problem is concerned with developing an aggregation model for EVs' assignment and charging, while considering the stochastic nature of EVs' arrivals.

Realistic models for residential demands and RES powers were used to develop the corresponding numerical results. The proposed scheduling algorithms do not require highly restrictive assumptions. The results proved that effectiveness of the proposed methodology

and algorithms in achieving a significant improvement in the problems' objectives. On the other hand, the algorithm used in EV assignment requires restrictive Markovian assumptions. Hence, we needed to verify our proposed analytical model with a more realistic simulation model. The results showed a good compliance between both models. Our proposed methodology helped in improving the average system time significantly, compared to that of a near-station-assignment policy.

This study is expected to have an important contribution from both research and application perspectives. From the research side, it will provide a tool for managing a large, diverse number of electric appliances by classifying them according to how much they can benefit the utility. From the application side, our work will help to include residential consumers in demand response (while current DR programs focus on the industrial sector only). It will also facilitate RESs and EVs on a large scale to help address environmental concerns.

Acknowledgements

This PhD thesis is dedicated to my parents, Jehan and Hassan Elghitani, to my sisters, Nehal and Lubna, and to my brother, Baraa.

Table of Contents

List of Tables

List of Figures

List of Symbols

A_j Area of region L_j.

$C(s,a)$ Single step incurred cost if the system is in state s and action a is selected.

C_{th} Thermal capacitance.

D_i Deadline for scheduling a demand block of type i.

$EI(x)$ Expected improvement function.

H_i Total number of EVs (served or queued) in station i.

K_i Duration of a demand block of class i.

L The location (region) from which a charging request is originated.

L^{rating} The power rating of the distribution transformer.

L_t Total energy consumption of residential consumers in time slot t.

L_t^c Controllable power consumption at time slot t.

L_t^{uc} Non-controllable power consumption at time slot t.

M_i Total number of ongoing EVs to station i.

N_c Number of charging stations.

N_g Number of non-renewable distributed generators.

N_q Number of demand block classes (queues).

N_r Number of residential consumers.

P^r Power consumed by the TCL appliance when it is turned on.

P_i^u Uncorrelated RES power for consumer i.

P_0 Correlated RES power.

P_i Power level of a demand block of class i.

$Q_i(t)$ Queued energy in queue i at time slot t.

R_i Number of chargers in charging station i.

R_{th}	Thermal resistance.
T	Number of time slots of the scheduling horizon.
$U(.)$	Unit step function.
V	Trade-off parameter between general delay and smoothing performances.
W_i	Waiting time of a demand block of type i.
$Z_i(t)$	Virtual queued energy in virtual queue i at time slot t.
Γ	Rejection penalty set.
Λ	Average arrival rate of charging requests per square meter.
$\boldsymbol{\pi}$	An MDP policy which maps the state space into the action space.
ψ	Steady-state probability distribution for system states.
δ	Minimum required quality of service level.
ϵ_i	Virtual arrived energy to virtual queue i.
$\epsilon_{th}(t)$	Random temperature deviation of a TCL appliance due to different sources of disturbance.
$\gamma(s)$	Electricity price at time slot s.
γ_i	Virtual incurred penalty if station i rejects a charging request.
λ_j	Average charging request arrival rate within region L_j.
$\mathbf{G}^{\boldsymbol{\pi}}$	Transition probability matrix if policy $\boldsymbol{\pi}$ was selected.
$\mathbf{q}_i(\mathbf{x})$	The gradient of QoS function at point $\mathbf{x}$.
$\mathcal{A}_s$	Set of all possible actions for state s (Action space).
$\mathcal{B}$	Set of all possible locations representing the geographical service area of the microgrid/ charging stations.
$\mathcal{GP}$	Multinomial Gaussian distribution.
$\mathcal{H}_k$	Sampling history at the k-th iteration.
$\mathcal{I}_i$	Set of interruptible deferrable appliances of consumer i.
$\mathcal{L}$	Set of regions which constitutes the service area.
$\mathcal{N}_i$	Set of non-interruptible deferrable appliances of consumer i.
$\mathcal{Q}$	Set of queues.

$\mathcal{S}$	Set of all possible system states (state space).
$\mathcal{T}_i$	Set of TCL appliances of consumer i.
$\mathcal{U}_i$	Set of non-controllable appliances of consumer i.
$\mathcal{Y}$	Set of tasks required to be scheduled.
μ	The reciprocal of the average charging time duration.
ν	The reciprocal of the average travel time duration.
ρ	Ramping rate of a distributed generator.
θ	Temperature controlled by a TCL appliance.
θ_e	Ambient (external) temperature.
θ_s	Temperature threshold for the TCL to send a demand request.
θ_{max}	Maximum required temperature level of a TCL appliance.
θ_{min}	Minimum required temperature level of a TCL appliance.
$a_i(t)$	Arrived energy to queue i at time slot t.
c_{it}	Cost incurred due to scheduling a demand block of class i at time slot t.
d_{ij}	Deadline for task scheduling for appliance j of consumer i.
$g_{ij}(t)$	Task pattern (power consumption profile) of appliance j of consumer i.
$h_i(\mathbf{x})$	Delay quality of service as a function of the capacity allocation vector $\mathbf{x}$.
$p_{ij}(t)$	Probability that appliance j of consumer i is turned on at time slot t.
$r(t)$	Aggregated net non-controllable demand at time slot t.
s	The state of the system.
$s(t)$	TCL binary switching function.
w_i	Weighting parameter to prioritize queue i.
$x_i(t)$	Scheduled (satisfied) energy from queue i at time slot t.
x_{it}	Allocated capacity for demand blocks of class i at time slot t.

List of Abbreviations

AS   Ancillary Services.

CPM   Cutting Plane Method.
CT-MDP   Continuous time Markov Decision Process.

DAP   Day-Ahead Pricing.
DG   Distributed Generator.
DR   Demand Response.
DRM   Demand Response Management.
DSM   Demand-Side Management.

EMC   Energy Management Controller.
ETP   Equivalent Thermal Parameter.
EV   Electric Vehicle.

HEM   Home Energy Management.

i.i.d.   Independent and Identically Distributed.
ICE   Internal Combustion Engine.
IP   Integer Programming.

MCS   Monte-Carlo Simulation.
MDP   Markov Decision Process.
MG   Microgrid.
MGCC   Microgrid Central Controller.
MILP   Mixed Integer-Linear Programming.

NERC   North American Electric Reliability Corporation.

ODE   Ordinary Differential Equation.

PMF   Probability Mass Function.
PPP   Poisson Point Process.
PSO   Particle Swarm Optimization.
PV   Photovoltaic.

QoS   Quality of Service.

r.v.   Random variable.
RA   Charging request arrival.
RES   Renewable Energy Source.

SAA   Sample Average Approximation.
SoC   Battery State of Charge.

TCL   Thermostatically-Controlled Load.
TNE   Transmission Network Expansion.

VA   Electric vehicle arrival.
VD   Electric vehicle departure.
VRP   Vehicle Routing Problem.

Chapter 1

Introduction

Smart Grid is a relatively new research area which aims to revolutionize existing power networks by embracing various new technologies and concepts. A smart grid is expected to be better than traditional electricity grids in terms of the efficiency of energy delivery, the utilization of environment-friendly energy sources, monitoring and recovery of power networks, and many other advantages. In this research, we focus on one important concept that a smart grid will be built on, which is demand response (DR). DR is the concept of achieving supply-demand matching by convincing energy consumers to modify their demands. DR can provide many benefits to electricity grids, especially when modifying the electricity supply is difficult or expensive. In this chapter, we first aim to provide the basics for understanding DR. After that, we discuss the objectives and motivations of this research. Finally, we present the outline of the thesis at the end of this chapter.

1.1   Demand-Side Management

The operation of electric power systems is traditionally based on demand following. The role of supply-demand matching of the electric energy is assigned to the generation-side of a power network, while the demand-side is assumed to be non-controllable and has to be satisfied regardless of its cost.

Demand following can be very expensive, especially during periods of peak demand. For example, generation units are usually committed in an ascending order according to their full load average cost [1]. During periods of peak demand, generation units of the highest cost are needed to be turned-on, as the low cost units are unable to cover all the required

demands. Therefore, utility companies began to realize the potential benefits of controlling consumers' demands, which is referred to as demand-side management (DSM) to contrast traditional generation-side decisions. DSM is defined by North American Electric Reliability Corporation (NERC) as "all activities or programs undertaken by any applicable entity to achieve a reduction in demand" [2]. Another term related to DSM is demand response (DR), which is defined according to US Department of Energy as "Changes in electric usage by end-use customers from their normal consumption patterns in response to changes in the price of electricity over time, or to incentive payments designed to induce lower electricity use at times of high wholesale market prices or when system reliability is jeopardized" [3]. Thus, DR is considered as a specific type of DSM that seeks demand modification via financial incentives.

Smart Appliances

Regardless of how a DR program is implemented, it will end up by modifying the normal power consumption of some electric appliances. The capability of modifying the power consumption (DR capability) varies from one appliance to another. The modification can be a reduction of the appliance's total energy consumption or completely turning it off. Other appliances have the ability to change their starting time without any reduction of the total energy consumed. Some appliances do not have any DR capability at all, e.g., television. A list of DR capabilities is provided in Table 1.1. Some appliances can have more than one DR capability. For example, a dish washer can have a load curtailment capability by reducing the heat energy required for drying the dishes, in addition to its original load-deference capability. We refer to an appliance as a "smart appliance" if it has 1) a DR capability, and 2) a control system that responds to a demand modification request (a DR signal).

1.2   Research Motivations

For a DR program to provide effective benefits to power networks, it should have a size comparable to the size of the power generated and transmitted. For example, we cannot expect that a congestion on a transmission line to be relieved by 1 kW demand reduction or that the electricity's wholesale price would be changed by a 10 kW DR offer. Thus, the large size of power networks forces DR programs to have comparable large sizes, i.e. in the order of MWs. Similar to power networks, environmental goals need a large-scale contribution of green energy sources. For example, decarbonizing the transport section

Table 1.1: DR capability classification

DR capability	Description	Example
Load curtailment	Appliance reduces its power consumption without requiring additional energy in the future	Light dimming
Non-interruptible load deference	When the appliance is turned on by its user, it does not work immediately, but rather waits for a DR signal to determine when it should start. However, once it starts, it cannot be interrupted until completion	Washing machine, dish washer
Interruptible load deference	Appliance can be interrupted as much as desired, as long as it is served with a predetermined energy within a certain time limit	Charging an electric vehicle
Thermostatically controlled loads (TCLs)	They are appliances related to temperature control. A TCL can contribute to DR by 1) changing its ON/OFF control signal without changing the temperature setting point, or 2) changing the temperature setting point itself	Air conditioning, electric water heater, refrigerator

will happen when thousands of vehicles run on the electric energy. Also, the integration of renewable energy source (RES) units should be in the level of several MWs in order to avoid the construction of new generators running on fossil fuel.

The operations of a power system should utilize power network's resources efficiently such that a matching between the supply and the demand is achieved. Resource management in many fields, such as economics, telecommunications, and power networks, usually involves different types of optimization, which depend on the model of resources, the model of system, and the optimization objective(s). In most cases, optimization algorithms work efficiently when there are a few numbers of resources to be managed. When the number of resources increases beyond a certain limit, optimization algorithms cannot work practically due to an increase of computational complexity. To deal with this problem, resources are classified into different groups, and each group is represented by a proper aggregation model. Thus, the large number of resources is replaced by a few numbers of new types of resources such that an optimization algorithm becomes solvable. In DR problems, the consumer demands are the resources to be optimized. We can conclude that the key to manage large-scale DR problems is to develop suitable models for demand aggregation. In this research, we plan to develop aggregated demand models for three different DR

applications, as described in the following subsections.

1.2.1 Reducing the cost of energy consumption

Efficient pricing schemes require the electricity price to be time-varying in order to reflect the dynamics of the electricity market. Given this condition, it can be useful for residential consumers to shift their demands from time periods of high electricity prices to time periods of low electricity prices. However, the capacity of the distribution transformers (and accordingly the capacity of the transmission network) is determined based on some level of diversity associated with the demand of consumers. The diversity means that the peak demands for different consumers normally do not coincide at some time intervals. If each consumer attempts to minimize the cost of his energy consumption independent of other consumers, this diversity will disappear, since most consumers will have a peak energy consumption at the periods of low electricity prices. With the time coincidence of peak energy demands of different consumers, their instantaneous aggregated power consumption can be larger than the capacity of the distribution transformer. Such event is undesired and hence the DR should be coordinated among residential consumers to prevent its occurrence. This coordination can be done by assigning the responsibility of controlling the appliances of all consumers to one external controller. As this controller will have to manage a large number of appliances, aggregated demand models for residential appliances are required.

In existing studies, deferrable loads are aggregated by assuming that each appliance is represented by a specific energy requirement and hence, the aggregated demand is represented by the sum of total energy required by all appliances. This assumption ignores the inter-temporal demand dependence associated with non-interruptible appliances. Under this assumption, the DR controller has no information about the duration of the energy consumption required by an appliance and, therefore, would schedule the appliance in the time slot of lowest price. This decision is not optimal if the duration of the energy consumption extends to multiple time slots, as the cost of the energy consumption is not determined only by the first time slot, but also by the next time slots. On the other hand, existing aggregation models for thermostatically-controlled loads (TCLs) are simply a reduced-order population model that is suitable for myopic control or performance evaluation. The model is too complex for multi-period optimization problems. Given the limitations of existing aggregation models for both deferrable and TCL appliances, our first research objective is to develop a framework for minimizing the cost of residential energy consumption, which includes both aforementioned types of appliances while considering the inter-temporal demand dependence.

1.2.2 Integration of Renewable Energy Sources

The second part of our research is concerned with the large-scale integration of RESs. Similar to non-renewable energy generators, the integration of RESs can be centralized or distributed. The centralized approach has the advantage of optimal site selection, i.e., selecting locations where the renewable energy is abundant. The disadvantage is that it will require a transmission network expansion (TNE) to carry the energy generation from the new site. An alternative way is to use the distributed integration, in which RESs are locally integrated into consumers' premises, and thus the TNE can be avoided. However, a consumer's location may not be optimal for RES production and, in addition, the consumer-level demand can have a behavior opposite to the power produced from the RES units. For example, the high production of a photovoltaic (PV) cell is usually around the noon time, when many consumers are away at work and hence their energy demand is low. Thus, efficient utilization of an RES unit is a major concern when it is integrated locally. One approach for utilization improvement is to use the DR in order to shift consumers' demand to periods of high RES energy production.

The intermittency of RESs is not an issue when the level of RES integration is low. However, at high scale integration, RESs will introduce large uncontrollable supply fluctuations, and supply-demand matching becomes more difficult. It is always desired to reduce the magnitude of supply-demand mismatch to avoid excessive use of ancillary services. One approach for minimizing the mismatch is to utilize DR such that demand is increased when there is a surplus of supplied energy and reduced when there is a deficiency in supplied energy. Unlike the first research problem which considers only the randomness in the demand arrivals, in our second research problem, the randomness of the RES needs to be addressed as well.

1.2.3 Assignment of Electric Vehicles to Charging Stations

The last part of our research is concerned with a large-scale penetration of electric vehicles to the transport sector. Electric vehicle (EV) users have different concerns from those of residential consumers, mainly related to the short travel range per battery charging and long charging duration of an EV. Due to the limited range, EVs will require to be charged at a higher rate than that of gasoline vehicles. With a high arrival rate, not every vehicle is guaranteed to be served immediately at a charging station due to limited battery stock in each station. If there is no available fully-charged battery, a newly arrived EV has to wait (queued) until one charger becomes available. From simple queueing principles, for a queue to become stable (i.e. not to grow indefinitely), the mean service rate should be

greater than the mean arrival rate. Due to the long charging time, the service rate (the rate at which an EV completes charging) is much lower than the service rate of a gasoline station. With a large penetration of EVs to the transport sector, the mean service rate for some station can possibly be less than the mean arrival rate and hence, the expected EV waiting time will become infinite. The service rate can be improved by utilizing high power chargers or equivalently deploying a larger number of low power chargers in each station. However, due to distribution network constraints, each station has a maximum power limit or equivalently a maximum number of chargers. One approach for achieving queue stability is to control the arrival rate by a proper assignment of EVs to charging stations, whenever an EV requires to be recharged.

There exist some studies related to the assignment of a small number of EVs, whereas most existing studies related to managing a large number of EVs are concerned only with EV charging. Our third research objective is to study the assignment of a large number of EVs in order to minimize the expected "time of service" of EV users. In existing studies, it is usually assumed that the arrival and departure of each EV is known in advance. The assumption is backed by the fact that many EV owners usually charge their EVs at time periods when they do not need their vehicles for long times, such as when the owner is at work or at home in the evening. This assumption is not suitable for charging stations, which are expected to serve consumers at any time. Thus, different from the existing studies, our study will take into consideration the random arrivals of EVs.

1.3   Research objectives

A flowchart for the main tasks of this thesis is given in Figure 1.1. The aforementioned shortcomings in the existing studies motivate us to set the following objectives for our thesis:

1) Developing a modelling methodology for managing a large number of residential appliances.

   - It has to be suitable for both deferrable and TCL appliances.
   - The inter-temporal demand dependence needs to be considered.

   The methodology will be used in two DR applications:

   - Minimizing the cost of residential energy consumption.

6

- Minimizing the fluctuations resulting from a large-scale integration of RESs.

2) Developing a modelling methodology for optimal assignment of EVs to different charging stations, which achieves the best possible EV user experience given a charging infrastructure.

- Factors needed to be considered include the time needed for the EV to reach the assigned charging station and its waiting time in that charging station.
- The methodology should be suitable for managing a large number of EVs.
- No prior knowledge for a charging request time or location.

1.4   Outline of the Thesis

This thesis is organized as follows. In Chapter 2, we present a brief literature survey on different demand response problems. The system model under consideration is given in Chapter 3. Chapters 4, 5, and 6 are concerned with the aforementioned three research problems. Finally, some conclusions on this PhD research thesis are given in Chapter 7.
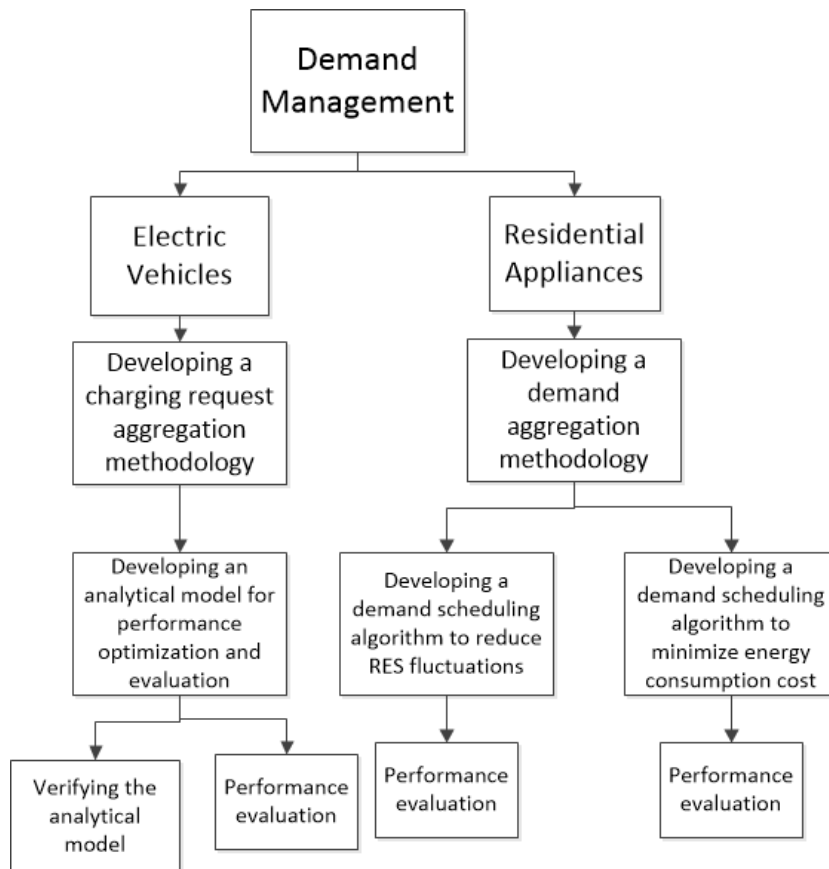
Figure 1.1: A flowchart for the main tasks in the Ph.D. thesis.

Chapter 2

Literature Survey

We define the standard DR problem as the opposite of classical generation dispatch problem: dispatch problems consist of multiple controllable generators serving a non-controllable aggregated load, while the standard DR problem consists of multiple controllable loads served by a one common source (supplier). Although there exist problems associated with multiple controllable sources and multiple controllable loads, we define the standard DR problem this way to distinguish pure generation dispatch and pure demand response, as shown in Figure 2.1. From the structure of DR problems, it is clear that two models needed to be defined, which are the supply model and controllable demand model. Supply models are widely studied in dispatch problems, and most research work done in demand response focus mainly on demand modeling. Hence, the goal of this chapter is to review different demand modeling approaches in existing studies.

(a)   (b)
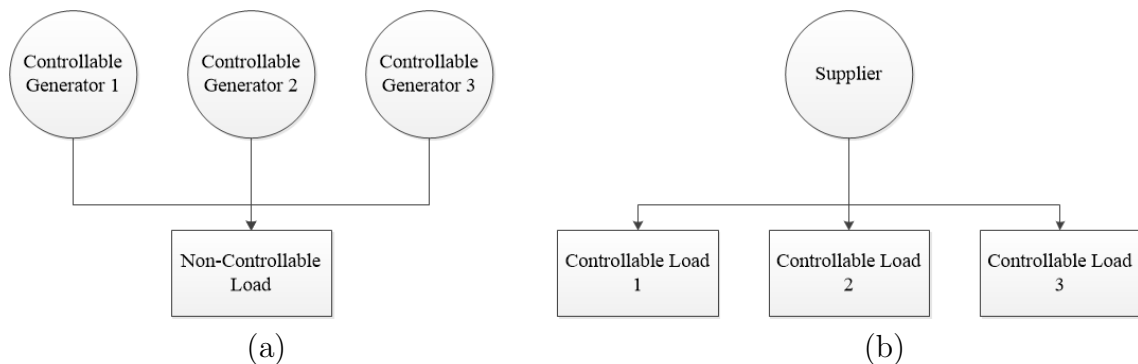
Figure 2.1: Comparison between (a) classical generation dispatch problem and (b) standard DR problem

Since electric appliances are the basic source of energy demands, it is natural to start with developing their individual demand models and scheduling algorithms to achieve different DR objectives. When the number of appliances becomes large, the computational complexity of scheduling algorithms increases. In order to avoid a prohibitive computational complexity, aggregation models for groups of appliances are developed so that scheduling algorithms deal with a reduced number of components. In turn, each demand aggregator will be responsible to schedule its corresponding appliances based on the control signal received from the DR controller. In the following, we discuss various existing individual and aggregated demand models.

2.1 Individual demand models

Deferrable Appliances

Different residential appliances can be modeled according to the state diagrams shown in Figure 2.2. Appliances that do not contribute in DR (inelastic demand) can be modeled by two states: off and on (active). When an appliance is in the active state it consumes electric energy at constant or time-varying power. The time duration that the appliance remains in the active state is usually not fixed, e.g. watching a TV or cooking on an electric oven. When the appliance is in the off state, it either consumes no energy or a small amount of energy representing stand-by power.

In the case of deferrable appliances, a third state is introduced which is the "inactive" state. When the appliance is in this state, it means that there is an energy demand that needs to be satisfied, but it is decided to be deferred. Thus, an appliance in the inactive state does not consume energy, similar to the off state. However, an appliance in the off state does not have any deferred energy demand. Different from an inelastic demand, the appliance energy demand profile is known in advance to the appliance controller, e.g. when turning-on a washing machine. This energy demand profile is usually referred to as a "task". Thus it is the controller's job to fulfill this task before the user-specified deadline. In the case of non-interruptible appliances, the controller has to decide if the task is to be scheduled at the current time slot or not. In the case of interruptible appliances, a task can be rescheduled and interrupted as many times as desired.

The majority of existing studies assume non-real time task arrivals, i.e. all appliances are initially in the inactive state. At the beginning of scheduling time horizon, there is a list of interruptible and non-interruptible tasks, which is known in advance to the appliance controller [4, 5, 6, 7, 8, 9, 10, 11]. This assumption is usually made to avoid dealing
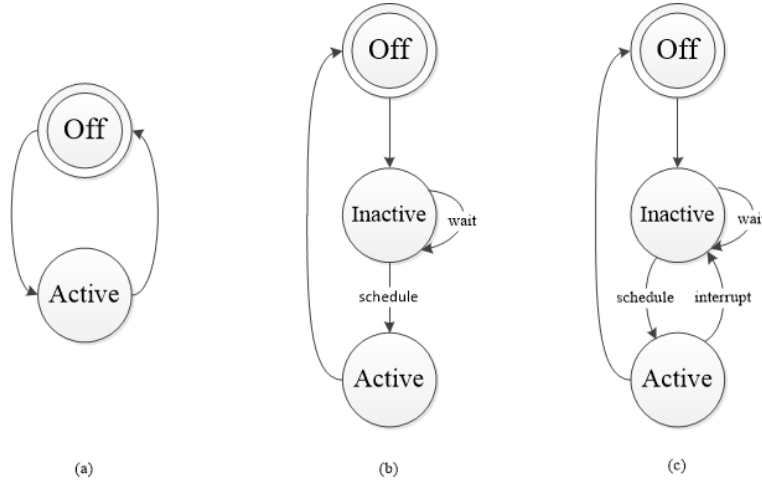
Figure 2.2: Different residential appliance demand models: (a) non-elastic demand, (b) non-interruptible deferrable demand, and (c) interruptible deferrable demand

with uncertainties from the demand side of the DR problem. Practically, this assumption will force consumers to decide which appliance they are planning to use at the beginning of each scheduling time horizon, e.g. at the beginning of a day. To make appliances scheduling more convenient for consumers, some studies assume real-time task arrivals, in which the appliance controller does not know about a task to be scheduled except when the consumer turns on an appliance. In other words, the arrival time of a task is random from the controller's point of view. Scheduling an individual appliance is studied in [12, 13], in which stochastic optimization methods are applied on each appliance separately to determine its optimal starting time. This is a suitable approach when appliances do not share a limited common resource such as in the cases when the power is supplied by a small distributed generator, a storage device, or when the household power capacity is limited. When there is a common resource, joint scheduling of appliances must be applied. In [14], a generic, theoretical framework for appliance-level demand response is presented. In this study, each appliance is first modeled as a Markov chain, then the global system state is defined as the concatenation of all appliance states. A less generic approach is given in [15], where it is assumed that each appliance should be scheduled one time only during the time horizon.

Thermostatically Controlled Loads

TCLs represent appliances that are responsible for temperature control such as air conditioners, refrigerators, and electric water heaters. Here, we discuss the operation of a

heating TCL, where the controlled temperature increases when it is turned on. Similar principles/strategies can be applied to cooling TCLs.

The simplest temperature control strategy can be described as follows: if the controlled temperature is below the setting temperature, then turn on the appliance; otherwise, turn it off. However, this control strategy can cause the appliance to be turned on and off at a very high rate, leading to appliance damage. For this reason, a small temperature variation tolerance is always acceptable. Minimum and maximum temperature thresholds are set such that the desired temperature setting point is between them. The temperature interval between the two thresholds is referred to as the "dead band". It means that, if the controlled temperature is outside this temperature interval, the appliance is not working properly. The new temperature control strategy can then be described as follows: if the controlled temperature is below the minimum temperature, turn on the appliance; if the controlled temperature is above the maximum temperature, turn off the appliance; otherwise, do nothing.

An individual TCL appliance can be represented by an equivalent thermal parameter (ETP) model, which models the evolution of the controlled temperature in the same way as the charging of an electric capacitor. According to this model, the temperature evolution is given by:

$$\theta(t + \Delta t) = \theta_e + P_{TCL}(\Delta t)R_{th} - [\theta_e + P_{TCL}(\Delta t)R_{th} - \theta(t)]e^{-\Delta t/R_{th}C_{th}} + \epsilon_{th}(t), \quad (2.1)$$

where θ_e is the surrounding temperature of the appliance, R_{th} is the thermal resistance, C_{th} is the thermal capacitance, and $P_{TCL}\Delta(t)$ is the electric power consumption of the TCL during Δt. Higher order models can be used to describe multiple surrounding temperatures. The term $\epsilon_{th}(t)$ is used to model any additional disturbance. Figure 2.3 shows an example of the evolution of temperature and power consumption of a TCL.

A TCL appliance can contribute to DR in two ways: 1) Non-intrusive control: TCL is switched in an optimal way (which can be different from the control strategy described earlier) such that the controlled temperature is constrained within the dead band. Long-term average power consumption is usually not affected by this approach; 2) Intrusive control: the approach is to change the temperature setting point, which will cause a decrease or increase of the average power consumption.

Next, we discuss why the existing non-TCL models cannot be directly applied to TCL appliances. Assuming non-intrusive control, a TCL can be freely switched on or off as long as the controlled temperature is within the dead band. If we choose to defer a TCL electric
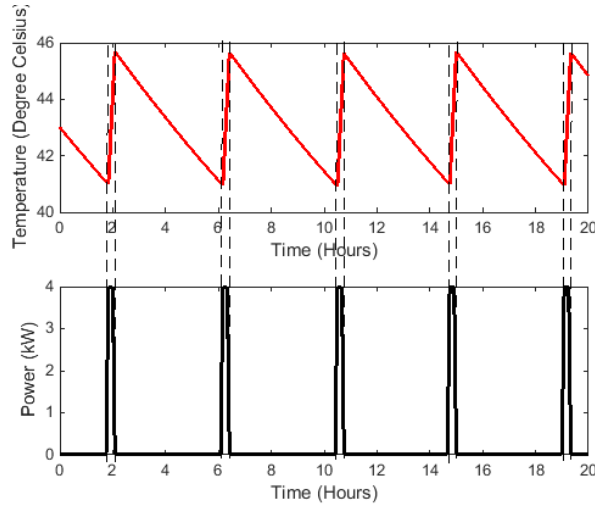
Figure 2.3: Temperature and power consumption evolution of an electric water heater (parameters taken from [16]). Temperature evolution is similar to charging and discharging of an electric capacitor, such that temperature does not deviate from the setting point (in this example 43°C) more than a predefined value (in this example 2°C). Power consumption takes binary levels (either on or off), which results a cyclic load pattern.

demand, part of the stored heat energy will be lost as the TCL is turned off. Hence, more electric energy demand will be needed in addition to the originally deferred one, in order to compensate for the temperature drop during the deference period. This is not the case in non-TCL appliances, where deferring an appliance demand does not affect the amount of energy demand to be satisfied.

Myopic control of a group of TCLs is suggested in some studies [17], in which TCLs are prioritized according to their capability of deferring or increasing their power consumption. For example, if aggregated power consumption of a group of electric heaters needs to be reduced, a heater which is close to upper temperature bound has the priority to be turned off. Similarly, if the aggregated power consumption needs to be increased, a heater which is close to lower temperature bound has the priority to be turned on. This approach is suitable for source following applications, in which the TCLs in the group receive a real-time target demand signal that they are supposed to track. However, this myopic policy is not suitable for other applications such as opportunistic demand scheduling, where one cannot simply decide whether to increase or decrease power consumption given the price of only the current time slot. Also, the temperature difference may not be an adequate measure for the capability of deferring or increasing power consumption. For example, a heater with a better thermal insulation can defer its power consumption for a longer time,

13

even if it is not close to the upper temperature bound.

Electric Vehicles

EVs are different from residential appliances in two aspects. First, their mobility can be exploited to control their demand spatially over a power distribution network by proper assignment of EVs to charging points; second, they can have the ability to supply electricity back to the grid as they have battery storage. The former aspect relates to an EV before it reaches the charging point, while the latter aspect relates to the EV after it reaches the charging point.

Due to limited EV traveling range per battery charging, an EV needs to recharge frequently. Hence, EV arrival at a charging station will be high in comparison with that of gasoline vehicles at a gasoline station. With long charging times, a station cannot accommodate a high EV arrival rate. As a result, vehicle routing algorithms are needed for efficient utilization of charging resources. These algorithms can be categorized into two types: 1) complete path planning from the trip origin to destination, referred to as vehicle routing problem (VRP); and 2) charging station assignment, which directs a vehicle to a proper charging station whenever it requests charging.

Although VRP is not a new problem, it has been revisited recently for electric vehicles [18, 19, 20, 21]. In the studies, the road network is modeled as a complete undirected graph, where the vertices represent charging stations and any other locations of interest, and the graph's edges represent the distance between vertices. Each edge is mapped with two quantities: associated cost (e.g. delay) and the amount of energy required to cover the distance. Both quantities can be vehicle-dependent. Given a finite number of vehicles, the routing problem is formulated as a mixed integer-linear programming (MILP) problem that minimizes the total routing cost.

A dedicated path schedule is suitable for managing a commercial fleet for delivery services (as the VRP was originally designed for). However, applying the VRP on regular passenger EVs is too constraining and inconvenient. In this case, assigning EVs to charging stations at the time of charging request is a more attractive approach. Similar to the VRP, non-real time charging station assignment is considered in [22, 23, 24].

After the charging station assignment, the main concern is to avoid distribution transformer overloading, which can happen if EV charging is uncoordinated. This concern is either studied explicitly as in [25, 26] or in the context of other problems, such as opportunistic demand scheduling [27, 28, 29, 30, 31] or generation dispatch [32]. From the

14

coordinator (demand controller) point of view, each EV is characterized by three parameters: its arrival time, departure time, and required amount of energy charging. Charging power is not a parameter as it is usually standardized. Most existing studies assume that these three parameters are given in advance to the demand controller. This assumption is supported by the fact that an EV is usually charged where and when it is expected to be parked for a sufficiently long time, such as when the consumer is at work in the afternoon or at home overnight. Thus both arrival and departure times can be predicted to a great extent, whereas the required charging energy is submitted by each EV upon its arrival. The main result of this assumption is that EV demand scheduling is usually done in non-real time (offline scheduling). However, it is not a valid assumption for a charging station where EVs can arrive at any time.

The scheduling objective can be the minimization of the aggregated EV peak charging load [25], which is a suitable objective if the EV loads represent a major part of the total network load. On the other hand, if non-EV loads (e.g. residential loads) are more dominant, it is desired to schedule EV demands in a way opposite to variations of non-EV loads (valley filling [26]). Although in reality, future demand is random, what is actually needs to be forecasted is the worst-case scenario, i.e. the largest possible power profile.

2.2 Aggregated demand models

Deferrable Appliances

A natural approach for demand aggregation is to aggregate demands of appliances that belong to each individual consumer. Such approach is used in [8, 9, 11], where demand control follows the hierarchy illustrated in Figure 2.4. According to this hierarchy, demand control is done using bi-level programming, where each consumer submits his aggregated appliances' demand profile to the demand controller. Based on the demand profiles, the demand controller deduces an optimal price profile (real or virtual) that achieves the demand response objective. This price profile is then submitted back to all consumers, who modify their appliances' demand such that the cost of individual consumers is minimized. Then, consumers resend their modified demand profiles to the demand controller and the process repeats until convergence to final demands and price profiles. In summary, the demand hierarchy splits the original DR problem into two levels: the lower level is a home energy management (HEM) problem, and the upper level is an optimal pricing problem. The two problems are solved iteratively until convergence.

There are two drawbacks associated with this hierarchical approach. First, one consumer may have many appliances, and the lower level HEM problem is itself difficult to
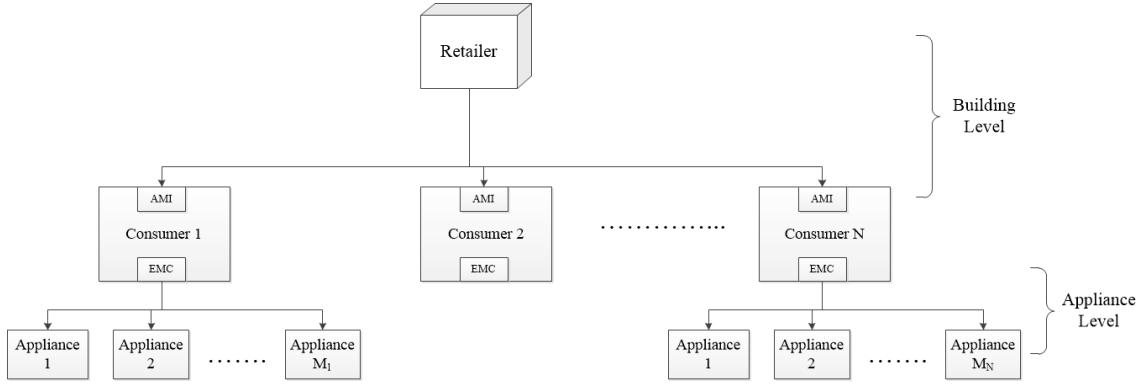
Figure 2.4: An illustration of power demand hierarchy, where arrows represent directions of power flow.

be solved; Second, convergence is not always guaranteed or the solution can converge very slowly [33, 34]. Due to computational time limitations, the problem solving will have to stop after a certain number of iterations. The final solution will largely depend on the initial starting point and can be far from optimal. In order to mitigate this issue, an assumption is usually made to discard all appliances' constraints. Each appliance is simply modeled by a specific amount of energy requirement, and there is no constraint on whether this energy should be satisfied in one time slot or over several time slots. Thus, the consumer's aggregated demand is a specific total energy requirement, which can arrive in non-real time [35] or real time [36, 37, 38, 39, 40]. The aforementioned assumption is accurate under two conditions: 1) the number of appliances per consumer is large, which can relax power constraints; and 2) each appliance's energy requirement can be satisfied in less than one time slot, and hence there are no inter-temporal constraints. As a result of the assumption, the lower-level problem discussed earlier completely disappears, and only the upper-level problem needs to be solved without any iteration.

When the number of consumers is large, even the upper-level problem can be difficult to solve. Hence, an alternate approach is to develop an aggregated demand model for a large number of consumers, rather than dealing with each consumer individually. Economic models based on demand elasticity/utility in literature represent this level of demand aggregation. Demand elasticity represents the amount of demand reduction for unit price increase, while demand utility represents user satisfaction (valuation in dollars) for consuming one unit of electric energy. Thus, demand elasticity and utility are two sides of one coin and are considered as one category of demand modeling. The utility function is usually an increasing, concave function of energy consumption. It can be time-varying [41] to represent consumers' different energy consumption valuation for different time periods across the day. In more complex models, cross-elasticity is considered, in which electricity

price affects power consumption not only in the current time slot, but in future time slots [42, 43]. A drawback of these models is that they are not built on residential demand characteristics, but rather based on historical data of the response of aggregated demand to price signals. This makes the model non-robust (as it can change easily due to any external factor) and very case-oriented (e.g., an elasticity model used for one location might not be suitable to represent demand of the same size in another location). Since errors can always happen when using such models, some research works add random noise to the demand elasticity models to capture uncertainty in consumer responses to price changes [44]. In other words, the average demand is determined by a deterministic function of electricity price, while the randomness is modeled as a zero-mean random variable.

Thermostatically Controlled Loads

We first discuss aggregation of a homogeneous population of TCLs, then extend it to a heterogeneous case. As suggested in [45, 46], TCLs are classified according to their current temperature and on/off operation status. For example, if the temperature interval is partitioned into 3 intervals, then there are a total of 6 different bins in which TCLs are classified into. The system state is represented by the probability mass function (PMF) over these different bins. An advantage is that the accuracy of the model depends on the resolution of the PMF, but not on the number of aggregated TCLs. The control signal represents the switching probabilities (turning on or off) that are submitted to each group of TCLs residing in the same bin. Since the population is homogeneous and if it is large enough, the system state transition (PMF change) is almost deterministic. For example, if the number of TCLs in some state bin is 10,000 and the decision is that each TCL in the bin can switch with a probability 60%, then almost 6000 TCL appliances will switch as the population is large. Since the population is also homogeneous, these 6000 TCLs will be transferred to the same bin. Thus, system evolution is approximately deterministic. Also, total power consumption can simply be deduced by calculating the probability that a TCL is on, then multiplying it by the total number of TCL population and the power rating of an individual TCL.

Some studies (such as [47]) attempt to use the same approach for heterogeneous TCLs. TCLs within each bin will not be transferred to the same bin in the next time slot since different TCLs will have different evolutions. Thus, due to heterogeneity, state transitions will be stochastic rather than deterministic. Calculating these transition probabilities is challenging, as it depends on the mixture of TCLs' types within each bin. In [47], it is assumed that this mixture is constant for all bins, which is the same mixture of the total TCL population. For example, if the mixture in the TCL population is 30% of type I and 70% of type II, when we select any bin at any time, we will find that the

probability of a randomly selected TCL of type I is 30%. This assumption can be highly inaccurate. If we aggregate the operation of cooling and heating TCLs, heating TCLs will be concentrated towards high temperature bins while cooling TCLs will be concentrated towards low temperature bins.

Electric Vehicles

There are very limited studies for developing aggregated models for EV routing or charging station assignment. One of the studies is [48], in which each charging station is modeled as a queue representing the number of EVs waiting to be served in that station. Using queueing theory, authors attempt to define an optimal station assignment policy such that EV's expected waiting time is minimized. However, EV mobility model is not considered. It is assumed that each EV can reach any station in zero time.

On the other hand, aggregated models for EVs' charging are frequently used. There are two ways for EV charging aggregation: 1) homogeneous EV aggregation [28, 30] in which EVs are classified into groups according to their arrival and departure times. Each group is treated as one big electric vehicle, and the problem is solved as a small-scale EV scheduling problem; 2) heterogeneous EV aggregation, in which each EV group can have different arrival and departure times [27, 31, 32]. The optimization problem is solved using bi-level programming: in the upper level, the controller receives aggregated EV demand profiles from each group and decides the corresponding electricity virtual price profile accordingly; in the lower level, each group receives this virtual price profile and attempts to schedule its corresponding EVs such that the total virtual demand cost is minimized. The bi-level problem is solved iteratively until convergence.

2.3   Summary

In this chapter, we discuss different existing individual and aggregated demand models for three different sources of electric energy consumption, which are deferrable appliances, thermostatically-controlled loads and electric vehicles. Existing aggregated demand models for deferrable appliances assumes perfectly dispatchable demand, without considering various appliance constraints. This is accurate when the energy consumption requirement can be satisfied within one time slot. However, if the energy consumption extends over multiple time slots, then the scheduling decisions will cause inter-temporal demand dependence and significantly impacts achieving the DR objective. Therefore, a new aggregated demand model should be developed to characterize the inter-temporal dependence resulting from scheduling decisions. On the other hand, existing aggregated models for TCLs

are reduced-order models, which are less complex than dealing with individual models for a large population of TCL appliances. These models are suitable for performance evaluation, but are computationally inefficient for many DR optimization problems. Hence, developing an efficient aggregated demand model for TCLs is essential to incorporate them in large-scale DR programs. Finally, EVs are modeled from two aspects, for first assigning them to charging stations and then charging their batteries. For the first aspect, there is almost no existing aggregated EV assignment model, only individual models exist. For the second aspect, aggregated models for EV battery charging assume a predetermined arrival and departure times. The assumption is not suitable for charging stations, in which EVs arrive randomly. Hence, an aggregated EV charging model is needed to properly capture both aspects.

Chapter 3

System Model

3.1 Microgrid

We consider a microgrid (MG), as shown in Figure 3.1. The geographical service area of the MG is represented by a bounded and convex set of locations $\mathcal{B} \subset \mathbb{R}^2$. The MG serves a number, N_r, of residential consumers and a number, N_c, of charging stations. If the MG is in the grid-connected mode, the electric energy is purchased from the day-ahead market. On the other hand, if the MG is in the island mode, the demands are satisfied using a number, N_g, of identical and non-renewable distributed generators (DGs). The regular operations of the MG are maintained by the microgrid central controller (MGCC). We extend the functions of the MGCC to include controlling the demand as well. In the following, the model of each part of the system under consideration is defined in details.
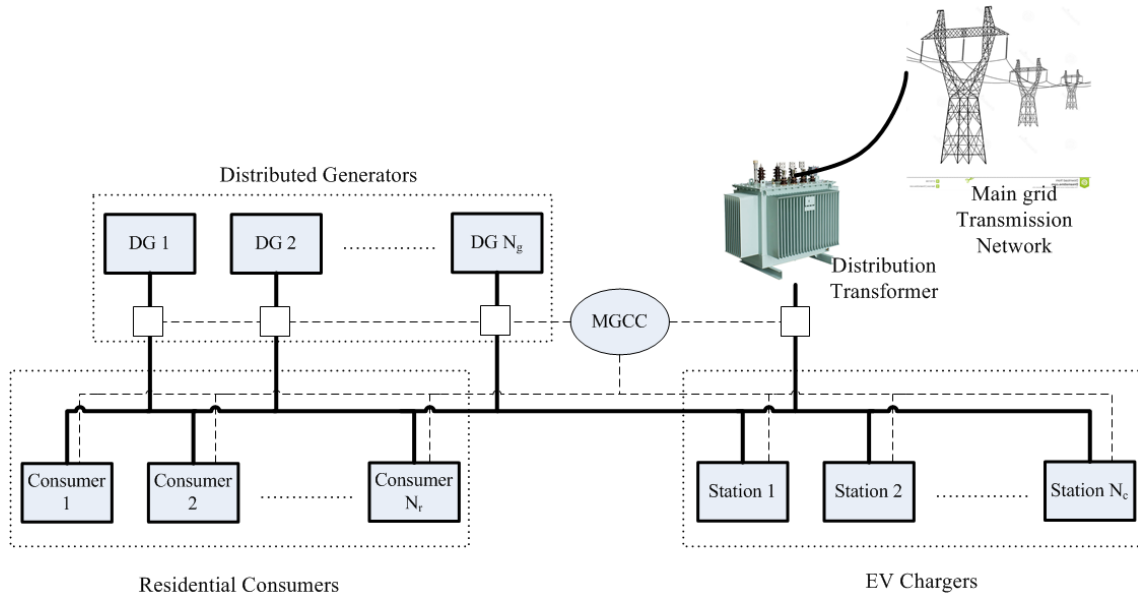
Figure 3.1: Block diagram of microgrid under consideration. Solid lines represent power distribution network, dashed lines represent communication network, and white squares represent circuit breakers that can be closed or opened by MGCC depending on the microgrid operation mode.

Supply Model

The supply model depends on the operation mode of the MG. In the grid-connected mode, DGs are turned off and the energy is entirely purchased from the main grid under a day-ahead pricing (DAP) scheme. The electricity price profile for the current day was submitted to the MGCC at the beginning of the day before. The electricity price is updated periodically every 5 minutes (similar to Ontario's electricity market clearance price [49]) and hence the profile is composed of 288 time intervals. If the MG is in the island mode, the demand is satisfied by the energy produced from the DGs. All the DGs are assumed to be identical with a maximum ramping rate ρ. The ramping rate represents the change of the DG's power per unit time. With identical DGs, they are equivalent to a single DG with a maximum ramping rate of ρN_g.

Residential Consumer Model

We follow a similar approach for residential demand modeling as in [50]. The general behavior of a consumer can be modeled as a Markov chain whose states represent different consumer's activities. There are three consumer states, i.e., absent, inactive, and active.

The "absent" state indicates that the consumer is not at home, the "inactive" state indicates that the consumer is at home but with a low activity level, while the "active" state indicates that the consumer is at home and has a high level of activity. The states affect the energy consumption of consumer's appliances. The probability that a user uses an appliance is higher when he is in the active state than that when he is in the inactive state.

Consumer appliances are classified into three categories: deferrable loads, thermostatically-controlled loads, and non-controllable loads, described as follows.

1) Deferrable loads: Each consumer, i, has a set $\mathcal{N}_i$ of non-interruptible appliances and a set $\mathcal{I}_i$ of interruptible appliances. Each appliance $j \in \{\mathcal{N}_i \cup \mathcal{I}_i\}$ is characterized by an arbitrary task pattern, $g_{ij}(t)$, a probability to be turned-on, $p_{ij}(t)$, and a deadline for the task completion, d_{ij}. Task requests arrive only when the consumer is in the active state.

2) TCLs: Each consumer, i, has a set $\mathcal{T}_i$ of TCL appliances. Each appliance follows a simple ETP model, as described in Chapter 2. Appliances have different physical and setting parameters. Physical parameters include thermal resistance, capacitance and active power consumption. Setting parameters include the temperature setting point and dead band. The TCLs' operation is independent of the consumer state.

3) Uncontrollable loads: Each consumer, i, has a set $\mathcal{U}_i$ of uncontrollable appliances. Each appliance is modeled as an (on/off) Markov chain whose transition probabilities depend on the consumer state. If the consumer is in the absent state, the appliance is always turned off. Each appliance $j \in \mathcal{U}_i$ consumes constant power as long as it is turned on, while it does not consume any energy when it is turned off.

In addition to appliance demands, each consumer has a local RES power generation capability. Since RES units are installed within a limited geographical area, the power profiles generated from all units are highly correlated. We model the power generated from the RES unit of consumer i as a weighted sum of two power profiles:

$$P_i^{RES} = \alpha P_0 + (1 - \alpha)P_i^u. \tag{3.1}$$

The first profile represents the nominal power profile P_0 resulting from the "spatially average" RES power in the considered geographical area. This profile is the same for all RES units, hence, it represents the correlated part of the RES power production. The second profile P_i^u represents the deviation from that nominal power profile as a result of any possible imperfections. The profile depends on the conditions of the corresponding RES unit
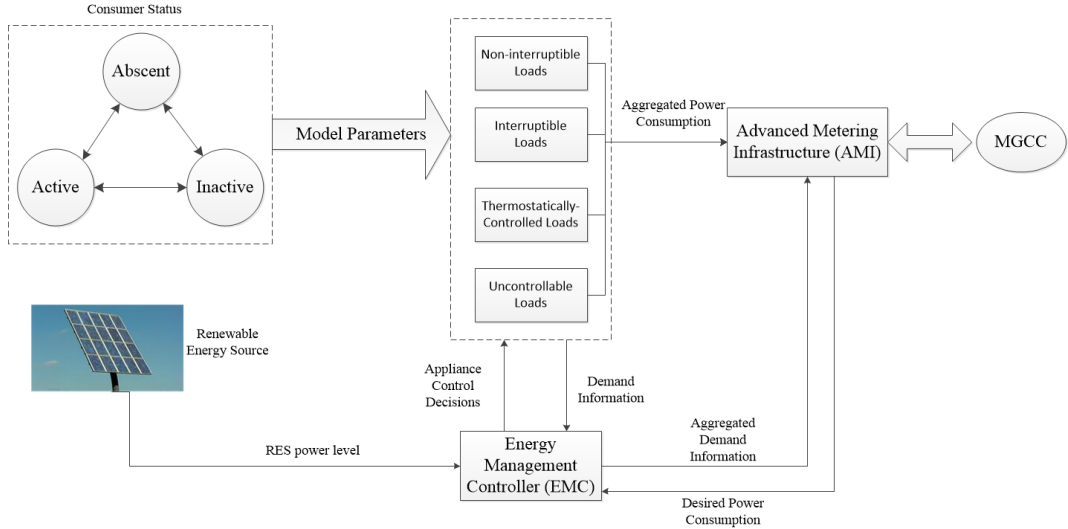
Figure 3.2: Residential consumer demand model. Each consumer has an EMC unit is responsible for appliance scheduling and an AMI unit which acts as an interface between the consumer and the MGCC.

and is independent on other units. The overall effect of the aggregated RES power is the contamination of the smooth aggregated demand profile with fluctuations. The complete residential consumer model is illustrated in Figure 3.2.

Electric Vehicle and Charging Station Models

A charging station i is characterized by two parameters: a location belonging to $\mathcal{B}$ and a number of chargers R_i. Each EV is assumed to be equipped with a wireless transceiver which enables a two-way communication with a central controller. Whenever a user needs to recharge his EV's battery, he sends a charging request to the controller and in return he receives a message indicating which charging station he is supposed to head to. The communication is assumed to be reliable with negligible transmission delay compared to EV's travel or waiting times.

Charging requests are assumed to arrive according to a homogeneous Poisson Point Process (PPP) with parameter Λ. All chargers are assumed to have the same power rating, accordingly the time needed to charge an EV's battery is independent on the assigned station. The time required for an EV to travel from point $A \in \mathcal{B}$ to point $B \in \mathcal{B}$ is assumed to be proportional to the Euclidean distance between A and B.

3.2 Summary

In this chapter, the system model under consideration is presented, including supply and demand models. Two categories of demands are considered: 1) residential appliances, and 2) electric vehicles. Both demands are controlled by a single entity referred to as MGCC, which is responsible for taking all DR decisions. The demands are served by either importing power from the main grid or by producing power from a set of DGs.

Chapter 4

Minimizing Energy Consumption cost for Residential Consumers

4.1 Problem definition

Consider that the MG in Fig. 3.1 is in the grid-connected mode. The cost of consuming a unit energy is time-varying according to the DAP. Minimizing the cost of energy consumption is done by shifting the demand from time slots having high electricity prices to time slots having lower electricity prices, whenever possible. One approach is to let each consumer schedules his appliances, independently from other consumers, in order to minimize his own energy consumption cost using one of the home energy management (HEM) algorithms. However, such uncoordinated demand modification will result in large aggregated power consumption at time slots of low electricity prices. The aggregated power may exceed the capacity of the distribution transformer and can possibly lead to MG operation failures. Therefore, all the appliances of residential consumers are scheduled using a single controller, the MGCC, in order to take the capacity of the distribution transformer into consideration.

According to the DAP, the electricity price profile of a current day is announced one day before. Hence, the MGCC knows exactly when the electricity price will be high and when it will be low. What the MGCC does not know in advance is when the appliances will be turned on. Thus, the arrivals of the appliance demands are the main source of uncertainty in this problem.

Regardless of the demand uncertainty, an aggregated demand model is needed to facilitate controlling a large number of appliances by the MGCC. To establish a model for

demand aggregation, it is unavoidable that some of individual appliances' information will be lost. Such information can include the power consumption profile of an appliance or the consumer's convenience settings such as task deadlines for deferrable appliances or temperature deadbands for TCL appliances. The loss of information can lead to a non-optimal appliance scheduling and/or consumer inconvenience. Therefore, when an aggregated demand model is needed, it is necessary to keep as much important information as possible, while reducing the problem complexity.

In existing studies, aggregated demand models for deferrable appliances depend on a simplifying appliance model by considering only the amount of required energy. The information about the duration of the appliance energy consumption is discarded. This assumption is valid if the appliance energy requirement can be satisfied in less than one time slot. In our problem, one time slot is equal to the price update interval, i.e. 5 minutes. Deferrable appliances such as washing machines can consume energy for 1 to 2 hours, corresponding to 12 to 24 time slots. Scheduling a washing machine in one time slot will not only affect the power consumption in that particular time slot, but also the power consumption in several future time slots. Without the knowledge of the energy consumption time duration, the MGCC schedules the appliance starting from the time slot of the lowest price. This will minimize the energy consumption cost for the first time slot of the scheduling, but may not be optimal for the rest part of the appliance energy consumption.

On the other hand, the existing aggregated models for TCLs (described in Chapter 2) are suitable for myopic control, i.e. achieving the DR objective over a single time slot only. The models are not suitable for the optimization over multiple time intervals as in our problem. Using the existing aggregated models, the space representing the collection of all possible states of the aggregated model is very large, even for a homogeneous TCL population. For example, if the temperature range is divided into three intervals, the state space will have six dimensions. If the population of the TCLs can be represented by a sample of 10 TCLs, the state space is in the order of 10^6. A large state-space is undesired in stochastic optimization problems, since it requires the evaluation of a large number of different scenarios to find the optimal decisions.

Given the limitations of existing models, our objective is to develop an effective aggregation model for both deferrable and TCL appliances. The new model should capture the durations of the energy consumption of different appliances and facilitates the contribution of TCL appliances in cost minimization problems.

4.2   Solution methodology

Our methodology for minimizing the energy consumption cost will be based on the following demand aggregation model. It is known that the lowest two layers (levels) of the demand hierarchy are the appliance layer and the building layer. We introduce a new layer between them, which is responsible for consumer demand management, referred to as the "Demand Response Management" (DRM) layer. This layer acts as an interface between different consumer appliances and the MGCC. The construction of a new layer means introducing new types of demand information and decisions, different from that existing in both the appliance and building layers. The input to the DRM layer is the demand requirements of deferrable and TCL appliances. The output of this layer is what we refer to as "demand blocks", which are our new units of demand information. Each demand block ideally has constant power consumption over a fixed duration, represented by a rectangular-shaped demand profile. A demand block can be constituted from the demand requirement of a single appliance or from a mixture of demand requirements of several appliances. The responsibility for the generation of demand blocks is assigned to the EMC unit that is located in the consumer premises. Demand blocks are classified into different classes according to three parameters: demand block duration, power consumption, and delay requirement. When demand blocks are generated, they are placed into different queues according to their classes, where each queue represents a distinct class of demand blocks, as shown in Figure 4.1. The set of all possible classes is defined in advance, and is the same for all residential consumers.

With the demand information in demand blocks, the MGCC schedules queued demand blocks from different classes for service at each time slot. In this way, the MGCC does not directly control a large number of appliances, but manages a much smaller set of queues. The inter-temporal demand dependence resulting from the scheduling of different demand blocks is now considered, since the duration and power of each demand block is given in advance to the MGCC.

The idea behind our approach is that we are not focused on an appliance identity, but rather on its DR capability or, in other words, how it can provide benefits to the power system. This DR capability is expressed through the three aforementioned parameters (energy consumption duration, power level, and delay requirements). If two appliances have the same values for these three parameters, they are considered as of the same type (class) from the MGCC point of view, regardless if they have different functions or if they belong to different consumers. The demand aggregation is done by grouping appliances of closer DR capabilities together (assign them to the same queue).

The DRM layer divides the cost minimization problem into two parts, demand mapping
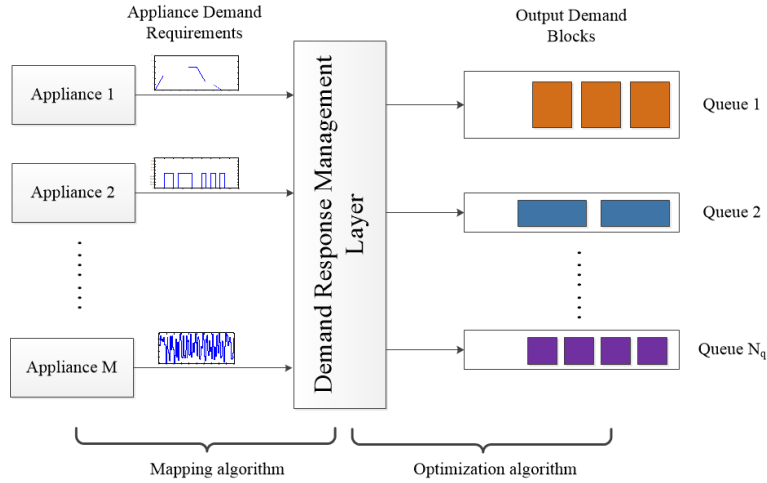
Figure 4.1: The function of the DRM layer: mapping different demand requirements of various appliances to standardized blocks of demand.

and demand optimization. Demand mapping defines how a demand requirement of an appliance is assigned to one queue of the given queue set. The mapping algorithm is run by the EMC unit within each consumer premises. On the other hand, demand optimization algorithm is run by the MGCC, and aims to determine the optimal scheduling of queued demand blocks such that the total energy consumption cost is minimized. These algorithms will be discussed in the next section.

As a byproduct of our methodology, the consumer privacy can be better preserved. If the information about demand blocks can be collected from the consumers by a trusted party, only the total numbers of demand blocks waiting within each queue are sent to the MGCC. When the MGCC decides to schedule a demand block, it will not know which consumer this demand block belongs to, and hence, the consumer's privacy is preserved.

4.3 Solution algorithms

4.3.1 The mapping algorithm

The goal of the mapping algorithm is to assign different appliance demand requirements to different given classes of demand. The mapping is done such that the total distortion resulting from the assignment process is minimized. The distortion resulting from assigning demand requirement profile $g(t)$ to class i is defined as
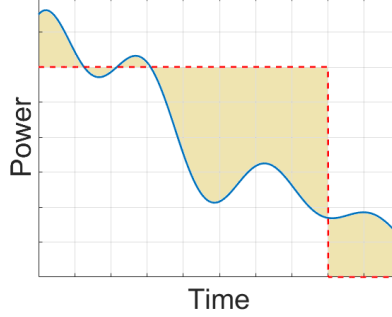
Figure 4.2: The deviation between an arbitrary demand profile (solid) and an ideal demand block (dashed).

$$\zeta_i(g(t)) \triangleq \frac{1}{P_i^2 K_i} \int_0^\infty \left[g(t) - P_i \left(U(t) - U(t - K_i) \right) \right]^2 dt, \tag{4.1}$$

where P_i and K_i are the power level and duration of a demand block of class i, and $U(.)$ is the unit step function. The distortion represents the amount of deviation of the task profile from the rectangular shape of an ideal demand block of class i (Figure 4.2).

TCL as a deferrable load

Knowing the demand requirement of a deferrable appliance is straight-forward, as the task pattern is given in advance. However, in TCL appliances, there is no predefined task pattern. Furthermore, the consumer's convenience from TCL appliances is defined by temperature constraints instead of delay constraints. Therefore, we need to deduce a method for representing demand requirements of TCL appliances similar to that of deferrable appliances. Our proposed method is described in the following.

Starting from the first-order ETP model, the evolution of the temperature controlled by a TCL appliance is given by [51]

$$C_{th} \frac{d\theta}{dt} = \frac{\theta_e - \theta}{R_{th}} + P^r s(t), \tag{4.2}$$

where θ is the temperature under control, P^r is the power consumed by the TCL appliance when it is turned on, and $s(t)$ is the binary switching function which takes a value of 1 when the appliance is on, and 0 otherwise. The model in Equation (4.2) represents a

29

heating TCL, since the controlled temperature increases when the appliance is turned on. However, cooling TCLs can follow a similar analysis. Equation (4.2) is a first-order ODE, whose solution is well-known and given by

$$\theta(t) = \theta_e + P^r s(t) R_{th} - (\theta_e + P^r s(t) R_{th} - \theta_i)e^{-t/R_{th}C_{th}}, \tag{4.3}$$

where $\theta_i = \theta(0)$ is the initial temperature. The temperature constraints are given by

$$\theta_{min} \leqslant \theta \leqslant \theta_{max}, \tag{4.4}$$

where θ_{min} and θ_{max} represent the minimum and maximum temperatures beyond which the operation of the TCL becomes inconvenient for the consumer. Now, we let the appliance send a request for energy demand whenever the temperature falls below a certain threshold $\theta_s \in [\theta_{min}, \theta_{max}]$, which can be, for example, the temperature setting point. The appliance will require a non-interruptible power consumption of level P^r for a duration K and a deadline D for satisfying the demand. From the DR perspective, it is desirable for an appliance to have short power consumption duration and a long deadline for demand satisfaction. However, as we shall see, there is a trade-off between both quantities.

After the demand request is sent, the appliance waits until it receives a permission from the demand controller to be turned-on. The maximum time that the appliance can wait without causing a discomfort for the consumer is the period that θ drops from θ_s to θ_{min}, as illustrated in Figure 4.3. Therefore, the maximum achievable deadline D_{max} can be deduced from eq. (4.3) as

$$D_{max} = R_{th}C_{th} \, ln\Big(\frac{\theta_s - \theta_e}{\theta_{min} - \theta_e}\Big) \tag{4.5}$$

Since the TCL appliance does not know in advance when it will receive the permission for power consumption, the duration of the power consumption, K, should be specified under worst-case conditions. First, the TCL power consumption duration should be sufficient for the controlled temperature to rise above θ_s. The worst-case will happen when the appliance receives the permission exactly at the end of the deadline, when θ is at its minimum value. Therefore, the minimum power consumption duration, K_{min}, is determined as the time required for θ to rise from the aforementioned minimum value to θ_s, as shown in Figure 4.4. The duration K_{min} can be deduced from (4.3) as:

$$K_{min} = R_{th}C_{th} \, ln\left[\frac{P^r R_{th} - (\theta_s - \theta_e)e^{-D/R_{th}C_{th}}}{P^r R_{th} - (\theta_s - \theta_e)}\right] \tag{4.6}$$
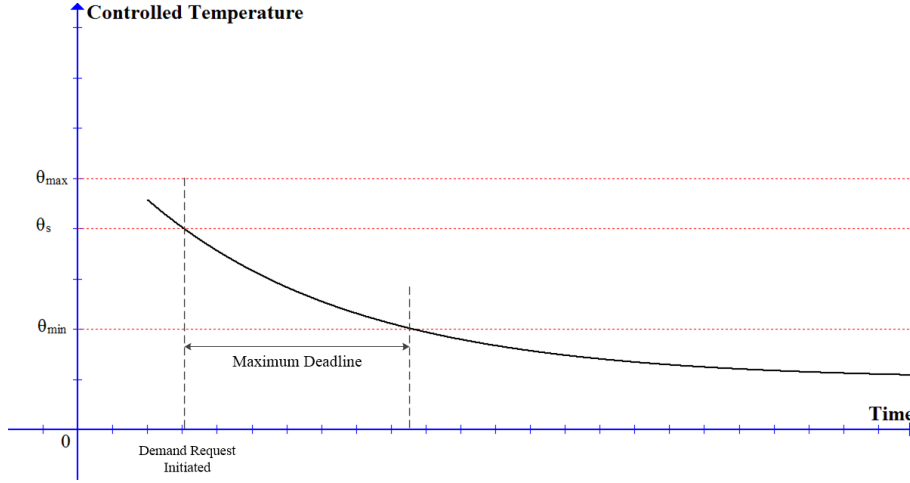
Figure 4.3: The evolution of a controlled temperature of a heating TCL when it is turned off. The maximum deadline for the satisfaction of a TCL demand request is calculated as the time needed for the controlled temperature to hit the minimum temperature level.

On the other hand, K should not be long enough for θ to rise above θ_{max}. In contrary, the worst-case condition happens if the appliance receives the permission to be turned-on immediately without any delay. Therefore, the maximum power consumption duration, K_{max}, is determined as the time required for θ to rise from θ_s to θ_{max}, as shown in Figure 4.4. The duration K_{max} can be deduced from (4.3) as

$$K_{max} = R_{th}C_{th} \, ln\Big(\frac{\theta_e + P^r R_{th} - \theta_s}{\theta_e + P^r R_{th} - \theta_{max}}\Big) \tag{4.7}$$

It is desirable to have a short duration for power consumption, therefore K is set by (4.6). However, (4.7) is important to make sure that $K_{max} \geqslant K_{min}$. If this condition does not hold, θ_s must be selected for a lower value.

By using the aforementioned approach, a TCL appliance can send its demand requirement in terms of power consumption level, P^r, duration, K_{min}, and the deadline for accepting the request, D, similar to that in deferrable appliances.

Mapping demand requirements

At each time slot, the input to the mapping algorithm is a set of tasks, $\mathcal{Y}$, representing different demand requirements from deferrable and TCL appliances. Each task $i \in \mathcal{Y}$ is characterized by a power consumption pattern $g_i(t)$ and a deadline D_i. The mapping algorithm is responsible for the best assignment of these tasks to available classes of demands.

31
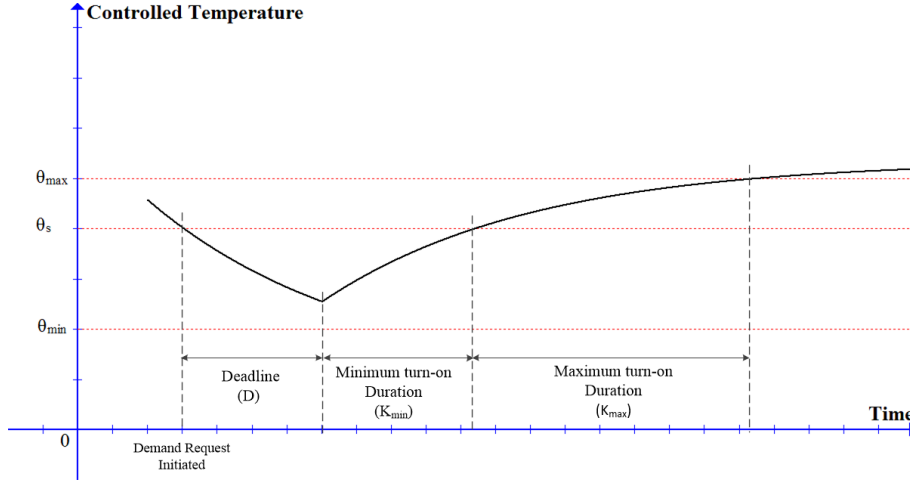
Figure 4.4: Illustration for the minimum and maximum turn-on durations

Our proposed mapping algorithm is based on enumeration. This approach is justified since, in practice, a residential consumer usually has a small number of appliances contributing to DR, which do not have to request energy demand at the same time.

As a result of the mapping algorithm, different demand blocks can be generated. A demand block can be constituted from a single task or multiple tasks. Therefore, the mapping algorithm accounts all the possible combinations for task grouping. For example, if we have three input tasks $\{a, b, c\}$, there are five possible ways for task grouping, which are $\{(a, b, c), (ab, c), (a, bc), (b, ac), (abc)\}$, such that ab represents a new task formed from adding the demands of task a and b. For each group, the tasks (original or mixed) are assigned separately to different classes of demand, based on the minimum distortion criterion, defined in (4.1). Therefore, each group will have its corresponding task mapping and the resulting total distortion. The mapping algorithm will finally choose the group corresponding to the minimum total distortion. The steps of the mapping algorithm are summarized in Algorithm 1.

32

Algorithm 1: The mapping algorithm

Input : The set of tasks required to be mapped at the current time slot t

1 Generate all the possible combinations, $\mathcal{G}$, for task grouping

2 **for** *group* $\mathcal{H}_i \in \mathcal{G}$ **do**

3 $\quad$ **for** *task* $j \in \mathcal{H}_i$ **do**

4 $\quad\quad$ Identify the deadline of the task, D_{ij}

5 $\quad\quad$ Identify the set of demand classes having the deadline parameter shorter than or equal to D_{ij}

6 $\quad\quad$ Using (4.1), calculate the distortion values resulting from the assignment of the task to each of the demand classes

7 $\quad\quad$ Store the result of the minimum distortion value and the corresponding class of demand

8 $\quad$ **end**

9 $\quad$ Store the complete task mapping for group i and the total amount of distortion resulting from the mapping process

10 **end**

11 Select the group corresponding to the minimum total distortion

12 Assign all the input tasks to demand classes according to the mapping of the selected group

---

4.3.2 The optimization algorithm

The goal of the optimization algorithm is to schedule different demand blocks such that the total consumer energy consumption cost is minimized. The problem has two types of constraints: 1) power capacity constraints due to the limited power rating of the distribution transformer, and 2) the delay QoS constraints for different types of demand blocks. The power capacity constraints can be written as

$$L_t \leqslant L^{rating}, \qquad \forall t = 1, 2, \dots, T, \tag{4.8}$$

where L_t is the total energy consumption of residential consumers in time slot t. For convenience, we simply refer to the energy consumption in a unit time slot as power consumption. Therefore, L_t also represents the total consumer power consumption at time slot t. Similarly, L^{rating} represents the power rating of the distribution transformer. The total number of time slots in the scheduling horizon is represented by T, which can be deduced by dividing the length of the scheduling horizon (1 day) over the length of a one

time slot (5 minutes). In our problem, the time horizon is composed of different 288 time slots.

The total power consumption is divided into two parts: controllable power consumption at t, L_t^c, which results from the scheduling of different demand blocks; and uncontrollable power consumption at t, L_t^{uc}, which results from the operation of the non-controllable appliances. The cost of the energy consumption from non-controllable loads cannot be minimized, however they limit the power headroom in which the controllable loads are allowed to be scheduled. Therefore, the non-controllable loads still need to be considered by the optimization algorithm. Hence, the constraint set in (4.8) is re-written as

$$L_t^c \leqslant L_t^{max}, \qquad \forall t = 1, 2, \ldots, T, \tag{4.9}$$

where $L_t^{max} = L^{rating} - L_t^{uc}$. The non-controllable power consumption is a random process from the controller's point of view. This uncertainty creates a risk that the capacity constraints become violated, especially when a large number of demand blocks are scheduled. In our work, we follow a conservative approach by considering the maximum possible (worst-case) values of L_t^{uc}.

On the other hand, the delay QoS constraints are given by the probability that the demand blocks are scheduled before their deadlines. The constraints are global, not associated with demand blocks generated at a specific time period. The QoS constraints are given by

$$\Pr\{W_i \leqslant D_i\} \geqslant \delta, \qquad \forall i = 1, 2, \ldots, N_q, \tag{4.10}$$

where W_i and D_i represent respectively the waiting time and the deadline of a demand block of class i, N_q represents the total number of queues (also the total number of demand block classes), and δ represents the minimum level of QoS.

The only source of randomness in the problem is the arrival process of different demand blocks, which evolves according to some general and non-stationary stochastic process. All other parameters are deterministic from the controller's point-of-view. Therefore, the system under consideration can be described as a multi-class, non-stationary $G_t/D/m$ queueing system.

A straight-forward approach to make optimal decisions under uncertainty is to use a stochastic optimization technique such as Markov decision process (MDP) or Monte-Carlo simulation (MCS). However, both approaches are computationally inefficient in solving our problem. Since demand rejection is not allowed (i.e., each demand block *has* to be admitted

34

to the queueing system), queue length can take any non-negative value. Therefore, the system's state-space and the decision-space are not finite, hence, it is difficult to use MDP for finding the optimal decisions. On the other hand, simulation is a powerful tool for evaluating the performance resulting from taking a single decision. However, the essence of MCS is to enumerate all the possible decisions, evaluate them, then to select the decision corresponding to the optimal value. MCS is not suitable as the decision-space is too large to be enumerated and evaluated.

Thus, we need to develop an efficient approach for the optimization other than using the existing straight-forward approaches. Our proposed approach works by dividing the decision-making process into two phases: 1) capacity planning, and 2) real-time scheduling. In the first phase, we set a maximum-limit for power consumption profiles for each queue such that all constraints are satisfied. In the second phase, demand blocks are scheduled in a greedy way regardless of the cost of energy consumption, but they should not exceed power consumption profiles defined in the first phase.

Let x_{it} denote the maximum number of demand blocks of class i that can be scheduled at time slot t, and $\mathbf{x} = \{x_{it} : i \in 1, 2, \ldots, N_q, \quad t \in 1, 2, \ldots, T\}$ denote the vector of allocated capacity of demand blocks for each class at each time slot. We denote the cost of scheduling a demand block of class i at time t by c_{it}, given by

$$c_{it} = P_i \sum_{s=t}^{t+K_i-1} \gamma(s), \tag{4.11}$$

where $\gamma(s)$ is the given electricity price at time slot s.

The capacity allocation vector, $\mathbf{x}$, is the decision variable for the first phase. Since arrivals of the demand blocks are random, there is no single choice of $\mathbf{x}$ that minimizes the energy consumption cost under all possible demand arrival scenarios. Instead, we seek to minimize the upper bound of the energy consumption cost which will happen if the allocated capacity $\mathbf{x}$ is fully utilized. The optimization problem is given by

$$\mathbf{P1}: \quad \min_x \left\{ \sum_i \sum_t c_{it} x_{it} \right\}$$
$$\text{s.t. } \mathbf{Ax} \leqslant \mathbf{L^{max}} \tag{4.12}$$
$$h_i(\mathbf{x}) \geqslant 0 \qquad \forall i \in \mathcal{Q} \triangleq 1, 2, \ldots, N_q$$
$$\mathbf{x} \in \mathbb{N}^{T \times N_q},$$

where $\mathcal{Q}$ represents the set of queues. The first set of constraints represent the power capacity constraints in (4.9), where $\mathbf{A}$ is a $T \times TN_q$ matrix that transforms the capacity allocation vector $\mathbf{x}$ (of length TN_q) into the total power consumption profile (of length T). The second set of constraints represent the QoS constraints in (4.10), where $h_i(\mathbf{x}) = \Pr\{W_i \leqslant D_i\} - \delta$, representing the difference between the actual QoS level and the target QoS level.

The difficulty of solving **P1** lies on how to evaluate $h_i(\mathbf{x})$ over its domain. We adopt an algorithm used for non-linear programming, called *cutting plane method* (CPM) [52, 53]. The approach is based on an assumption that $h_i(\mathbf{x})$ is a concave function. The assumption is justified in our problem as follows: it is intuitive that the delay performance improves as we add more power (demand block) capacity. Therefore, $h_i(\mathbf{x})$ is a non-decreasing function. However, the maximum possible value for $h_i(\mathbf{x})$ cannot exceed $1 - \delta$, which means that the function saturates at sufficiently high values of $\mathbf{x}$. Thus, $h_i(\mathbf{x})$ should be concave at least at high QoS values, which are the main region of interest.

The CPM principle is close to that of the popular branch-and-bound method. The original problem **P1** is relaxed by removing the second set of constraints, $h_i(\mathbf{x}) \geqslant 0$. Thus, **P1** is transformed into a pure integer programming (IP) problem, which can be solved by its regular techniques. The relaxed problem is

$$\mathbf{P2}: \quad \min_{x} \left\{ \sum_i \sum_t c_{it} x_{it} \right\}$$
$$\text{s.t. } \mathbf{Ax} \leqslant \mathbf{L^{max}}$$
$$\mathbf{x} \in \mathbb{N}^{T \times N_q} \tag{4.13}$$

After obtaining the optimal solution of **P2**, $h_i(\mathbf{x})$ is evaluated at that particular solution, $\mathbf{x}_r^*$, using a simulation or analytical method. If all the constraints are satisfied, $h_i(\mathbf{x}_r^*) \geqslant 0, \forall i \in 1, \ldots, N_q$, the relaxed solution is the optimal solution of the original problem $(\mathbf{x}^* = \mathbf{x}_r^*)$. If one or more constraints are violated, then for each violated constraint a linear constraint is created such that the "failed" relaxed solution is removed *without* changing the feasible region of **P1**. However, adding these constraints will reduce the feasible region of the relaxed problem, **P2**. The new solution of the relaxed problem will again be used to test if the constraints are satisfied or violated. The process is repeated, and with each iteration, the feasible region of the relaxed problem shrinks until a relaxed solution is reached that satisfies all the constraints of **P1**. The benefit of the approach is that we do not need to characterize $h_i(\mathbf{x})$ over its domain, but rather evaluate it at a specific finite number of points.
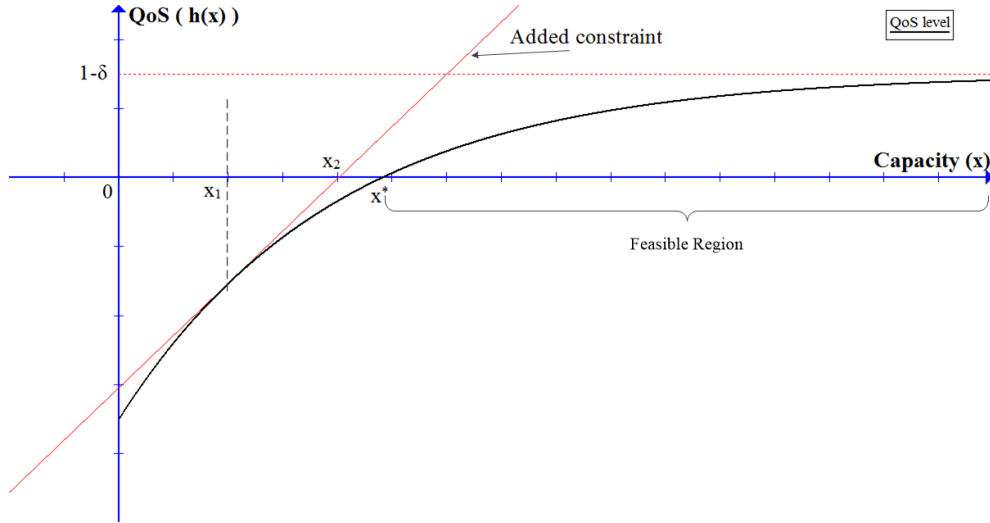
Figure 4.5: Illustration of the cutting plane method in a single dimension

We describe how linear constraints are added whenever one or more of the QoS constraints are violated. For clarification, we describe how the CPM works in one dimension as shown in Figure 4.5. Denote the solution of the relaxed problem by x_1. When $h(x_1)$ is evaluated, it is found that the constraints are violated since the value of $h(x_1)$ is less than zero. We define the added linear constraint as the tangent to the QoS function at x_1, which cuts the feasible region of the relaxed problem at x_2. The (wrong) solution x_1 is outside the feasible region after adding the linear constraint, while the optimal solution x^* is still within the new feasible region. The algorithm will run again at x_2, and the feasible region will continue shrinking until the algorithm reaches the feasible optimal solution x^*. From Figure 4.5, it is clear why the concavity assumption is essential for the CPM to work. If $h(x)$ were a convex function, the added constraint would cut the feasible region of the original problem, which can lead the algorithm to reach a sub-optimal or even infeasible solution.

Determining x^* in this example can be done using simple iteration algorithms. However, for a multi-dimensional QoS functions (as in our problem), such algorithms are computationally inefficient. For the multi-dimensional case, since $h_i(\mathbf{x})$ is assumed concave, then:

$$h_i(\mathbf{x}) - h_i(\mathbf{x}_r) \leqslant \mathbf{q}_i(\mathbf{x}_r) \cdot (\mathbf{x} - \mathbf{x}_r), \qquad (4.14)$$

where $\mathbf{q}_i(\mathbf{x})$ is the gradient of $h_i(\mathbf{x})$ at point $\mathbf{x}$. If we add the following linear constraint to the relaxed problem:

37

$$h_i(\mathbf{x}_r) + \mathbf{q}_i(\mathbf{x}_r) \cdot (\mathbf{x} - \mathbf{x}_r) \geqslant 0 \tag{4.15}$$

then we guarantee that the infeasible solution $\mathbf{x}_r$ is excluded, since $h_i(\mathbf{x}_r) < 0$. Also, this constraint will not affect the feasible region of the original problem **P1**, because at any feasible point $\{\mathbf{x} : h_i(\mathbf{x}) \geqslant 0\}$, the added constraint in (4.15) is not violated (using inequality (4.14)). Therefore, the constraint defined in (4.15) can be used to cut the feasible region of the relaxed problem **P2**.

Before evaluating the QoS performance with either analytical or simulation methods, the rules for real-time scheduling of different demand blocks must be defined. In the capacity planning phase, we define the allocated capacity of demand blocks for each class at each time slot. However, the allocated capacity for some classes may not be fully utilized in real-time. Therefore, we need to develop a rule for utilizing the leftover capacity to serve other classes of demand blocks. First, the duration of the accepted demand blocks should not exceed the duration of the allocated capacity. Given this condition, we use the following heuristic. We prioritize demand blocks according to the shortest deadline. If two demand blocks have the same deadline, they are prioritized according to the longer duration. The proposed optimization algorithm is summarized in Algorithm 2.

Sample Average Approximation

It is difficult to evaluate the performance of a multi-class, non-stationary queueing system using analytical methods. Therefore, we use simulation to generate samples of demand block arrivals and use the sample average approximation (SAA) to approximate the values of $h_i(\mathbf{x})$. For each simulation run (day) j, a total number, N_j^i, of demand blocks of type i are generated. Let S_j^i denote the fraction of N_j^i that are satisfied within their deadlines. Both S^i and N^i are random variables. The approximation is done by replacing $h_i(\mathbf{x})$ by $\bar{h}_i(\mathbf{x}, m)$ as follows:

$$h_i(\mathbf{x}) \approx \frac{\sum_{j=1}^m S_j^i}{\sum_{j=1}^m N_j^i} - \delta \triangleq \bar{h}_i(\mathbf{x}, m) \tag{4.16}$$

Notice that $\bar{h}_i(\mathbf{x}, m)$ is also a random variable. The optimization problem **P1** will be updated to **P3** as follows:

$$\mathbf{P3}: \quad \min_{x} \left\{ \sum_{i} \sum_{t} c_{it} x_{it} \right\}$$
$$\text{s.t. } \mathbf{Ax} \leqslant \mathbf{L^{max}} \tag{4.17}$$
$$\bar{h}_i(\mathbf{x}, m) \geqslant 0 \qquad \forall i \in \mathcal{Q}$$
$$\mathbf{x} \in \mathbb{N}^{T \times Q}$$

Let X denotes the feasible set of problem **P1**, while X^* and X_m^* denote the set of optimal solutions to **P1** and **P3** respectively. Assume $\mathbf{x_m} \in X_m^*$. The solution $\mathbf{x_m}$ will have the following properties: 1) it satisfies the original linear set of constraints (power capacity constraints), 2) it is "possible" that $\mathbf{x_m}$ violates the QoS constraints, i.e. $\exists i \in \mathcal{Q}:$ $h_i(\mathbf{x_m}) < 0$, and 3) it is "possible" that $\mathbf{x_m}$ to be a suboptimal solution. For SAA to be justified, we need to prove that $X_m^* \subseteq X^*$ almost surely as $m \to \infty$, which is addressed in the following theorem:

Theorem 4.1. *If there exist at least one feasible solution to problem **P1** (i.e. X is non-empty), then $\mathbf{x}_m$ is feasible almost surely as $m \to \infty$ (i.e. $X_m^* \subseteq X$). Furthermore, if there exist at least one optimal solution such that $h_i(\mathbf{x}) > 0, \forall i \in \mathcal{Q}$, then $\mathbf{x}_m$ is also optimal almost surely as $m \to \infty$.*

Proof. See Appendix B. □

Algorithm 2: The optimization algorithm

   Input : Day ahead electricity price profile $\gamma(t)$, arrival processes of demand
                blocks of different classes

1 Solve the relaxed problem (**P2**) defined in (4.13). The relaxed solution vector is
   denoted by $\mathbf{x}_r^*$.
2 Identify the set of violated constraints $\mathcal{V} = \{i : h_i(\mathbf{x}_r^*) < 0, \ i \in 1, \ldots, N_q\}$
3 **while** $\mathcal{V}$ *is non-empty* **do**
4   **for** $i \in \mathcal{V}$ **do**
5   Update problem **P2** by adding a linear constraint to it using (4.15)
6   **end**
7   Solve problem **P2**. Update $\mathbf{x}_r^*$
8   Update $\mathcal{V}$
9 **end**
10 The optimal capacity allocation vector will be given by $\mathbf{x}^* = \mathbf{x}_r^*$.
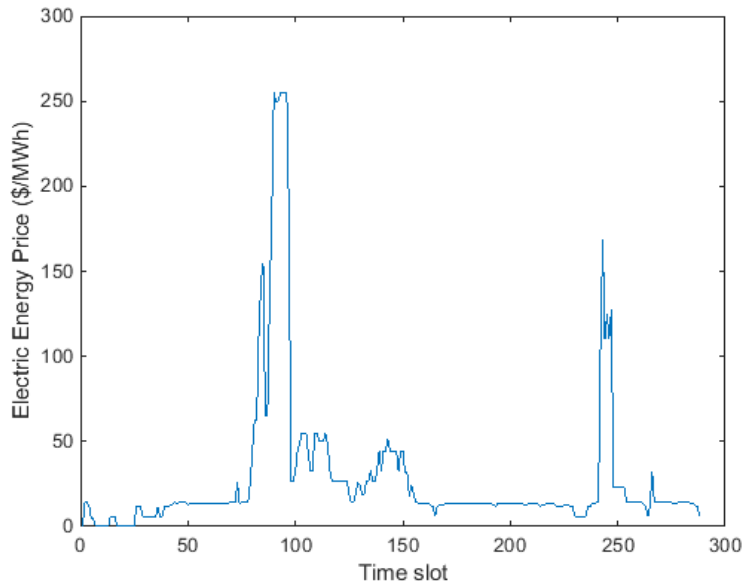
Figure 4.6: Ontario's electricity market clearance profile for 12th of June, 2015. The profile is considered in our study as the profile of the day-ahead electricity price.

4.4 Numerical results

4.4.1 Raw Data

We attempt to utilize data for the electricity price and the residential demand as close to reality as possible. For the day-ahead electricity pricing, we select an Ontario's electricity market clearance profile of a random day, as shown in Figure 4.6.

The data collected for the residential demand should be an appliance-level with a temporal resolution of at least 5 minutes. The power drawn by an appliance when it is turned-on can usually be easily deduced or given in the appliance's data sheet. However, the consumer's behavior towards using this appliance cannot be easily deduced. The same appliance can be used differently by different consumers. Therefore, a statistical, appliance-level demand data should be collected by monitoring each appliance for a large number of consumers. Unfortunately, such data is not abundant, since the concern of the operators and planners of power networks is the aggregated demand of many consumers, not the appliance-level demand. Nevertheless, there exists a study by [54] which recorded the appliance-level residential demand for a period of almost two years (2012-2014), with three

Table 4.1: Non-controllable appliances' parameters (extracted from measurements in [54])

Appliance	Power level (kW)	Turn-on probability	Duration Distribution
TV	0.1	0.07	Exponential(12)
Lighting	0.5	5.6×10^{-4}	Exponential (4)
Kettle	2	0.0013	Fixed (1)

different temporal resolutions (6 seconds, 1 second, and 62.5 µs !). However, the study is for a small number of consumers (4 consumers only). Our approach is to use the demand data of one of these consumer to represent the demand behavior of all the consumers in our system. While this is not a realistic approach, it is the best we can do given the available measurements.

The data of the first consumer considered by [54] consists of the measurements of 52 different appliances. For simplicity, we consider only the appliances of significant energy demand. We also consider the 6-seconds resolution version of the data, which exceeds our minimum resolution requirement (5 minutes). The appliances which we will consider in our study are discussed in the following.

Non-controllable appliances

We consider three non-controllable appliances having significant energy consumption, which are TV, the kettle and the lighting circuit. Both TV and the lighting circuit can be used when the consumer is in the inactive mode, while the kettle can be used when the consumer is in the active mode. From the measurement data, we extract the parameters shown in Table 4.1. The parameters include the appliances' power rating, the probability that an appliance is turned on at any given time slot, and the approximating distribution of their power consumption duration (with its mean given between brackets in units of time slots).

Deferrable appliances

We consider two appliances whose demand can be deferred without interruption which are the washing machine and the dish washer. The appliances' turn-on probabilities are 0.0024 and 0.001, respectively. The profiles of their power consumption when they are turned-on are illustrated in Figure 4.7.
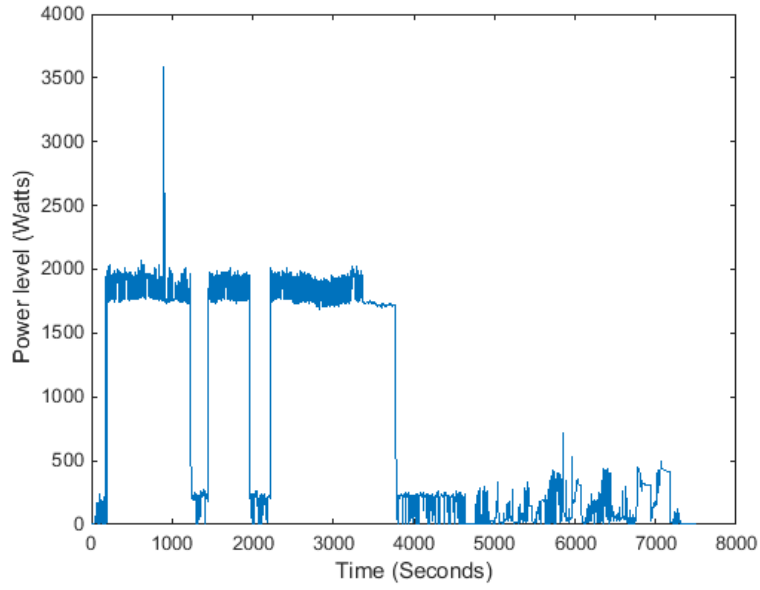
(a)
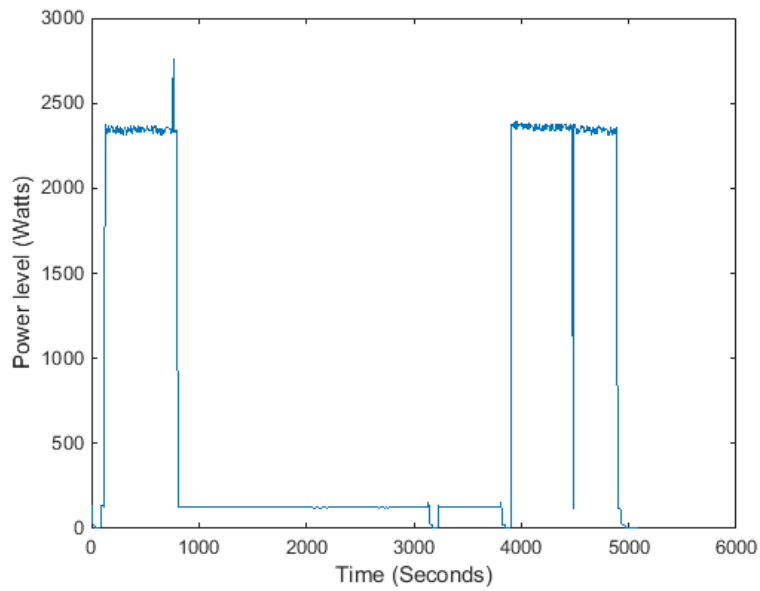
(b)

Figure 4.7: Task profiles for (a) the washing machine and (b) the dish washer. Data extracted from [54].

Table 4.2: TCL appliances' parameters

Appliance	Power level (kW)	R_{th} (°C/kW)	C_{th} (kJ/°C)	θ_e (°C)	Setting point (°C)	Dead band (°C)
Fridge [46]	0.2	100	2880	20	4	0.25
A/C [17]	5	2.5	9000	30	20	1

TCL appliances

The measurements include two TCL appliances, the fridge and the A/C system. However, it is difficult to deduce different TCL parameters from the power measurements alone. Hence, we use TCL parameters from other studies as shown in Table 4.2.

Demand Diversity

The aforementioned extracted parameters reflect the energy consumption behavior of a single consumer only. Due to the limited available measurements for other consumers, we make use of the extracted parameters to represent the demand of a large number of consumers (1000). We diversify the demand by altering these parameters randomly from a consumer to another. Details about demand diversity can be found in Appendix A.

4.4.2   Simulation Results

We first study effects of the uncoordinated cost minimization, i.e. when each consumer minimizes its own energy consumption cost, disregarding the capacity of the distribution transformer (such as 600 kW). Aggregated load profiles for all consumers before and after implementing demand response are shown in Figures 4.8 and 4.9, respectively. It is clear from Figure 4.9 that the power consumption of the controllable loads is concentrated at specific time periods, where the electricity price is minimal. However, since there is no coordination among consumers, the power consumption exceeds from time to time the capacity of the distribution transformer. Therefore, it is beneficial to use our optimization framework to avoid transformer overloading.
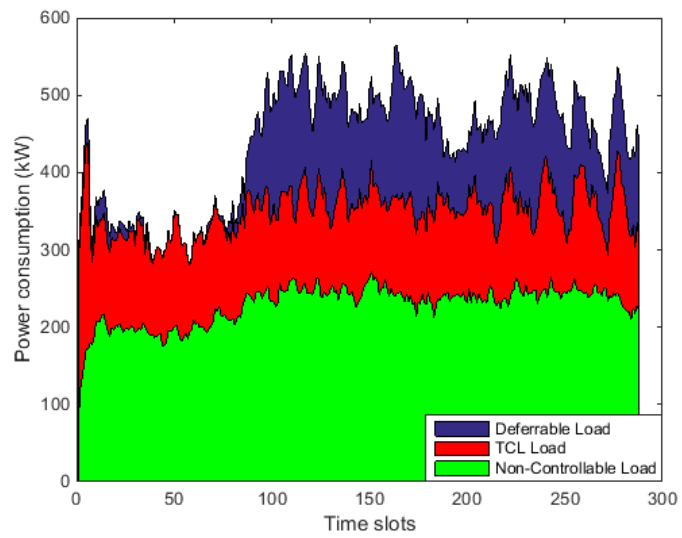
Figure 4.8: Aggregated demand profiles for controllable and non-controllable loads without implementing demand response

44
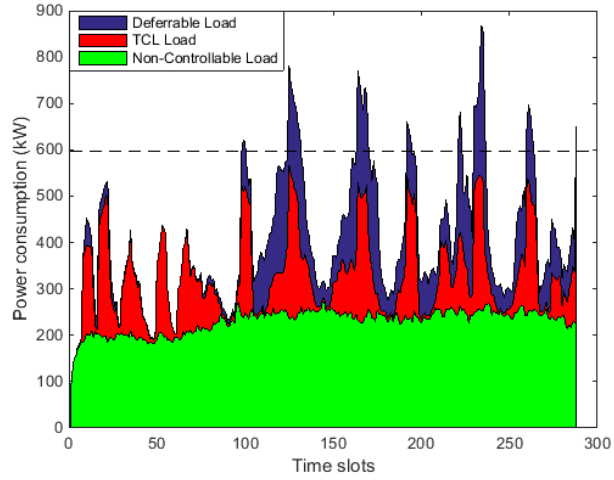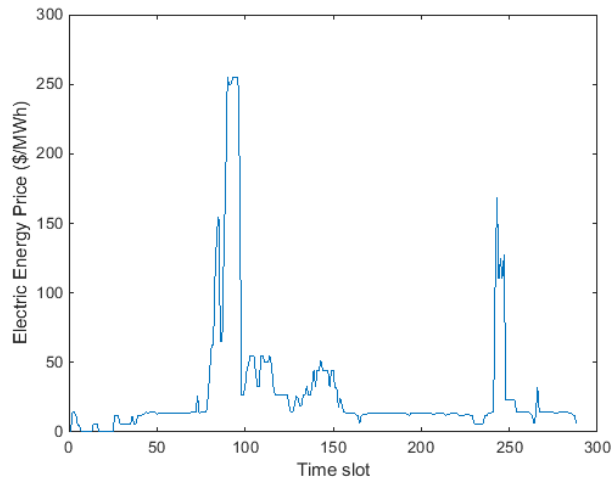
Figure 4.9: (a) Aggregated demand profiles for controllable and non-controllable loads after implementing an uncoordinated demand response (b) Electricity price profile. Note that the controllable power consumption is high whenever the electricity price is low and vice versa.

45
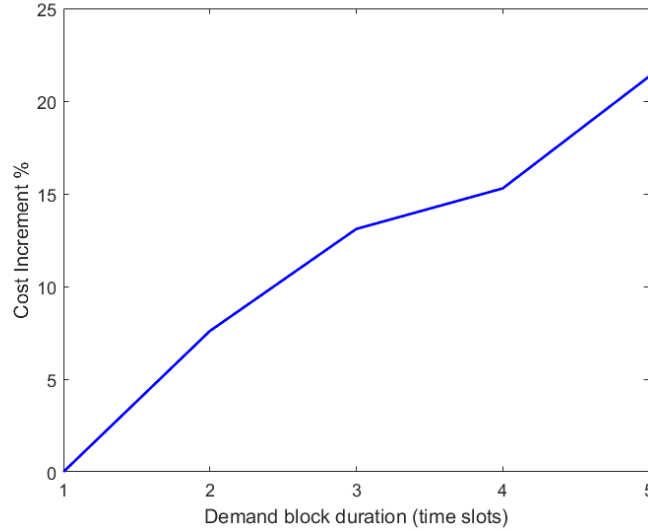
Figure 4.10: The percentage of the increase of energy consumption cost due to assuming a perfectly flexible demand (cost increment). The result is plotted as the duration of the demand block is increased while keeping the mean energy rate constant.

We show why it is better to consider the duration of appliances' power consumption in determining optimal power allocation. Consider a single queue of demand blocks of power consumption level of one unit and a deadline of 10 time slots. We solve the optimization problem assuming the perfectly flexible case, when the demand block duration is one time slot. The resulting solution is verified for different demand block durations but of a constant mean energy rate. This means that as the duration of the demand block is increased, its mean arrival rate decreases by exactly the same amount. The cost increments due to ignoring demand block durations are plotted in Figure 4.10. As we can see, cost increment becomes more significant as the duration of the demand blocks increases. The obtained results largely depend on the price profile used and/or the profile of the power capacity headroom. In general, ignoring the demand duration can cause the solution to be far from optimal when the aforementioned profiles are highly fluctuating.

Table 4.3: Parameters of demand classes considered

Class #	Power level (W)	Duration (Time slots)	Deadline (Time slots)
1	2000	17	12
2	2000	13	12
3	7000	6	14
4	200	28	6

Consider a set of demand classes such that their parameters are close to the characteristics of the input appliances. The parameters are listed in Table 4.3. The CPM is used for optimal allocation of different demand block capacities. The total allocated power profile is illustrated in Figure 4.11 and the actual power consumption profile after implementing DR is illustrated in Figure 4.12.
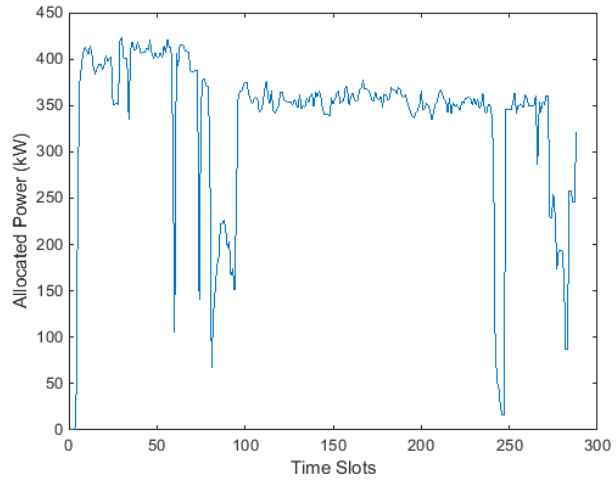
(a)
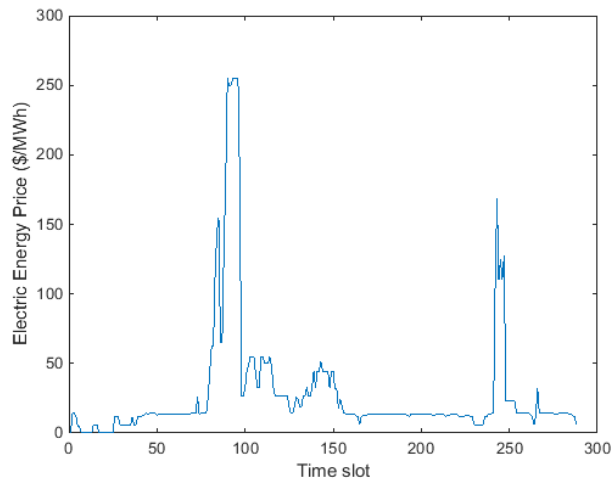
(b)

Figure 4.11: (a) Allocated power profile (b) Electricity price profile. We notice that power is allocated such that power consumption is reduced during the two major price peaks.
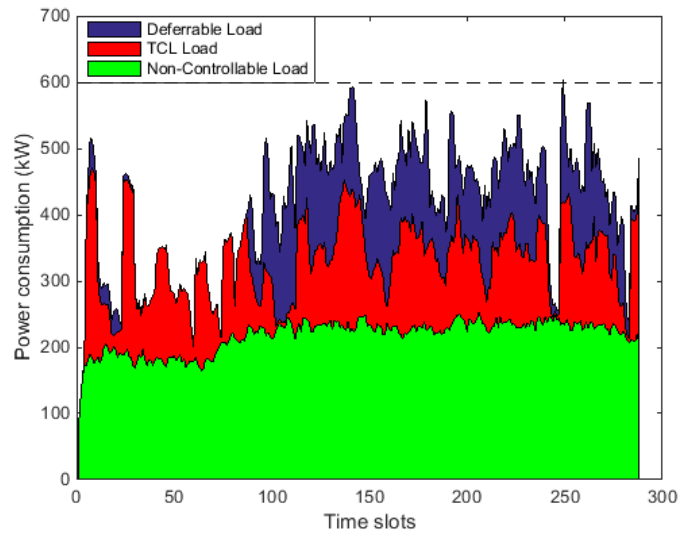
Figure 4.12: Aggregated demand profiles for controllable and non-controllable loads after implementing a coordinated demand response. Notice that the aggregated power consumption does not exceed the capacity of the distribution transformer.
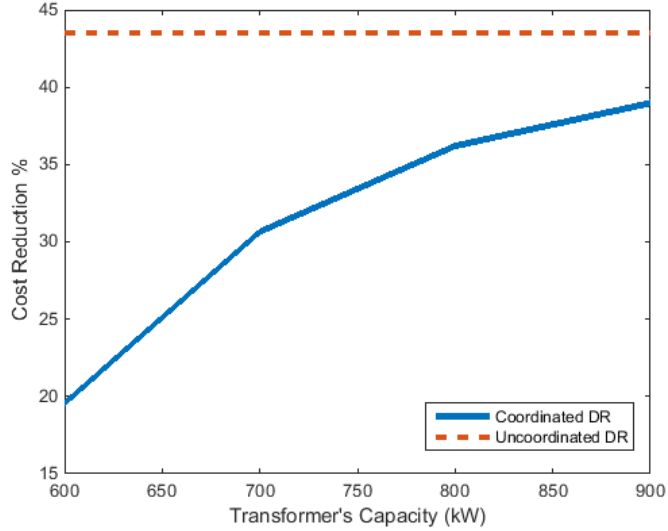
Figure 4.13: Energy consumption cost reduction as a percentage of the energy cost without applying DR.

Finally, we need to evaluate the performance of the proposed demand management framework. Our performance metric is the amount of energy cost reduction due to applying DR. The best possible demand reduction corresponds to the case of the uncoordinated DR. We plot the amount of demand reduction as the capacity constraint is gradually relaxed, as illustrated in Figure 4.13. It is observed that, as the capacity constraint becomes practically ineffective (at 900 kW), the achievable demand reduction (39%) is close to the ideal one (43%).

4.5   Summary

This chapter is concerned with managing a large number of residential appliances to minimize the cost of their energy consumption, given a time-dependent electricity price. Existing studies related to residential demand management suffer from three shortcomings: 1) an increasing computational complexity when the number of controllable appliances increases, 2) inter-temporal demand dependence is not considered, and 3) no aggregation model available for heterogeneous TCL appliances. Therefore, we proposed a novel demand aggregation model where residential demand is classified according to three parameters, power level, duration, and deadline for satisfying the demand. We showed how any TCL

appliance can be treated as a deferrable load, and accordingly can be assigned to the proper class of demand. The proposed algorithm for demand scheduling is an offline algorithm based on the *cutting-plane method*, which was effective in mitigating the complexity introduced by delay QoS constraints. The numerical results were based on realistic data, and the performance of our methodology approaches the ideal performance of uncoordinated demand as the capacity of the distribution transformer increases.

Chapter 5

Large-Scale Integration of Renewable Energy Sources

5.1   Problem definition

The continuous growth of the electric energy demand is inevitable due to the growing world population. This fact sparks worries about the environmental impacts of the required electric energy production. Traditional thermal generators produce a large amount of harmful gases as a result of the combustion of fossil fuel used in the energy generation. These gases have a negative impact on the environment, such as the formation of acidic rain and resulting in a global climate change [55, 56]. The environmental concerns are the main motivation for using renewable energy sources (RES)s, such as wind and solar energies, as alternative sources to fossil fuel for the production of electric energy. Due to their crucial advantages, RESs are considered one of the major pillars for smart grids, which are expected to increase the deployment of RESs in large scales.

Although utilizing RESs is not a new idea, there are several challenges for integrating them in existing power networks in terms of grid stability and power system operations [57, 58, 59]. The latter's challenges are attributed to output power fluctuations from wind turbines or photovoltaic cells. These fluctuations are characterized by being stochastic, making the generation non-dispatchable, which leads to two major operational concerns. First, large fluctuations may result in a supply-demand imbalance which can contribute to a high area control error [60, 61]. The second concern is to provide adequate reserves to accommodate the uncertainties in the net demand, i.e., the remaining demand after

reducing the portion satisfied by the RESs. High uncertainties implies more reserves to be purchased [62, 63], which can lead to a significant increase in the cost of operations.

Many research studies were made to smooth power fluctuations resulting from RES integration, which can be classified into two major approaches. The first approach is to deploy an electric energy storage element, which stores a part of the RES energy when the RES output power is high. The stored energy is then released at periods of low RES power production [64, 65]. However, existing storage technologies suffer some difficulties to be implemented on large scales [66]; For example, the technology of pumped hydro storage needs special site requirements to be implemented. Battery energy storage suffers from low energy densities and short lifetimes [67]. Besides, deploying storage systems requires additional installation and operational costs [68].

The second approach is to use DR to modify electric energy demand in a way that helps in smoothing power fluctuations. The majority of the existing solutions are based on resource management (optimization) frameworks, in which demand modification is the resource to be dispatched. Reducing power fluctuations can appear explicitly in the objective function [69, 70], or implicitly by assuming a convex cost function of the aggregated power profile [71, 72]. Existing studies allocate different types of demands in an offline manner based on the forecast of the RES output power. However, the forecast might not be accurate, especially for long time horizons. Also, offline scheduling is not suitable for managing residential appliances, because it is hard to predict when a consumer will exactly need to turn an appliance on. Finally, demand allocation decisions are usually the solution of a mixed-integer linear programming (MILP) problem, which becomes computationally difficult as the number of demands to be allocated increases.

Given the aforementioned limitations, our objective for this research problem is to propose a suitable methodology for smoothing power fluctuations resulting from RES integration, using the DR of a large number of residential appliances. In this case, the MG in Figure 3.1 is assumed to be in the island mode, where the energy is supplied only by the set of DGs. Unlike the main grid, the DGs cannot satisfy a highly fluctuating demand because of their limited ramping rate. Hence, a demand smoothing methodology is essential for proper MG operation.

5.2   Solution methodology

We use the same methodology for appliances' scheduling similar to what we used for solving problem 1, which is composed of two main steps: 1) classifying demands into a predefined
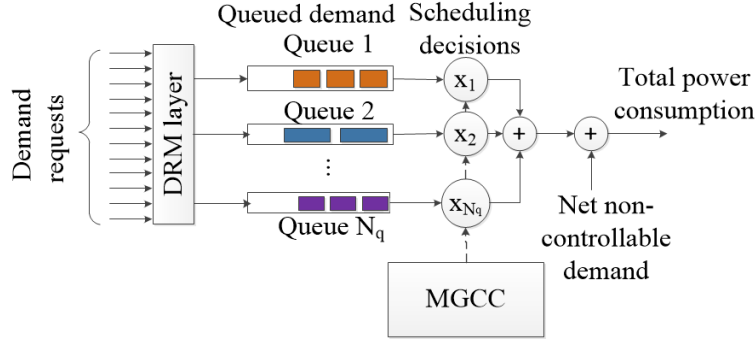
Figure 5.1: Demand scheduling methodology for research problem 2. Unlike problem 1, the scheduling objective is to regulate a stochastic signal which is the net non-controllable demand.

set of classes (mapping algorithm), and 2) deducing a proper scheduling policy for these classes of demand (optimization algorithm). The methodology is depicted in Figure 5.1.

The same mapping algorithm (Algorithm 1) can be used, but we need to develop a new optimization algorithm. In our previous research problem the main control signal, which is the electricity price profile, is deterministic. In the current problem, however, the main control signal (the aggregated non-controllable profile) is stochastic. Applying algorithm 2 using the mean profile as a deterministic signal is an inefficient approach; For example, assume the stochastic profile is i.i.d., then the mean profile will be flat, accordingly demand scheduling will be useless. Thus we need to develop a new optimization algorithm which runs online, such that decisions are made based on the actual recent data, instead of an offline algorithm as Algorithm 2.

5.3 Solution algorithm

We use Lyapunov optimization [73, 74, 36] to schedule demand requests. Each queue $i \in \mathcal{Q}$ is updated according to

$$Q_i(t+1) = [Q_i(t) - x_i(t)]^+ + a_i(t), \tag{5.1}$$

where $Q_i(t)$, $x_i(t)$, and $a_i(t)$ are the deferred, scheduled and newly arrived demands of class i at time slot t, respectively. The function $[x]^+$ is defined as $max\{x, 0\}$. The set $\{x_i(t)\}$ represents the decision variables of our problem, whereas $\{a_i(t)\}$ is a set of exogenous variables which we have no control over them.

In order to take consumers' comfort into consideration, one can set different limits (constraints) on the length of each queue, i.e., $Q_i(t) \leqslant Q_i^{max}$. However, this approach just provides a soft deadline guarantee, i.e., there can be a non-zero probability that a demand request waits beyond the deadline. In order to provide a hard deadline guarantee, we follow the same approach as in [36], where we introduce a set of virtual queues, each is associated with one of the real queues. The virtual queues are updated as follows:

$$Z_i(t+1) = [Z_i(t) - x_i(t) + \epsilon_i \mathbb{1}_{\{Q_i(t)>0\}}]^+, \tag{5.2}$$

where $\epsilon_i \geqslant \mathbb{E}\{a_i(t)\}$ is a positive constant, and $\mathbb{1}_{\{.\}}$ is an indicator function that equals one when the condition between the braces is satisfied and zero otherwise. By setting different limits on these virtual queues such that $Z_i(t) \leqslant Z_i^{max}$, the maximum waiting time for a request in queue i is given by [36]:

$$D_i^{max} = \lceil (Q_i^{max} + Z_i^{max})/\epsilon_i \rceil. \tag{5.3}$$

On the other hand, the variables $\{x_i(t)\}$ should be controlled dynamically to reduce the fluctuations imposed by the non-controllable net demand profile $r(t)$. Our measure for these fluctuations is the time average of the second moment of the total power consumption:

$$\bar{c} \triangleq \lim_{T \to \infty} \frac{1}{T} \sum_{t=0}^{T-1} \mathbb{E}\left\{ \left(r(t) + \sum_{i=1}^{N_q} x_i(t) \right)^2 \right\}.$$

Hence, our goal is to minimize $\bar{c}$. We will first propose an algorithm for scheduling the controllable demands $\{x_i(t)\}$. Afterwards, the performance of the proposed algorithm will be addressed by Theorems 1 and 2. Our proposed algorithm is described in Algorithm 3. The algorithm needs a set of positive constants $\{V; w_i, \quad \forall i \in \mathcal{Q}\}$ as an input, which we will latter describe their effect on the performance of Algorithm 3. The algorithm is online, where scheduling decisions are made based on the current realization of the input stochastic processes $\{r(t); a_i(t), \quad \forall i \in \mathcal{Q}\}$ and on the system's history demonstrated in the variables $\{Q_i(t), Z_i(t), \quad \forall i \in \mathcal{Q}\}$. The algorithm does not need any form of prediction for the stochastic processes $\{r(t); a_i(t), \quad \forall i \in \mathcal{Q}\}$.

Next, the performance of Algorithm 3 is described by Theorems 1 and 2, which will be defined shortly. The first theorem is related to the long-term *average* behavior of the cost function, while the second theorem is related to the short-term *sample path* behavior of the cost function.

Algorithm 3: Demand scheduling algorithm for research problem 2

Input : $V; w_i, \quad \forall i \in \mathcal{Q}$

1 for $t \in 0, 1, 2, \ldots$ **do**

2   Measure/read the following variables: $r(t), Q_i(t), Z_i(t), \quad \forall i \in \mathcal{Q}$

3   Calculate the total optimal scheduling energy $x_s(t)$ by the following equation:

$$x_s(t) \triangleq \sum_{i=1}^{N_q} x_i(t) = \frac{\sum_{i=1}^{N_q} w_i \left[Q_i(t) + Z_i(t)\right]}{2N_q V} - r(t). \qquad (5.4)$$

4   First individual energy allocation is given by
    $x_i(t) = \min\{x_s(t)/N_q, Q_i(t)\}, \quad \forall i \in \mathcal{Q}.$

5   Distribute the remaining energy $x_r(t) = x_s(t) - \sum_{i=1}^{N_q} x_i(t)$ among queues
    arbitrarily wherever possible.

6   Update $Q_i(t+1)$ according to eq. 5.1, and $Z_i(t+1)$ according to eq. 5.2,
    $\forall i \in \mathcal{Q}.$

7 end

We begin by setting a benchmark for performance comparison, c^*. For the long-term behavior, we define c^* as the infimum of the solution of the following stochastic optimization problem:

$$
\begin{aligned}
\mathbf{P1}: \quad &\min_{x_i, \forall i \in Q} \bar{c} \\
&\text{s.t. eq.}(5.1) \\
&\bar{Q}_i \triangleq \lim_{T \to \infty} \frac{1}{T} \sum_{t=0}^{T-1} \mathbb{E}\{Q_i(t)\} < \infty, \forall i \in \mathcal{Q},
\end{aligned}
\qquad (5.5)
$$

where $\bar{Q}_i$ is the time average of the mean length of queue i. Problem **P1** represents an extreme case when consumers are willing to wait as long as it takes to achieve the best possible performance, c^*. Practically, residential consumers will set deadlines for scheduling their demand requests, e.g., as in eq.(4.5). The long-term performance of Algorithm 3 is described in the following theorem:

Theorem 5.1. *Assuming all queues are initially empty, $Q_i(0) = 0$ and $Z_i(0) = 0, \forall i \in \mathcal{Q}$, and assuming system inputs $\boldsymbol{\omega}(t) = \{r(t); a_i(t), \quad \forall i \in \mathcal{Q}\}$ are i.i.d. and bounded, then applying the Algorithm 3 yields the following results:*

1) *All queues, both real and virtual, are upper bounded by Q_i^{max} and Z_i^{max}, defined by:*

$$Q_i^{max} \triangleq \frac{2N_q V}{w_i} \left\{ N_q a_i^{max} + r^{max} \right\} + a_i^{max}$$

and

$$Z_i^{max} \triangleq \frac{2N_q V}{w_i} \left\{ N_q \epsilon_i + r^{max} \right\} + \epsilon_i$$

2) *The finite time horizon average cost satisfies:*

$$\frac{1}{T} \sum_{i=1}^{T-1} \mathbb{E} \left\{ \left(r(t) + \sum_{i=1}^{N_q} x_i(t) \right)^2 \right\} \leqslant c^* + B/V,$$

where B is a constant given by:

$$B \triangleq \sum_{i=1}^{N_q} w_i \left[\frac{(x_i^{max})^2 + (a_i^{max})^2}{2} + \frac{\max\left[\epsilon_i^2, (x_i^{max})^2\right]}{2} \right]. \qquad (5.6)$$

Proof. See Appendix C. □

Theorem 5.1 describes the long-term average performance. We will now describe the performance of Algorithm 3 from a sample path perspective. We should first find another measure for performance comparison, other than c^*. We follow a sample path comparison, in which we assume that inputs $\{r(t); a_i(t), \forall i \in \mathcal{Q}\}$ are given in advance for a finite time horizon T. We use this information to define the following deterministic optimization problem:

$$\mathbf{P2}: \quad \min_{x_i, \forall i \in Q} c_k \triangleq \frac{1}{T} \sum_{t=kT}^{kT+T-1} \left(r(t) + \sum_{i=1}^{N_q} x_i(t) \right)^2$$

$$\text{s.t. eq.}(5.1)$$

$$\sum_{t=kT}^{kT+T-1} [x_i(t) - a_i(t)] \geqslant 0, \forall i \in \mathcal{Q} \quad (5.7)$$

$$\sum_{t=kT}^{kT+T-1} [x_i(t) - \epsilon_i] \geqslant 0, \forall i \in \mathcal{Q}.$$

We here divided the infinite time horizon into a series of frames, each of length T, where the scheduling cost of frame k is given by c_k. Hence, our new comparison benchmark will be the optimal solution of problem $\mathbf{P2}$. Assume we run Algorithm 3 for a number of K frames, then the sample path performance is given by the following theorem:

Theorem 5.2. *Assuming all queues are initially empty, $Q_i(0) = 0$ and $Z_i(0) = 0, \forall i \in \mathcal{Q}$, then applying Algorithm 3 for a number of K frames yields the following sample-path result:*

$$\frac{1}{KT} \sum_{t=0}^{KT-1} \left(r(t) + \sum_{i=1}^{N_q} x_i(t) \right)^2 \leqslant \frac{1}{K} \sum_{k=0}^{K-1} c_k^* + BT/V$$

Proof. See Appendix D.

$\square$

5.4   Numerical results

5.4.1   Raw Data

For demand generation, we use the same data that were used in problem 1. However, this time the residential consumers are allowed to use RESs, which satisfy part of their energy demands and introduce fluctuations to their aggregated demand profile. We assume a single type of RES which is wind energy. The correlated portion P_0 is generated from a wind speed data extracted from [75] of one-minute temporal resolution. The wind turbine model used is a medium sized (11 kW) wind turbine described in [76]. RES power is
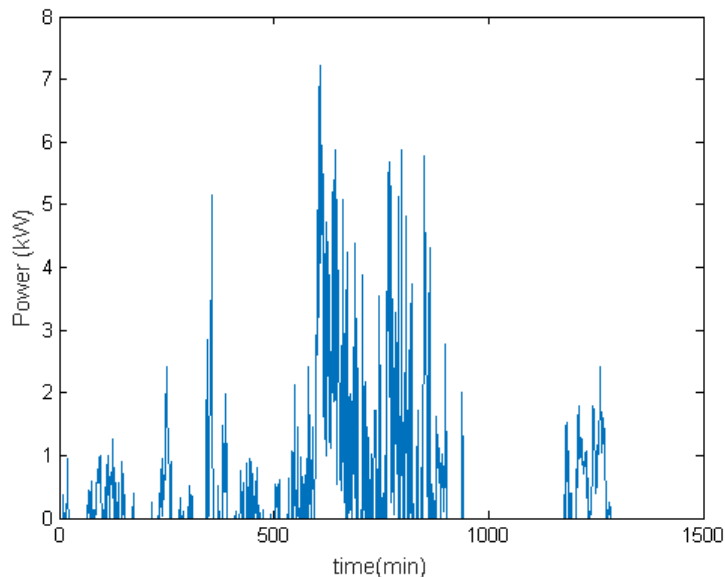
Figure 5.2: Random sample for an RES power production of a single consumer.

simulated by feeding wind speed data to the power-wind curve in [76]. The uncorrelated portion P_i^u is uniformly distributed of the same mean as P_0. The weighting factor α is taken to be 0.9. A sample of an RES power profile of a single consumer is shown in Figure 5.2. As a result of RES integration, a large magnitude of rapid fluctuations is introduced to the aggregated non-controllable demand (Figure 5.3).

5.4.2   Performance Evaluation

The objective of Algorithm 3 is to minimize the fluctuations in the aggregated demand profile of all consumers. The impact of these fluctuations in our problem is addressed as follows. Due to the non-zero ramping time of the DGs, they can only supply the slowly fluctuating portion of the demand. Any supply-demand mismatch is covered by purchasing expensive ancillary services (AS). To account for both regulation-up (AS that are available to increase output power) and regulation-down (AS that are available to decrease output power), we assume that their cost is a quadratic function of the mismatch. We decompose the total aggregated demand profile into two profiles: 1) the demand supplied directly by the DGs, 2) the mismatch purchased from the AS market. For simplicity, we calculate the first profile as the moving average of the original profile with a window size same as the

59
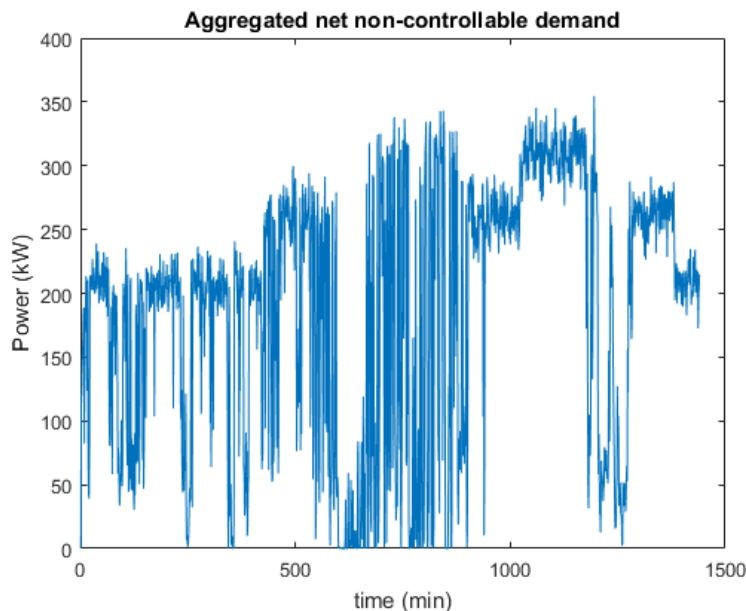
Figure 5.3: Aggregated net non-controllable demand assuming a large-scale integration of RESs.

generator's ramping time Ψ. Hence, the first profile represents a smoothed version of the original profile. The mismatch profile is simply calculated by taking the difference between the original profile and its smoothed version as illustrated in Figure 5.4.

Several total demand profiles under our proposed methodology are depicted in Figure 5.5. For simplicity, we assumed a single class of controllable demands. From Figure 5.5, it is clear that the fluctuations are reduced as the demand scheduling deadline increases.

We compare our proposed methodology to a simple naive policy, where controllable demand is scheduled such that the total aggregated demand profile tracks the average total demand. Whenever a demand request reaches the deadline, it has to be scheduled immediately (forced scheduling). The policy is naive since it attempts to flatten the total demand profile without taking into consideration the penalty of forced scheduling. Our performance measure is the relative cost of AS purchase which is the ratio between the cost under DR and without DR (no delay). For simplicity, we consider a single class of controllable demand. Figure 5.6 plots the relative cost versus deadline for four different cases: 1) our methodology (Lyapunov), 2) naive policy assuming perfect time average prediction (naive), 3) naive policy assuming $+20\%$ error in time average prediction (naive $+20\%$), and 4) naive policy assuming -20% error in time average prediction (naive -20%). Such prediction errors are common due to the high uncertainties of the RES power production. As
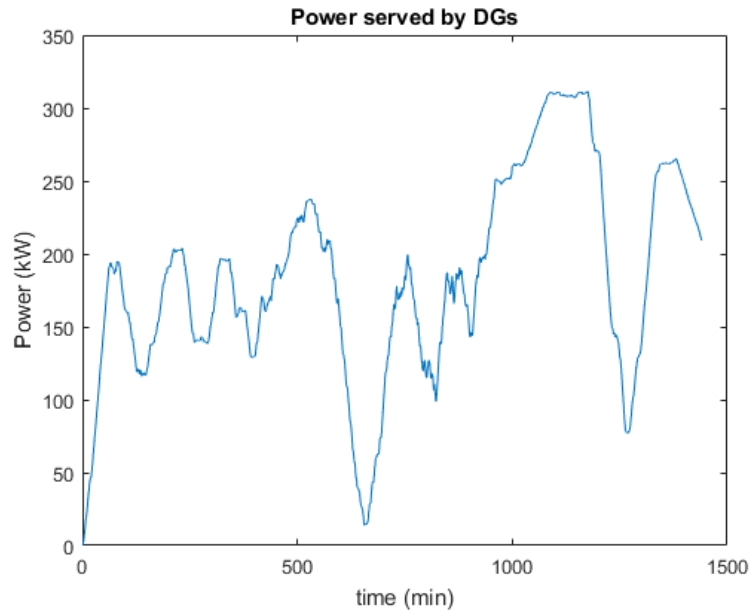
(a)
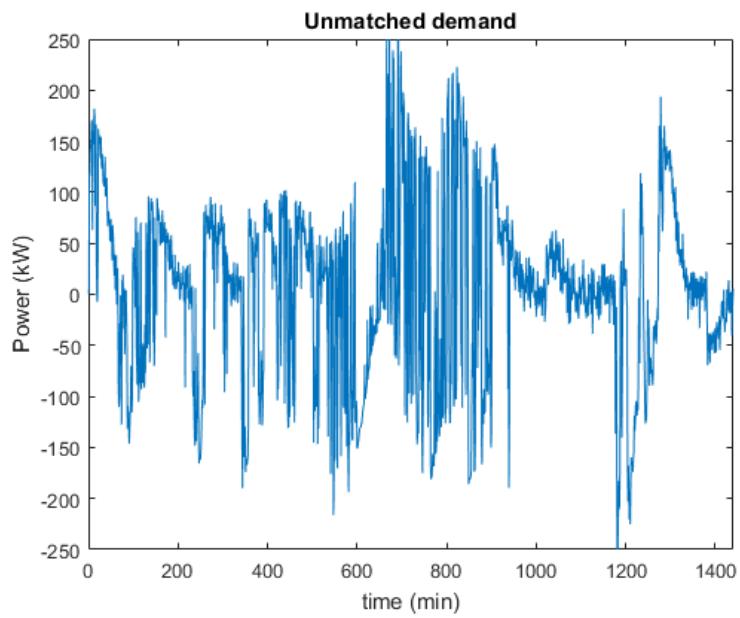
(b)

Figure 5.4: Decomposing demand profile in Figure 5.3 into: (a) a smoothed profile and (b) an unmatched demand profile ($\Psi = 60$).

61
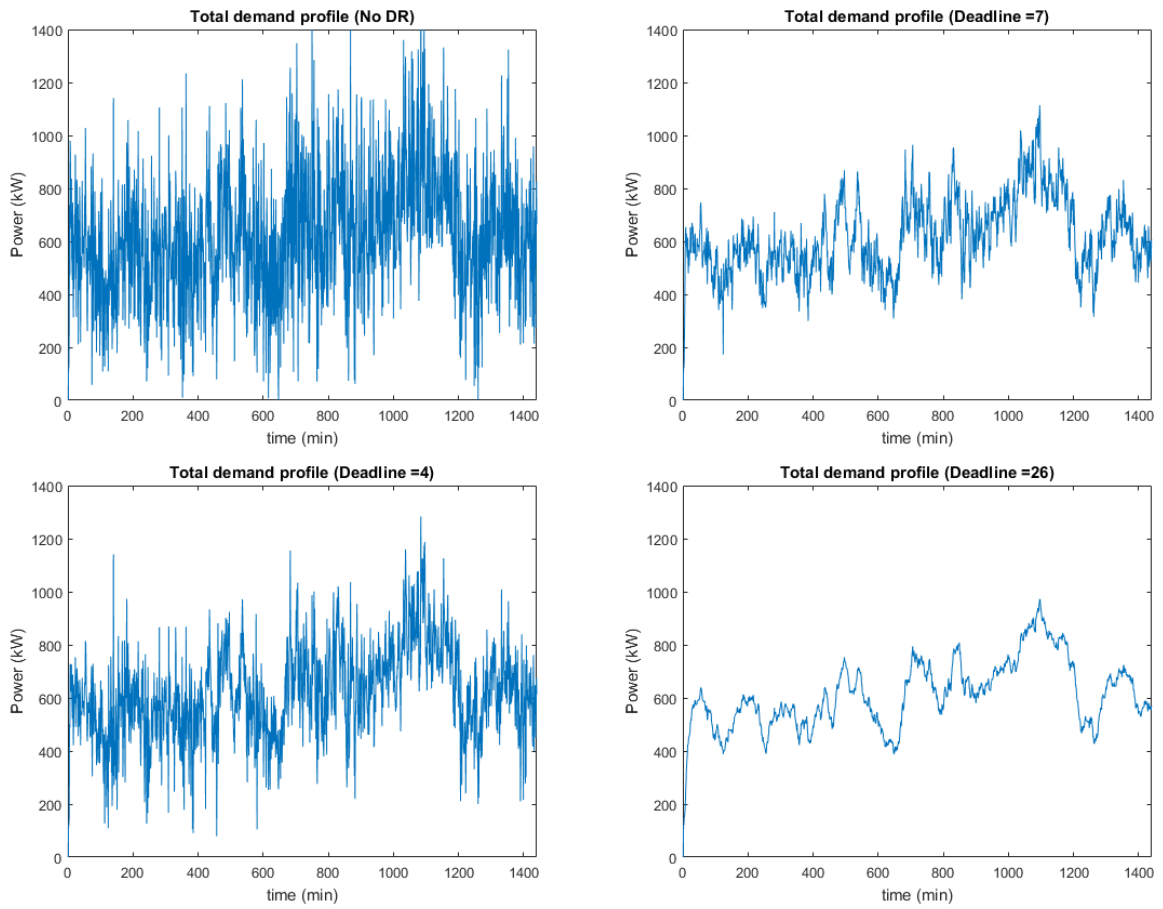
Figure 5.5: Total demand profiles for different demand scheduling deadlines.
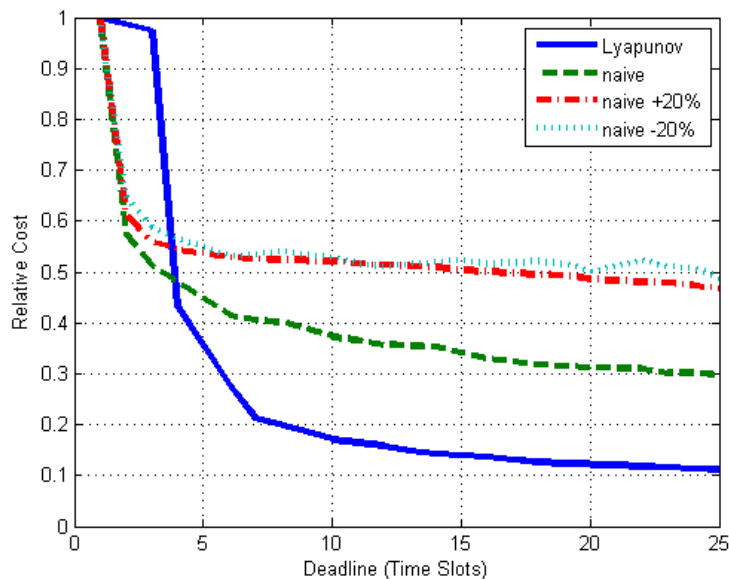
Figure 5.6: Comparison between the proposed methodology and naive tracking policy

the deadline increases, our methodology outperforms the naive policy even under perfect prediction.

Finally, we investigate the benefit of using a multi-class queueing system. Increasing the number of queues allows more efficient assignment of controllable demand requests, however it decreases the arrival rate per queue which in turn decreases queues' capability for regulation. Hence, we can expect that for each distribution of demand requests, there is an optimal number of queues that achieves the best performance (lower cost). The cost of purchasing AS for different number of queues (normalized to the cost under single queue) is shown in Figure 5.7. The figure shows that the performance improves rapidly as the number of classes increases until the number of classes reaches seven, after which the cost starts to increase slowly.
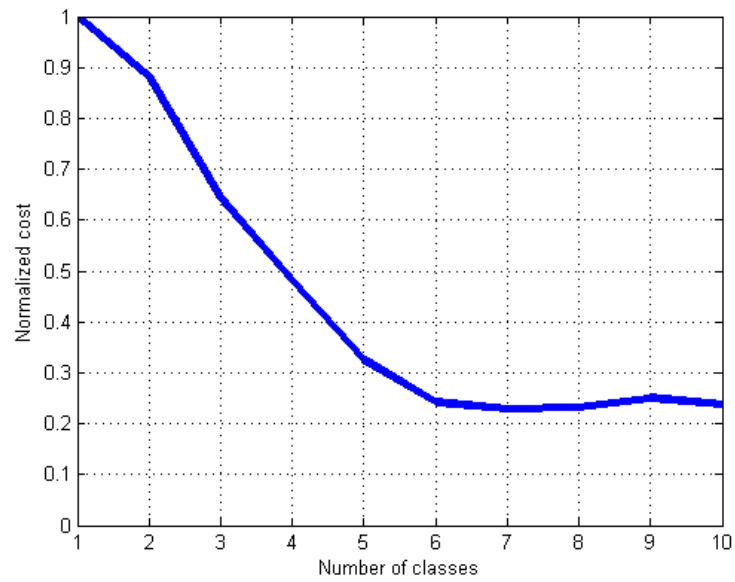
Figure 5.7: Performance under different number of queues normalized to the performance of single queue

64

5.5 Summary

Similar to chapter 4, this chapter is concerned with managing a large number of residential appliances. However, different from chapter 4, the DR objective is to reduce the fluctuations resulting from a large-scale integration of RES units. The main driving signal is the net non-controllable demand profile which is stochastic, unlike the deterministic driving signal used in chapter 4, which is the day-ahead pricing. The offline algorithm used in chapter 4 is inefficient due to the stochastic nature of the driving signal. Hence, we had to define a new algorithm for demand scheduling that runs online. Based on Lyapunov optimization, the performance of our proposed algorithm is defined from two criteria: long-term average performance and short-term sample-path performance. Numerical results proved the effectiveness of our proposed algorithm in reducing the fluctuations. We also showed that the performance does not improve indefinitely as the number of classes increases. There is, however, an optimal number of classes that achieves the best performance.

Chapter 6

Optimal Assignment of Electric Vehicles to Charging Stations

6.1 Problem definition

The presence of electric vehicles (EVs) is now noticeable; There were 665,000 EVs on the road by the end of 2014 [77]. From a user point of view, EV has some attractive features, such as its maintenance simplicity and reduced noise compared to the ordinary internal combustion engine (ICE) vehicle [77]. Also, the advance in the EV technology will help in reducing the manufacturing cost; For example, it is expected that the cost of Lithium-Ion battery pack will reach $100/ kWh in 2025 compared to $1126/ kWh in 2010 [78], which will help in stimulating the demand. Moreover, many countries are concerned with increasing the market penetration level of EVs in order to decarbonize the transport sector and to diversify their sources of fuel[79]. In order to accomplish these goals, governments had set EV adoption targets. Combined EU targets amount to 8-9 million EVs on the road by 2020 [80]. The US targets 3.3 million zero-emission vehicles by 2025 [81].

Although EV is not a new idea, the penetration levels are still negligible if compared to that of ICE vehicles; For example, sales of EVs in Europe excluding hybrids are less than 1% of total new car sales [80]. There still exist technological and social barriers which make the improvement of EV penetration levels a challenging task. For example, if we consider the EV specifications in [82], we find that the EV has a range of 80 km and a battery capacity of 16 kWh. The battery alone weighs around 198 kg. The time required for charging the battery from its minimum state-of-charge to its maximum state-of-charge depends on the power rating of the charger. Nowadays, there exist three standard charger's ratings [83]

level I (1.4 kW, household charger), level II (4 kW), and level III (50 kW, DC fast charger). Their corresponding charging times for a 10 kWh battery are 7 hours, 2.5 hours, and 12 minutes respectively. The aforementioned data used to be the typical specifications for an EV several years ago. Our first notice is the limited range of the EV which causes the fear that the EV battery becomes empty before reaching the destination (range anxiety). Larger ranges would have required a battery of larger capacity, which would have required larger volume and larger mass, making the EV more expensive. The second inconvenience is the relatively long-charging times, compared to the refill of fuel tank in ICE vehicles. The most convenient charging time happens when DC fast chargers are used. One of the drawbacks of EVs is the tradeoff between the first and second inconveniences: improving EV range will require a larger battery capacity and accordingly a longer charging time.

In order to accommodate a large number of EVs on the road and to allow them to make longer trips, an extensive charging infrastructure must be deployed, which is composed of charging stations that are publicly available within EVs' range. For each station, EV queueing might occur if the number of vehicles in the station exceeds the number of available chargers. Hence, an EV user will not only wait for charging his vehicle, but possibly for some other EVs to complete their charging as well. Increasing the number of chargers may reduce the average waiting time for EV users; However, it will require not only additional installation costs, but possibly upgrading the power network as well. Hence, this solution must be the last resort after making sure that existing charging resources are efficiently utilized, which can be achieved by two ways. The first way is to use the technology of battery-swapping: the EV's empty battery is replaced by a fully charged one upon EV's arrival to the station. The empty battery is left to be charged so that it can serve another EV and so on. The battery swapping concept can help in improving the performance as it provides some form of "demand buffering": during high demand, empty batteries will be swapped and then charged during low demand. However, such technology requires a high degree of standardization of battery types. Further, battery swapping is not an ultimate solution, since if the mean EV service rate of a single station is lower than its mean EV arrival rate, the queue will grow indefinitely, independent of the available battery stock in that station. The second way is through the optimal assignment of EVs to the proper charging stations, which is the concern of our problem. While it is natural to assign the EV to the closest station, it might be beneficial for the user to be assigned to a farther station if the first one was heavily loaded. The benefit we get here is from the "resource sharing", where a charging station not only serve vehicles within its area of operation, but vehicles from other areas as well.

Existing algorithms that are concerned with finding the best path for vehicles can be classified into static and dynamic routing algorithms [84]. In the first category, the under-

lying model is static: charging requests and locations are given in advance to a controller, which will use them for planning the best paths for vehicles. The static model assumes no new requests arrive over time. In the related studies [18, 19, 20, 21, 24, 22, 23], the road network is modeled as a complete undirected graph, where the vertices represent charging stations and any other locations of interest, and the graphs edges represent the distance between the vertices. Each edge is modeled by some associated cost which can be, for example, travel distance, travel time, energy consumption, ...etc. These quantities can be vehicle-dependent. Given a finite number of vehicles, the routing problem is formulated as a mixed integer-linear programming (MILP) problem that minimizes the total routing cost. Static routing is not suitable for our problem for two reasons; First, travel and charging times are relatively long; Hence, assuming that no new charging requests appear until the assigned vehicles finish their tasks is not practical. The second reason is that computational complexity of the MILP can be prohibitively large as the number of vehicles to be assigned increases. Therefore, static routing algorithms are more suitable for managing a limited fleet of commercial vehicles rather than a large number of regular passenger vehicles.

On the other hand, studies related to dynamic routing algorithms for charging EVs are scattered and do not represent a solid research body. In [48, 85], load balancing algorithms were developed to minimize the total average queueing lengths. However, the algorithms ignore the vehicle's travel time, i.e., a vehicle can be assigned to a faraway station even under light load just to perfectly distribute the load over all charging stations. The authors of [86] assume no queueing at all, i.e., if the chargers in all stations where busy, new charging requests will be denied.

Based on the aforementioned discussion, we conclude that the existing studies lack a proper queueing model which takes EVs' mobility into consideration, hence, they are not suitable for managing a large-scale penetration of EVs. Our third problem is concerned with addressing this particular shortcoming. The contributions of our work can be summarized as follows: 1) developing a queueing model for EV assignment and charging, 2) developing a dynamic routing algorithm which coordinates between continuous-time Markov decision process and Bayesian optimization to minimize the average system time, which is composed of the time required for the EV to travel to the assigned charging station in addition to the waiting time the user spends in that station until the EV starts to be served.

6.2 Solution methodology

Our solution methodology is based on formulating the problem as a continuous-time Markov Decision Process (CT-MDP) problem. The reason for choosing continuous time over discrete time modeling is that in the former, decisions and information exchange are event-driven, which has two advantages: 1) it allows taking decisions vehicle-by-vehicle, and 2) EV receives the decision immediately when it sends its charging request, whereas in discrete time, an EV needs to wait until the next pre-specified time instance to receive the controller's decision. As in any MDP problem, there are four quantities that need to be defined: 1) system state s (accordingly, the state-space), 2) action-space for each state $\mathcal{A}_s$, 3) transition probabilities for each state-action combination, and 4) the incurred cost for each state-action combination. The output of an MDP problem is a policy $\boldsymbol{\pi}\colon s \to a \in \mathcal{A}_s$, which is a function that maps the state-space into the action-space. In simpler words, the policy $\boldsymbol{\pi}$ tells us which action (decision) to select from the action space $\mathcal{A}_s$ if the system was in state s.

We define the system state by $2N_c + 1$ variables: the number of EVs residing at each station, $\{H_1, H_2, \ldots, H_{N_c}\}$, the number of ongoing EVs that were assigned for each station, $\{M_1, M_2, \ldots, M_{N_c}\}$, and the location of the new charging request L. H_i is composed of EVs being served and EVs waiting to be served. Since we assumed continuous time modeling, at most one EV can send a charging request at any given time instance. On the other hand, the action represents the station to which the new charging request is assigned. Hence, we have a number of N_c different actions: $\mathcal{A}_s = \{CS_1, CS_2, \ldots, CS_{N_c}\}$. A depiction of how different state variables are calculated is shown in Figure 6.1.

The definitions for state transition probabilities and instantaneous cost function will be described in the next subsection. Although an MDP policy is applied online, deducing the optimal policy itself requires an offline algorithm. Normally, offline algorithms can tolerate long computational times, since there are no restrictive computational delay constraints as in real-time algorithms. However, one of the drawbacks of using MDP is *curse of dimensionality* problem: adding more state variables leads to the exponential growth of the state-space size and accordingly the computational burden for solving the MDP can be practically prohibitive. In the system state definition, the number of state variables increases by 2 as the number of stations increases. In order to avoid the *curse of dimensionality* problem, we develop a distributed approach, where decisions for EVs assignment are made in a distributed manner based on the individual state of each station. For each individual station, the number of state variables will be fixed to 3 variables only: $\{L, M_i, H_i\}$, which will help in reducing the computational burden.
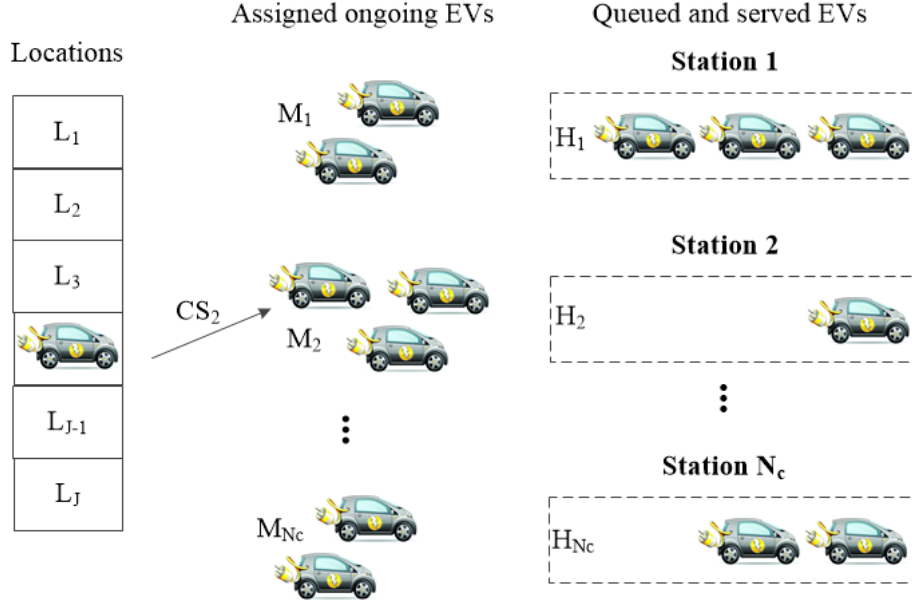
Figure 6.1: A depiction of different variables used to compose the state of the system.

6.3 Solution algorithm

Before describing the distributed approach for solving our problem, it is essential to describe the centralized approach first, which is the original approach to follow if we have the sufficient computational power.

6.3.1 Centralized approach

Finite state space

Our first obstacle is that the state space resulting from the definition in the previous section is infinite, which is attributed for two reasons: 1) there are infinite number of locations from which charging requests can appear, and 2) variables H_i and M_i are unbounded, i.e., they can reach any large positive value. It is usually hard to solve infinite state-space problems in a straight-forward manner. In order to make the state space finite, the service area is divided into J non-overlapping regions; hence, we have a finite set of locations $\mathcal{L} = \{L_0, L_1, L_2, \ldots, L_J\}$. The element L_0 denotes a virtual location representing the case when no new charging request happens. Second, we truncate the state space by setting
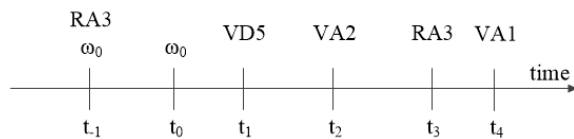
Figure 6.2: An example of a possible series of events that are responsible for the system's evolution.

upper bounds for variables H_i and M_i, such that they should not exceed H_i^{max} and M_i^{max}, respectively.

Transition probability matrix

There are three types of events responsible for a system state transition, which are charging request arrival (RA), EV's arrival to the assigned charging station (VA), and EV's departure from the charging station after completing its service (VD). For mathematical tractability, we assume that the inter-arrival times of these events are exponentially distributed. Since we assumed that charging requests arrive according to PPP, the inter-arrival times between two successive requests from location L_j is exponentially distributed with parameter $\lambda_j = \Lambda A_j$, where A_j is the area of region L_j. The time required for an EV to reach the assigned charging station is exponentially distributed with parameter ν. The charging time of an EV's battery is exponentially distributed of parameter μ. The main advantage exponential distribution assumption is its Markovian (memoryless) property. For clarification, assume the series of events shown in Figure 6.2. The current time is t_0. The last change in the system happened when a charging request at location 3 was initiated at time t_{-1}, making the system state to become ω_0. According to our assumption, $t_3 - t_{-1}$ is exponentially distributed with parameter λ_3. The Markovian property means that the residual time $t_3 - t_0$ is also exponentially distributed with the same parameter λ_3. Similarly, $t_1 - t_0$ is exponentially distributed with parameter μ and $t_2 - t_0$ is exponentially distributed with parameter ν. The Markovian property allows us to ignore how much time have passed since last event arrival and the system evolution depends only on the current state ω_0 and not on whether the current time is t_0 or t_{-1}.

The evolution of the system depends on the event that will arrive faster. For example, in Figure 6.2, the next event will be an EV arrival to station 2 if $t_2 < \min\{t_1, t_3, t_4\}$. In order to obtain the probability of that condition, we use two properties of the exponential distribution. First, the minimum of several exponentially distributed random variables (r.v.)s is also an exponentially distributed r.v., whose parameter is equal to the sum of all the parameters of the input distributions. Second, the probability that an exponentially distributed r.v. is smaller than another exponentially distributed r.v. is equal to the

Table 6.1: State transitions due to different events given the current state is $\{L_j, M_1, H_1, \ldots, M_i, H_i, \ldots, M_{N_c}, H_{N_c}\}$ and action CS_i is selected

Event type	j	Future state
Charging request from location L_k	$\neq 0$	$\{L_k, M_1, H_1, \ldots, \min\{M_i + 1, M_i^{max}\}, H_i, \ldots$ $, M_{N_c}, H_{N_c}\}$
Charging request from location L_k	0	$\{L_k, M_1, H_1, \ldots, M_i, H_i, \ldots, M_{N_c}, H_{N_c}\}$
EV's arrival to station CS_k	$\neq 0$	$\{L_0, M_1, H_1, \ldots, \min\{M_i + 1, M_i^{max}\}, H_i, \ldots$ $, M_k - 1, \min\{H_k + 1, H_k^{max}\}, \ldots, M_{N_c}, H_{N_c}\}$
EV's arrival to station CS_k	0	$\{L_0, M_1, H_1, \ldots, M_i, H_i, \ldots, M_k - 1, \min\{H_k + 1, H_k^{max}\},$ $\ldots, M_{N_c}, H_{N_c}\}$
EV's departure from station CS_k	$\neq 0$	$\{L_0, M_1, H_1, \ldots, \min\{M_i + 1, M_i^{max}\}, H_i, \ldots$ $, M_k, H_k - 1, \ldots, M_{N_c}, H_{N_c}\}$
EV's departure from station CS_k	0	$\{L_0, M_1, H_1, \ldots, M_i, H_i, \ldots, M_k, H_k - 1, \ldots, M_{N_c}, H_{N_c}\}$

ratio of the parameter of the first to the sum of both distributions' parameters. Assuming $\omega_0 = \{L_j, M_1, H_1, M_2, H_2, \ldots, M_{N_c}, H_{N_c}\}$, there would be a number of $J + 2N_c$ possible future events: charging request arrivals from J possible locations each of parameter λ_j, EV arrivals to N_c possible stations, each of parameter $M_i \nu$, and EV departures from N_c possible stations, each of parameter $\min\{H_i, R_i\}\mu$. Let σ_k be the parameter of event k, then by using the two aforementioned properties of the exponential distribution, the conditional probability of the event's occurrence is given by:

$$\Pr\{k|\omega_0\} = \frac{\sigma_k}{\sum_{i=1}^{J+2N_c} \sigma_i} \tag{6.1}$$

As a result of the occurrence of any event, the system will transit to a new state as given in table 6.1.

One-step cost function

The final part that needs to be defined is the cost function $C(s, a)$, which represents the immediate incurred cost as a result of taking action a when the system is at state s. The cost is composed of two parts, the expected travel time of the EV to the assigned station and the expected waiting time of EVs in all stations. The expected travel time from region j to station i is given by:

$$T_{ji}^r = \iint\limits_{L_j} t_i^r(x, y) f_j(x, y)\, dx\, dy, \tag{6.2}$$

where $t_i^r(x, y)$ is the expected travel time for an EV from the location (x, y) to station CS_i, and $f_j(x, y)$ is the conditional probability density function for the charging request location given it occurred within region L_j. On the other hand, the expected waiting time for station CS_i is given by:

$$T_i^w = \Pr\{\text{VA}_i\}\mathbb{E}\{T_i^w | \text{VA}_i\}, \tag{6.3}$$

where $\Pr\{\text{VA}_i\}$ is the probability that an EV arrives to station CS_i in the next event occurrence, which can be deduced from eq.(6.1) as:

$$\Pr\{\text{VA}_i\} = \frac{M_i\nu}{\sum_{i=1}^{N_c}\{M_i\nu + \min\{H_i, R_i\}\mu\} + \sum_{j=1}^{J}\lambda_j} \tag{6.4}$$

On the other hand, $\mathbb{E}\{T_i^w | \text{VA}_i\}$ represents the expected waiting time for a vehicle *just arrived* to station CS_i. The waiting time is zero, if there is at least one empty charger. If all the chargers where busy and no vehicle was queued, then the expected waiting time is the minimum of charging completion times of the vehicles being served, which is given by $\frac{1}{\mu R_i}$ (given the exponential distribution assumption). If there are some queued vehicles upon the new EV's arrival, then the expected waiting time will be the expected waiting time of the last queued vehicle in addition to $\frac{1}{\mu R_i}$. By induction the formula of the expected waiting time will be given by:

$$\mathbb{E}\{T_i^w | \text{VA}_i\} = \frac{1}{\mu R_i}[H_i - R_i + 1]^+ \tag{6.5}$$

Accordingly, The total one-time step cost function will be given by:

$$\begin{aligned}
&C(\{L_j, M_1, H_1, \ldots, M_i, H_i, \ldots, M_{N_c}, H_{N_c}\}, CS_i) \\
&= T_{ji}^r + \sum_{i=1}^{N_c} \frac{M_i\nu}{\sum_{i=1}^{N_c}\{M_i\nu + \min\{H_i, R_i\}\mu\} + \sum_{j=1}^{J}\lambda_j} \times \frac{1}{\mu R_i}[H_i - R_i + 1]^+
\end{aligned} \tag{6.6}$$

With all the four parts of the MDP problem defined, it is theoretically straight-forward to determine an optimal policy $\boldsymbol{\pi}^* : s \to a$ which minimizes the long term time-average cost:

$$\bar{c} = \lim_{k \to \infty} \frac{\sum_{k=0}^{K-1} \mathbb{E}\{C(s_k, \boldsymbol{\pi}(s_k))\}}{\sum_{k=0}^{K-1} t_k} \tag{6.7}$$

Algorithms for minimizing $\bar{c}$ can be found in [87]. Unfortunately, the number of computational requirements (memory/calculation) by these algorithms is at least in the order of square the size of the state space. As the state-space of our problem has $1 + 2N_c$ dimensions, the state-space size can grow easily. Further, the algorithms are not scalable: their computational requirements grow exponentially with the problem size (the number of stations). To avoid the *curse of dimensionality*, we follow a distributed approach for decision making as described in the next subsection.

6.3.2 Distributed approach

In this approach, an EV's assignment is done through a series of sequential decisions, where each station decides whether to accept an incoming charging request or reject it. The decisions are made in order, starting from station CS_1. A request rejected by station CS_i should be passed to the next station CS_{i+1} which in turn decides whether to accept or reject it and so on. If the request reaches the last station, CS_{N_c}, this means it has been rejected by all the previous $N_c - 1$ stations; Hence, station CS_{N_c} must accept any charging request arrives to it (Figure 6.3).

Individual (local) CT-MDP

The decision made by a station CS_i is based on its own current state $\{M_i, H_i\}$ and is independent on the individual state of other stations. The individual decision making is based on the CT-MDP approach discussed in the previous subsection. However, this time the state-space will have three dimensions only: $\{L_j, M_i, H_i\}$. The action-space will become binary: either accept "1" or reject "0". If we use the same cost function defined in (6.6), all stations will choose to reject the charging request and all requests will be assigned to station CS_{N_c}. Accordingly, we introduce a virtual cost for rejecting a request. If station CS_i rejects a request, it will get an instant virtual penalty of γ_i. The modified cost function will become:
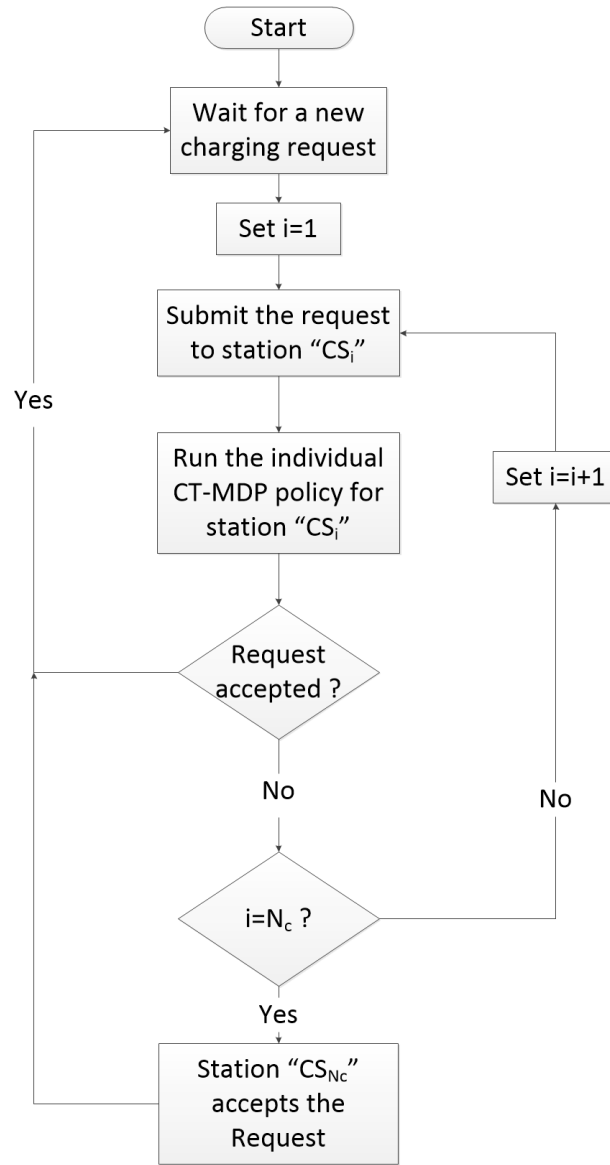
Figure 6.3: A flow chart for determining the EV assignment decision in the distributed approach.

$$C_i(\{L_j, M_i, H_i\}, a) = (1-a)\gamma_i + aT_{ji}^r + \frac{M_i\nu}{M_i\nu + \min\{H_i, R_i\}\mu + \sum_{j=1}^{J} \lambda_j^i} \frac{1}{\mu R_i} [H_i - R_i + 1]^+,$$

$$(6.8)$$

where λ_j^i is the average charging request arrival rate for station CS_i from region L_j, which is equal to the difference between λ_j and the portion accepted by previous stations. Intuitively, $\lambda_j^1 = \lambda_j$. The portion of charging requests accepted by any station will depend on its optimal admission policy. Accordingly, given a penalty set $\Gamma = \{\gamma_i, \ \forall i = 1, 2, \ldots, N_c - 1\}$, we cannot solve individual MDP problems in parallel, but rather in a sequential fashion.

In order to determine λ_j^i and other performance metrics for an MDP problem, it is necessary to find the steady-state probability distribution "ψ" of the station's state over the state-space $\mathcal{S}$, i.e., for each state $s \in \mathcal{S}$, $\psi(s)$ the probability that a station becomes in state s after an arbitrary long period. Given a policy π, the distribution ψ can be deduced from the transition probability matrix $\mathbf{G^\pi}$ as its left eigenvector; i.e., it satisfies $\psi = \psi \mathbf{G^\pi}$. The regional admission probabilities will be given by:

$$p_j^a = \sum_s \psi(s)\pi(s)\mathbb{1}_{\{L(s)=L_j\}}, \quad (6.9)$$

where, $L(s)$ denotes the location variable of state s, and $\mathbb{1}_{\{.\}}$ is the indicator function which is equal to 1 if the condition between braces is satisfied and zero otherwise. The average charging request arrival rate from region L_j for station CS_{i+1} is given by:

$$\lambda_j^{i+1} = \lambda_j^i(1 - p_j^a) \quad (6.10)$$

Thus starting from $\lambda_j^1 = \lambda_j$, we solve each individual MDP problem i to deduce the arrival rates from eq.(6.10), to be used for the next individual MDP problem $i + 1$. Other performance metrics that need to be deduced are the expected travel and waiting times. The contribution of station CS_i to the average EV travel time is given by:

$$\bar{T}_i^r = \frac{\sum_{j=1}^{J} p_j^a \lambda_j^i T_{ij}^r}{\sum_{j=1}^{J} \lambda_j} \quad (6.11)$$

The average EV travel time disregarding which station they are assigned to is simply given by $\bar{T}^r = \sum_{i=1}^{N_c} \bar{T}_i^r$. On the other hand, the expected waiting time for a vehicle arrived to station CS_i can be driven from the expected queue length using Little's law:

$$\bar{T}_i^w = \frac{\mathbb{E}\{Q_i\}}{\lambda_0^i} = \frac{\mathbb{E}[H_i - R_i]^+}{\sum_{j=1}^J p_j^a \lambda_j^i}, \tag{6.12}$$

where λ_0^i represents the total average rate of admitted requests from all regions to station CS_i. The average EV travel time disregarding which station they are waiting in is given by:

$$\begin{aligned}
\bar{T}^w &= \sum_{i=1}^{N_c} \Pr\{\text{EV assigned to station } i\} \bar{T}_i^w \\
&= \sum_{i=1}^{N_c} \frac{\lambda_0^i}{\sum_{j=1}^J \lambda_j} \bar{T}_i^w.
\end{aligned} \tag{6.13}$$

Global performance

The average system time is simply the sum of the average travel and waiting times, which depend on the virtual penalty set Γ. Let us denote this dependency by a multi-dimensional function $F(\Gamma)$, i.e.,

$$F(\Gamma) \triangleq \bar{T}^r(\Gamma) + \bar{T}^w(\Gamma) \tag{6.14}$$

Our problem is to find the optimal virtual penalty set $\Gamma^* = \{\gamma_1^*, \gamma_2^*, \dots, \gamma_{N_c-1}^*\}$ such that the average system time is minimized. Since we have no evidence that $F(.)$ is convex, we will use a heuristic approach to find a global optimal solution. The approach is based on Bayesian optimization (Figure 6.4), which is a useful search method when the evaluation of the objective function is computationally expensive [88]. In this approach, the objective function is treated as a black box, i.e., we assume we have no information about the function structure such as the gradient. The only available information is the sampling history $\mathcal{H}_k = \{(x_1, y_1), (x_2, y_2), \dots, (x_k, y_k)\}$, which is a set of k evaluated samples, where $x_i = \Gamma_i$ represents the sample point $\#i$ and $y_i = F(\Gamma_i)$ represents the evaluation of that point. Since the function $F(.)$ is assumed to be unknown for us, we develop a probabilistic model, $\tilde{F}(\Gamma)$, which describes the stochastic relationship between values at different points. Based on that model, we attempt to deduce which point to be sampled next (point $\#k+1$) which is *more likely* to have a better solution than that of the points in $\mathcal{H}_k$. In a similar approach to that in [88], the probabilistic model is selected to be Gaussian process, which

means that the values at any given set of points (which are unknown to us due to the black box assumption) are jointly-Gaussian; i.e., $\tilde{F}(\vec{x}) \sim \mathcal{GP}(\mathbf{m}, \mathbf{Z})$, where $\mathbf{m}$ and $\mathbf{Z}$ represent the mean vector and covariance matrix for the "random" function values at points $\vec{x}$, respectively. We select $\mathbf{m} = 0$ and $\mathbf{Z}(x, x') = \exp\left(-\frac{1}{2}\|x - x'\|^2\right)$. Our selection can be interpreted as follows: assuming we have no sampling history, the value of the function at any given point x is a Gaussian distributed random variable with zero mean and unit variance. The value at a neighboring point x' is also random variable which is statistically dependent on the value at point x. This dependence is directly related to the Euclidean distance between the two points. As the distance tends to zero, the covariance tends to unity meaning that the values at the two points are perfectly dependent. On the other hand, as the distance increases, the covariance tends to zero meaning that the values at the two points are independent. The aforementioned behavior is consistent, because (at least for smooth functions) we expect that the value at one point becomes closer to that at a neighboring point as the distance between the two points decreases. The next step is to incorporate the sampling history to improve the probabilistic model. It is easy to prove that the conditional probability density function of the value at a candidate point x' given a sampling is also normally distributed with mean m' and variance r' which are given by:

$$m' = \mathbf{Z}^T(k+1, k+1) - \\ \mathbf{Z}^T(k+1, 1:k)\mathbf{Z}^{-1}(1:k, 1:k)\mathbf{Z}(k+1, 1:k) \tag{6.15}$$

and

$$r' = \mathbf{Z}^T(k+1, 1:k)\mathbf{Z}^{-1}(1:k, 1:k)\mathbf{y}_{1:k} \tag{6.16}$$

The final step is to determine the next point to sample. Our selection criterion is based on the expected improvement over the best solution $y_k^* = \min \mathbf{y}_{1:k}$. The improvement is simply given by: $I(x) = [\tilde{F}(x) - y_k^*]^+$. From the mean and variance given in (6.15) and (6.16) respectively, it is straightforward to determine the expected improvement at any point, $EI(x)$. The point to be sampled next is determined from:

$$x_{k+1} = \arg\max\{EI(x)\}. \tag{6.17}$$

The function $EI(x)$ is referred to as the acquisition function. Finding the optimal solution of (6.17) can be done using one of the heuristic optimization algorithms such as particle swarm optimization (PSO). Unlike the original objective function $F(x)$, the acquisition
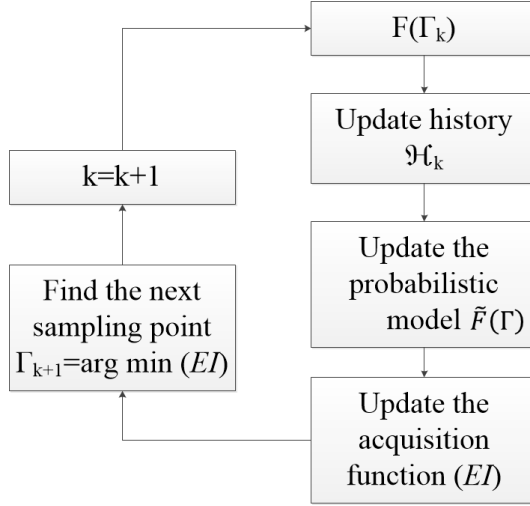
Figure 6.4: A flow chart for Bayesian optimization.

function is computationally cheap to sample. Accordingly, solving the problem in (6.17) is much quicker than solving the original problem.

We can now summarize the proposed algorithm for determining EVs' assignment policy in algorithm 4.

6.4 Numerical results

6.4.1 Model verification

We assume the service area to be a $10~km \times 10~km$ square. The area is divided into 9 regions. The charging infrastructure is composed of four charging stations located in the center of the four corner regions as shown in Figure 6.5. Charging requests arrive according a homogeneous PPP of average rate 0.2 requests/minute. We assume all chargers are DC fast chargers, with an average charging time of 15 minutes. Each of stations 1 and 4 has two chargers, while each of stations 2 and 3 has one charger. The average EV speed is $15~km/hr$.

Since we have made several approximations in our analytical model, our first step will be to verify the model with simulation. In the simulation model, many simplifying assumptions are relaxed: 1) Charging requests can arrive anywhere within the service area, instead of discrete regions' centers, 2) No truncation applied on queues' lengths or on

---
Algorithm 4: Proposed system-time optimization algorithm

Input : $Iteration\_max, \mu, R_i, \lambda_j, T^r_{ij}, \quad \forall i \in \{1, 2, \ldots, N_c\}$ and $j \in \{1, 2, \ldots, J\}$

Output: $\mathcal{P}^{best}$

1 Initialize $\Gamma_1, k = 0, \mathcal{H}_0 = \{\}, y^{best} = \infty, Iteration = 0$

2 **while** $Iteration <= Iteration\_max$ **do**

3   Initialize $\lambda^1_j = \lambda_j, \forall j \in \{1, 2, \ldots, J\}, \mathcal{P} = \{\}$

4 $k = k + 1$.

5 $Iteration = Iteration + 1$.

6   **for** $i \in \{1, 2, \ldots, N_c\}$ **do**

7   Determine station i's optimal accepting/rejecting policy $\boldsymbol{\pi}_i$ by formulating a CT-MDP problem. The inputs to that problem are: 1) the average request arrival rates from different regions are given by $\lambda^i_j, \forall j \in \{1, 2, \ldots, J\}$, 2) the average charging duration is given by $1/\mu$, 3) the number of chargers are given by R_i, and 4) the rejection penalty $\gamma_i = \Gamma_k(i)$

8 $\mathcal{P} = \mathcal{P} \bigcup \boldsymbol{\pi}_i$.

9   Deduce the probability distribution for different states of station i.

10   Calculate the regional admission probabilities (eq.(6.9)) to update the average arrival rates for the next station λ^{i+1}_j (eq.(6.10)).

11   Update the individual station performance parameters $\bar{T}^r_i$ (eq.(6.11)) and $\bar{T}^w_i$ (eq.(6.12)).

12   **end**

13   Update the global performance parameters and find the average system time

14   **if** $y_k < y^{best}$ **then**

15 $y^{best} = y_k$.

16 $\mathcal{P}^{best} = \mathcal{P}$

17 $Iteration = 0$.

18   **end**

19 $\mathcal{H}_k = \mathcal{H}_{k-1} \bigcup (\Gamma_k, y_k)$

20   Update the acquisition function using $\mathcal{H}_k$.

21   Solve (6.17) using PSO to get the next search point (Γ_{k+1}).

22 **end**
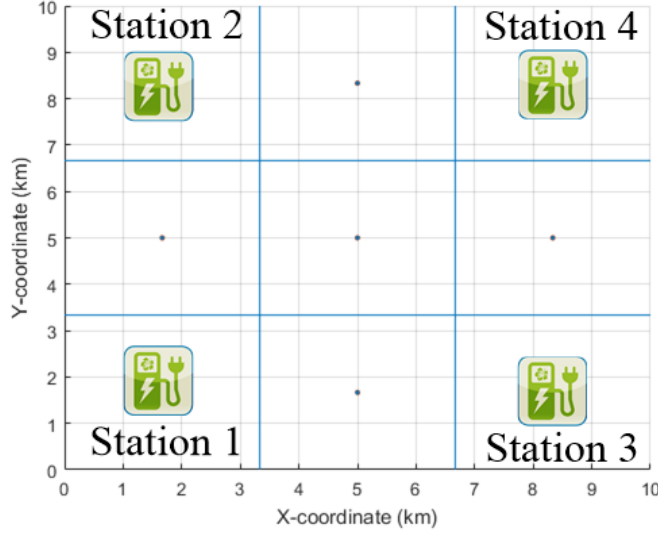
Figure 6.5: Service area under consideration for subsection 6.4.1.

the number ongoing vehicles; i.e., the simulation model is lossless and queue lengths are allowed to grow indefinitely, and 3) Uniform distribution for the charging duration is used instead of the exponential assumption. Model verification is applied on the first station only, where the performances under both analytical and simulation models are compared versus different rejection penalty values.

Figure 6.6 shows the general EV admission (acceptance) probability regardless of where the charging request occurs. Analytical and simulation results almost match each other. As the rejection penalty increases, the admission probability approaches to 1. The function is not smooth, because the performance depends on the optimal scheduling policy, which can only be selected from a discrete set of policies. Figure 6.7 shows the EV admission (acceptance) probability for each region. We notice that as the rejection penalty increases, the station starts to accept vehicles from the closest regions first, then the farther regions next. The mean travel and waiting times are shown Figures 6.8 and 6.9 respectively. The deviation between the analytical and simulation results for Figure 6.8 is attributed to the discretization of charging request locations, while the deviation in Figure 6.9 is attributed to using a uniform distribution for charging duration instead of exponential.

We proceed by testing algorithm 4 for a two-station system which is composed station 1 and station 4 only. For such system, it is easy to determine the exact optimal solution by enumeration, since the only decision variable is the rejection penalty for the first station

81
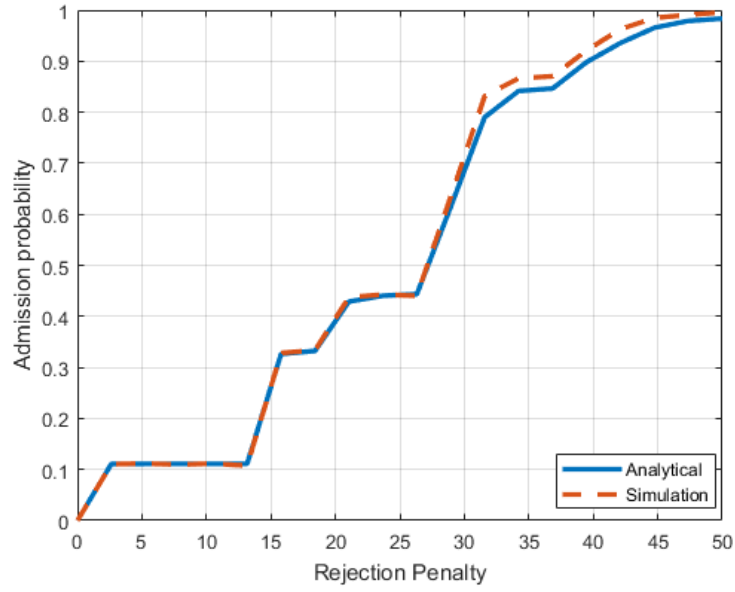
Figure 6.6: General EV admission probability for station 1.
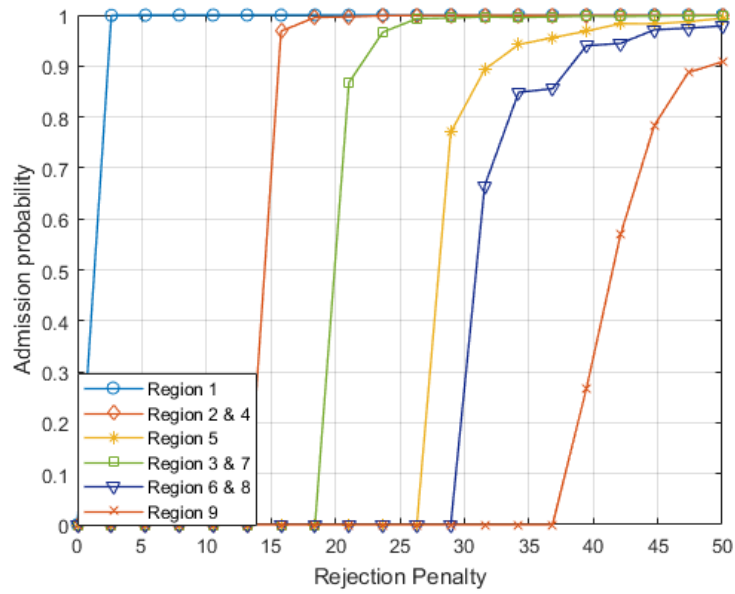
Figure 6.7: Regional EV admission probability for station 1.
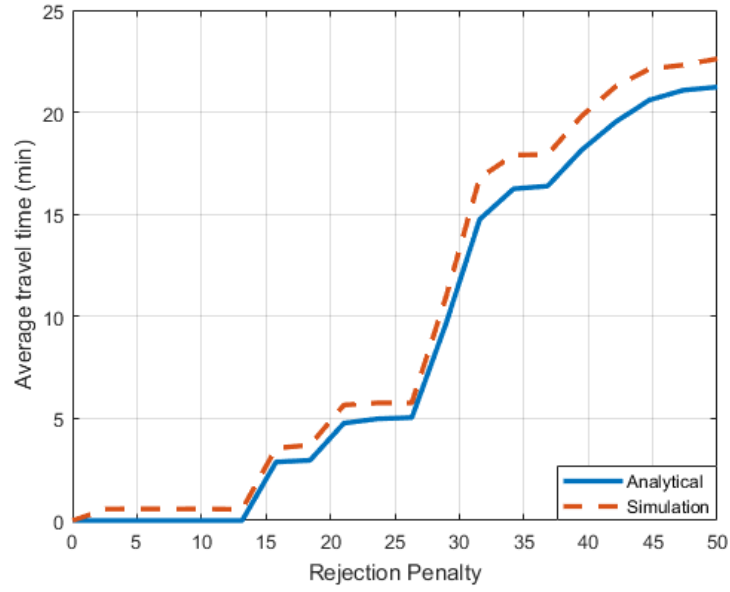
Figure 6.8: Average EV travel time to station 1.
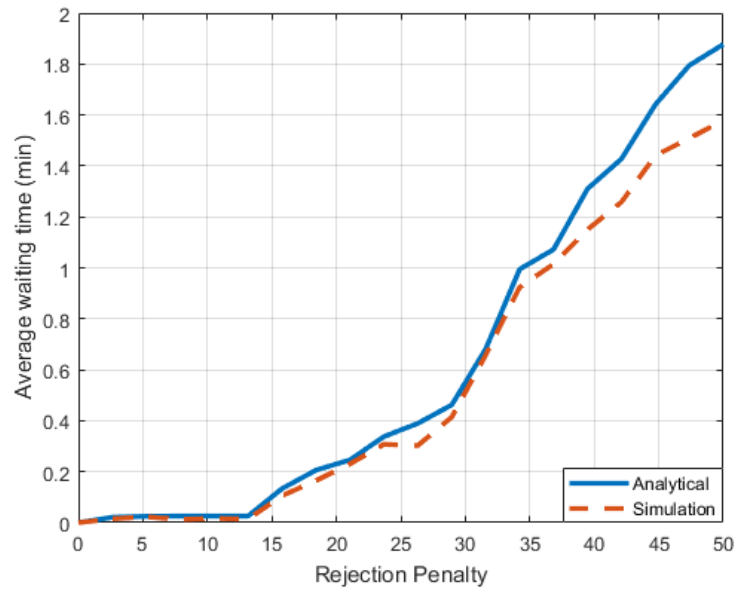
Figure 6.9: Average EV waiting time in station 1.
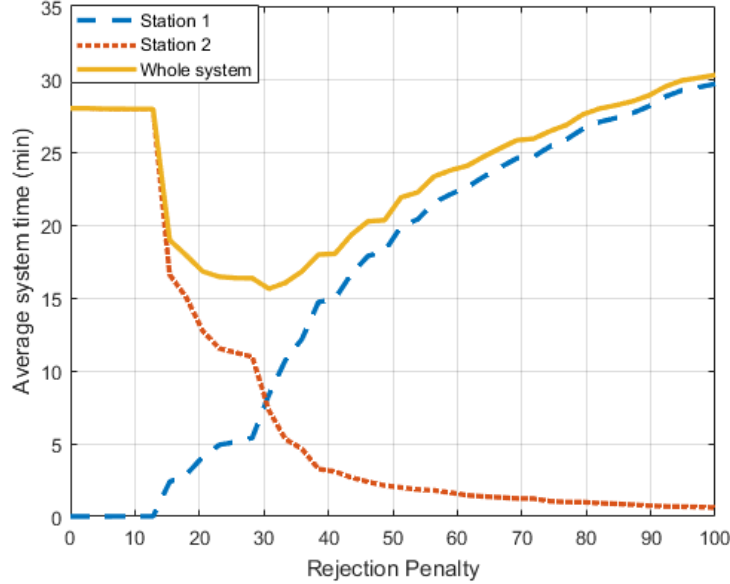
Figure 6.10: Average system time for a two-station system vs. the rejection penalty of the first station. The contribution of each station to the average system time is given by the dashed and dotted plots.

(there is no rejection penalty for the second station as it has to accept all charging requests rejected from station 1). Figure 6.10 plots the mean system time against the rejection penalty. The system time achieves one minimum of 15.62 minutes when the penalty is about 30.7. The contribution to the mean system time by each station is also shown in Figure 6.10. As the penalty increases, the contribution of station 1 increases and that of station 2 decreases. At the optimal point, the contributions of both stations are equal which is expected because of the symmetry of the system. Figure 6.11 shows how fast algorithm 4 approaches the optimal result. By the third iteration, the performance is about 29.6% larger than the optimal result. The performance becomes almost optimal at the 11th iteration.

Finally, the performance of Algorithm 4 is tested when all the stations are operating. Figure 6.12 shows the average system time under different traffic intensities, while Figure 6.13 shows the average power consumption for each station, normalized to the power rating of a single charger. The algorithm was run for 150 iterations for each point. The performance is compared to that of the nearest station policy, which simply assigns each EV to its closest station. From Figure 6.12 we deduce the following. First, the algorithm's
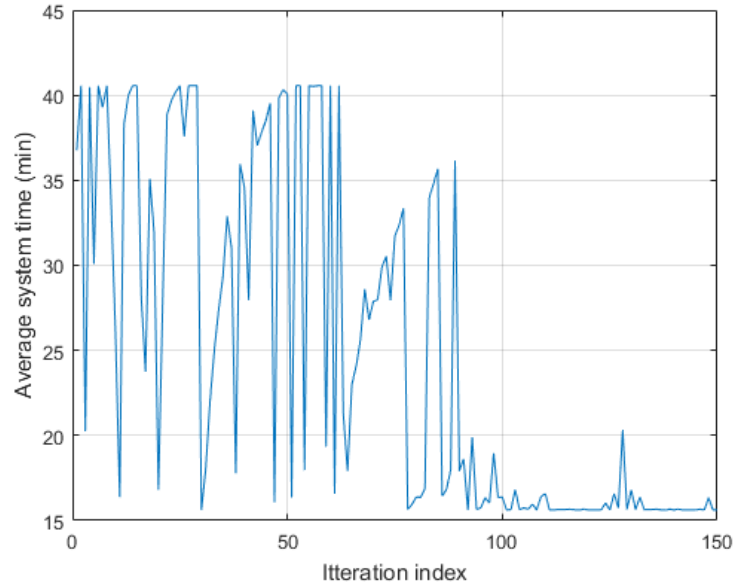
Figure 6.11: Performance evaluation for the two-station system under 150 consecutive iterations.

performance is not monotonic, because 150 iterations were not sufficient for some points to reach their optimal values. Second, the algorithm performs better at high traffic intensities, which is expected, because at low traffic intensities the EV's waiting time is most likely to be low and there is no need for the EV to be assigned to a farther station.
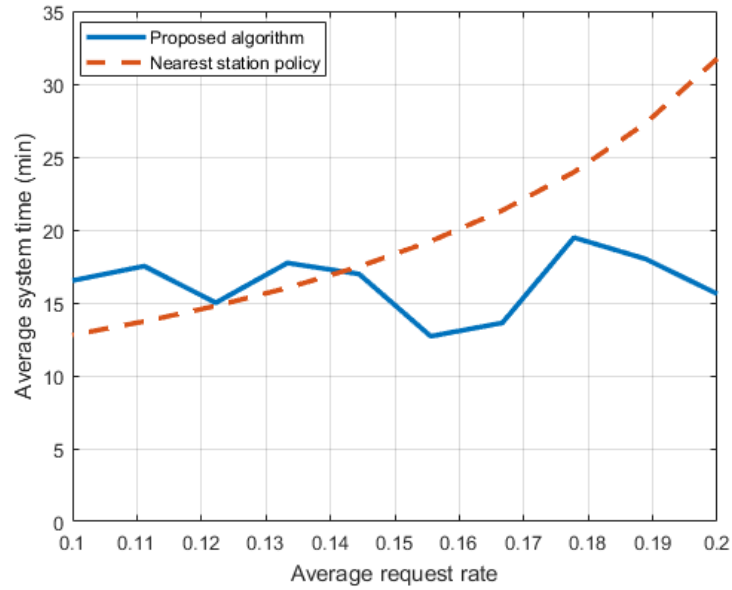
Figure 6.12: Performance evaluation for the four-station system under 150 consecutive iterations.
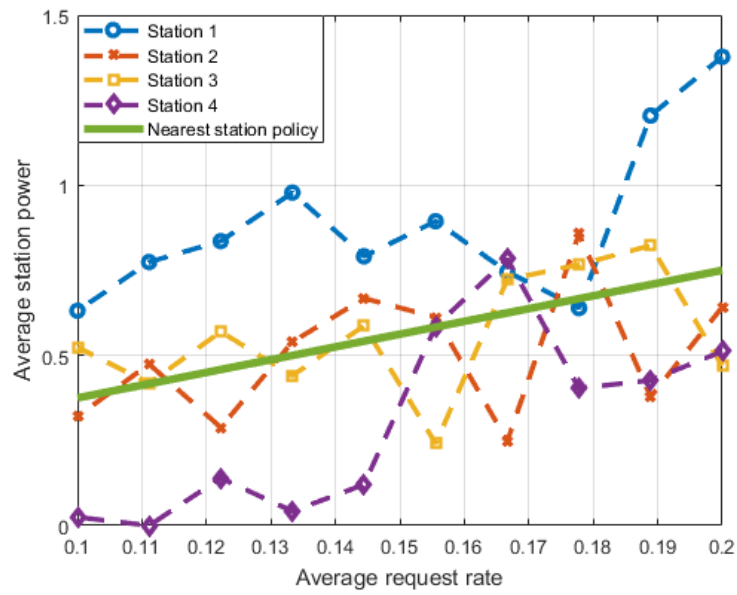
Figure 6.13: Average power loading for each station under our proposed algorithm (dashed), compared to that of the nearest station policy (solid).
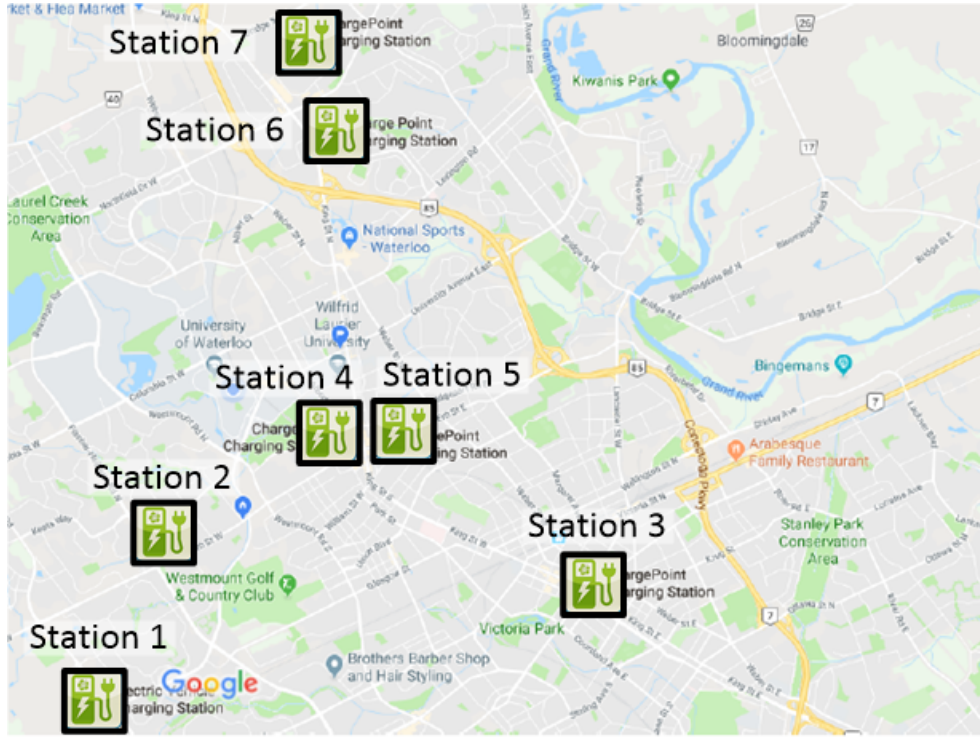
Figure 6.14: Service area under consideration for subsection 6.4.2.

6.4.2 Case study

In this subsection, we investigate utilizing our methodology assuming a high EV penetration within the town of Waterloo, Ontario, Canada. Figure 6.14 shows the location of 7 different stations within Waterloo. We assume a high charging request arrival rate $\lambda = 3$ requests/ min, which means that our methodology will assign on average more than 4000 EVs/ day. The number of chargers has to accommodate such high arrival rate, and was selected to be $\{3, 7, 5, 9, 6, 7, 10\}$ for Station 1 to Station 7, respectively.

We apply our methodology two times: first, when the order of assignment is the same as the order shown in Figure 6.14, and second, when the order of assignment is a descending order according to the number of chargers available in each station. The average system time for both cases was found to be 11.35 and 10.77 minutes, respectively. Figure 6.15 shows the average load for each station under both cases. We can conclude that the performance might be slightly better if we used a descending order of station assignment, given the same number of iterations.

87
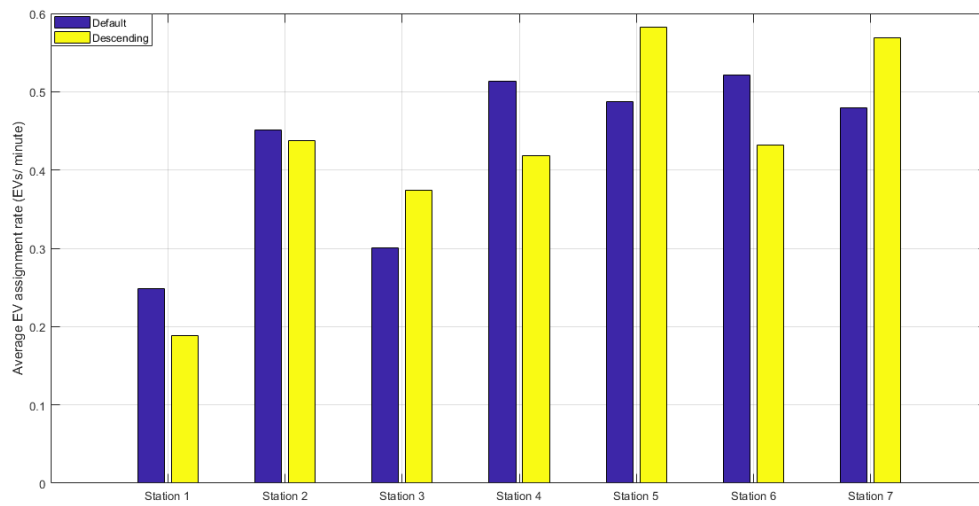
Figure 6.15: Average load for each station under 1) default order of assignment (blue), and 2) descending order of assignment (yellow).

6.5 Summary

A large penetration of electric vehicles (EVs) to the transport sector can easily overload the power network. Before taking the expensive decision of upgrading the power network, it is essential to make sure that the existing charging infrastructure is efficiently utilized. Depending on the concept of resource sharing, we aim to propose a methodology for optimal EVs' assignment to different charging stations. The core of our methodology is formulating our problem as a CT-MDP problem. In order to avoid the *curse of dimensionality*, we proposed a distributed approach for solving the original problem, where the decision of accepting/ rejecting an EV is taken in turns. We assigned a virtual rejection penalty for each station to "encourage" it to accept an incoming charging request. We then used Bayesian optimization to determine the optimal values of the virtual rejection penalties. The numerical results showed good compliance between the proposed analytical and simulation models. Our proposed methodology was effective in reducing the average system time for an EV user, especially during high traffic intensity.

Chapter 7

Conclusions and Future Works

7.1 Conclusions

Giving the demand a bigger role in supply-demand matching is one of the basic concepts that future power grids are expected to be built on. One of the approaches for controlling electric energy demand is through demand response (DR), which is concerned with modifying demand via providing various financial incentives to consumers. Demand modification can take many forms, which can be divided into two main categories: 1) demand curtailment, and 2) demand deferral. Our research work belongs to the second category, were different energy demands can be deferred in time, but they have to be completely satisfied at the end. While the majority of current DR programs prefer dealing with large energy consumers (like industrial consumers), our work aims to exploit the significant DR potential of small consumers (like residential and electric vehicles (EVs) consumers). The DR of these consumers has several challenges. First, since the individual consumer demand is small, residential/ EV DR programs should incorporate a large number of consumers to provide a significant benefit to the DR operator. Second, it is difficult to determine in advance when these consumers will demand energy, i.e., the arrival times of the demands are random. We explored these issues for three different DR applications: 1) using residential DR for energy cost minimization, 2) using residential DR for reducing the fluctuations resulting from integrating large number of RESs, and 3) managing the assignment of a large number of EVs to charging stations.

As optimization algorithms work efficiently when there are a few numbers of resources to be managed. The key to manage large-scale DR problems is to develop suitable methodologies for demand aggregation. In these methodologies, demands are classified into different

groups, each group is represented by a proper aggregation model. In our research work, queueing theory was used as the core of our aggregation methodologies. Each queue represents one type of demand classes. The decision variables used are queue scheduling and routing decisions. Admission control decisions were not used, since our system is lossless, and every demand has to be satisfied.

The demand requirements of different residential appliances were classified to fixed classes of demands. Each class of demands is defined by three parameters, power consumption level, energy duration, and a deadline for satisfying its requirement. Following this approach, new units of demand were defined, referred to as "demand block", where each unit represents a certain class of demands. The routing of demand requirements to different classes was done using the mapping algorithm, which is based on a minimum distortion criterion, independent of the DR objective. On the other hand, scheduling decisions have to be tailored for each DR problem. In the first problem, the main driving signal is the day-ahead pricing, which is deterministic. Hence, an offline scheduling (optimization) algorithm was suitable. The algorithm was based on the cutting plane method in which relaxed constraints were evaluated using simulation. Simulation has the advantage of allowing the algorithm to be applied on any general, non-stationary demand arrival process. On the other hand, the algorithm is not suitable for the second problem, where the main driving signal is the net non-controllable demand which is stochastic. For this problem, we developed an online scheduling algorithm based on Lyapunov optimization. The performance of the algorithm was addressed from two criteria: 1) Long-term time-average criterion, and 2) short-term sample-path criterion. The first criterion requires an i.i.d. assumption for the demands' arrivals and the driving signal, whereas the second criterion does not require such assumption.

Realistic demand, price, and wind data were used to evaluate our proposed methodology/algorithms. For the first problem, we showed how the aggregated demand profile was modified such that the energy consumption cost was reduced while not exceeding the capacity of the distribution transformer. As the capacity constraint become relaxed, the magnitude of cost reduction become close to that of the ideal case when there is no coordination between consumers. For the second problem, we showed that the fluctuations in the aggregated demand profile are reduced as the controllable demand portion becomes more delay tolerant. We also showed that there is an optimal number of queues for our given residential demand data, beyond which the performance is not improved.

The last part of our research is to manage the assignment of EVs to charging stations. In this problem, we explored the benefit of resource sharing, where each charging station not only serve charging requests within its region of operation, but from other regions as well. Each queue simply represents EVs corresponding to their assigned station. We

91

differentiated between queued and ongoing EVs. Unlike the previous problems, the decision variables are queue routing decisions, not queue scheduling. We preferred continuous-time control over discrete time for computational simplicity and user's convenience. The core of our routing algorithm is to use MDP to generate a queue routing policy. In order to avoid the curse of dimensionality, we used a distributed approach for solving the MDP problem based on Bayesian optimization. The use of MDP required several simplifying assumptions, e.g., the inter-arrival times between successive events are assumed to be exponentially distributed. Hence, our first concern was to compare our proposed analytical model with a more realistic simulation model. Our results showed good compliance between both models. Our algorithm proved to effectively reduce the system time especially under high traffic intensity.

The contribution of this thesis can be summarized as follows:

1) We developed a methodology for managing a large number of residential appliances. The methodology is based on aggregating the demand into several classes defined by power level, power duration and deadline for satisfying the demand. The methodology is composed of two algorithms: 1) mapping algorithm, which maps different appliance demand requirements to the predefined set of demands, and 2) optimization algorithm, which is responsible for scheduling different classes of demand to achieve the DR objective. The optimization algorithm is tailored to fit the DR objective and the system model.

2) We developed a technique for treating TCL appliances as deferrable loads. This facilitated using mathematical tools for managing them such as queueing theory which cares about time performance instead of temperature performance.

3) We developed two demand scheduling algorithms, one is offline based on cutting-plane method, which exploits the information of the deterministic driving signal of DAP, and the other algorithm is online based on Lyapunov optimization, which is robust against the stochastic nature of the driving signal of the net non-controllable demand profile.

4) We developed a methodology for assigning a large number of EVs to charging stations. The core of our methodology is formulating our problem as a CT-MDP problem. In order to avoid the *curse of dimensionality*, we proposed a distributed approach for solving the original problem, where the decision of accepting/ rejecting an EV is taken in-turn. We assigned a virtual rejection penalty for each station to "encourage it to accept an incoming charging request. We then used Bayesian optimization to determine the optimal values of the virtual rejection penalties.

7.2 Further Research Topics

In the future, the impact of DR algorithms on distribution networks is worth to be investigated. Instead of the simplified distribution network model used in our work, a realistic distribution network should be used instead. The model should incorporate real power losses, reactive power flow, voltage and current constraints, . . . etc. The objective of this topic is to design future power networks to become flexible for accommodating versatile types of DR programs.

Setting deadlines for satisfying residential consumers' demand might not be sufficient to achieve good consumer's convenience. Giving the consumer the freedom to use his controllable appliances, even if they were queued by the DR operator, is a better approach to address different consumers' potentials. However, this approach will cause uncontrollable queue scheduling, from the operator's perspective; Hence, proposed DR algorithms may need to be changed. Consumers receive compensations according to the magnitude of their contribution to DR. Understanding consumers' behavior towards different compensation (rewarding) schemes is essential to model the uncontrollable queue scheduling.

There are several useful extensions to the EV part of our work. First, it is practical to include more parameters to classify EVs' charging requests other than their charging locations. For example, if the current SoC is included, we can know which stations are reachable for each particular charging request. Also, including re-routing decisions, i.e., re-assigning ongoing EVs, can improve the utilization of existing charging resources. Finally, the total charging power margin might be limited and variable, e.g., the power network operator might prioritize serving residential consumers. Accordingly, charging stations might not be able to operate at their maximum charging capacities, which will require adding queue scheduling decisions to the original queue routing decisions. All these suggested extensions will require additional computational burden which need to be taken into consideration.

References

[1] K. Bhattacharya, "Lecture notes in Power Systems Operation (ECE 666)," January 2014.

[2] "Website of North American Electric Reliability Corporation," Available online: http://www.nerc.com/, Jan. 2016.

[3] "Benefits of demand response in electricity markets and recommendations for achieving them," *US Department of Energy*, Feb. 2006.

[4] Z. Chen, L. Wu, and Y. Fu, "Real-time price-based demand response management for residential appliances via stochastic optimization and robust optimization," *IEEE Transactions on Smart grid*, vol. 3, no. 4, pp. 1822–1831, Sept. 2012.

[5] Y. Li, B. L. Ng, M. Trayer, and L. Liu, "Automated residential demand response: Algorithmic implications of pricing models," *IEEE Transactions on Smart Grid*, vol. 3, no. 4, pp. 1712–1721, Sept. 2012.

[6] Z. Zhao, W. C. Lee, Y. Shin, and K.-B. Song, "An optimal power scheduling method for demand response in home energy management system," *IEEE Transactions on Smart Grid*, vol. 4, no. 3, pp. 1391–1400, June 2013.

[7] S.-J. Kim and G. Giannakis, "Scalable and robust demand response with mixed-integer constraints," *IEEE Transactions on Smart Grid*, vol. 4, no. 4, pp. 2089–2099, Apr. 2013.

[8] P. Samadi, H. Mohsenian-Rad, V. W. Wong, and R. Schober, "Real-time pricing for demand response based on stochastic approximation," *IEEE Transactions on Smart Grid*, vol. 5, no. 2, pp. 789–798, Feb. 2014.

[9] A.-H. Mohsenian-Rad, V. W. Wong, J. Jatskevich, R. Schober, and A. Leon-Garcia, "Autonomous demand-side management based on game-theoretic energy consumption scheduling for the future smart grid," *IEEE Transactions on Smart Grid*, vol. 1, no. 3, pp. 320–331, Dec. 2010.

[10] A.-H. Mohsenian-Rad and A. Leon-Garcia, "Optimal residential load control with price prediction in real-time electricity pricing environments," *IEEE Transactions on Smart Grid*, vol. 1, no. 2, pp. 120–133, Aug. 2010.

[11] P. Chavali, P. Yang, and A. Nehorai, "A distributed algorithm of appliance scheduling for home energy management system," *IEEE Transactions on Smart Grid*, vol. 5, no. 1, pp. 282–290, Jan. 2014.

[12] P. Yi, X. Dong, A. Iwayemi, C. Zhou, and S. Li, "Real-time opportunistic scheduling for residential demand response," *IEEE Transactions on Smart Grid*, vol. 4, no. 1, pp. 227–234, Feb. 2013.

[13] T.-H. Chang, M. Alizadeh, and A. Scaglione, "Real-time power balancing via decentralized coordinated home energy scheduling," *IEEE Transactions on Smart Grid*, vol. 4, no. 3, pp. 1490–1504, Aug. 2013.

[14] K. Turitsyn, S. Backhaus, M. Ananyev, and M. Chertkov, "Smart finite state devices: A modeling framework for demand response technologies," in *Proceedings of 50th IEEE Conference on Decision and Control and European Control Conference (CDC-ECC)*, Dec. 2011.

[15] P. Samadi, H. Mohsenian-Rad, V. W. Wong, and R. Schober, "Tackling the load uncertainty challenges for energy consumption scheduling in smart grid," *IEEE Transactions on Smart Grid*, vol. 4, no. 2, pp. 1007–1016, 2013.

[16] J. Mathieu, M. Dyson, D. Callaway, and A. Rosenfeld, "Using residential electric loads for fast demand response: The potential resource and revenues, the costs, and policy recommendations," *Proceedings of the ACEEE Summer Study on Buildings, Pacific Grove, CA*, vol. 1000, no. 2000, p. 3000, Aug. 2012.

[17] H. Hao, B. M. Sanandaji, K. Poolla, and T. L. Vincent, "A generalized battery model of a collection of thermostatically controlled loads for providing ancillary service," in *Proceedings of 51st IEEE Annual Allerton Conference on Communication, Control, and Computing (Allerton)*, Oct. 2013.

[18] F. Alesiani and N. Maslekar, "Optimization of charging stops for fleet of electric vehicles: A genetic approach," *Intelligent Transportation Systems Magazine*, vol. 6, no. 3, pp. 10–21, 2014.

[19] A. Afroditi, M. Boile, S. Theofanis, E. Sdoukopoulos, and D. Margaritis, "Electric vehicle routing problem with industry constraints: trends and insights for future research," *Transportation Research Procedia*, vol. 3, pp. 452–459, 2014.

[20] M. Bruglieri, F. Pezzella, O. Pisacane, and S. Suraci, "A variable neighborhood search branching for the electric vehicle routing problem with time windows," *Electronic Notes in Discrete Mathematics*, vol. 47, pp. 221–228, Feb 2015.

[21] Á. Felipe, M. T. Ortuño, G. Righini, and G. Tirado, "A heuristic approach for the green vehicle routing problem with multiple technologies and partial recharges," *Transportation Research Part E: Logistics and Transportation Review*, vol. 71, pp. 111–128, November 2014.

[22] M. P. Fanti, A. M. Mangini, G. Pedroncelli, and W. Ukovich, "Assignment of electrical vehicles to charging stations by a distributed approach," in *Proceedings of IEEE European Control Conference (ECC)*, June 2014.

[23] A. Ruzmetov, A. Nait-Sidi-Moh, M. Bakhouya, and J. Gaber, "Towards an optimal assignment and scheduling for charging electric vehicles," in *Proceedings of IEEE International Renewable and Sustainable Energy Conference (IRSEC)*, 2013.

[24] M. Wang, H. Liang, R. Zhang, R. Deng, and X. Shen, "Mobility-aware coordinated charging for electric vehicles in VANET-enhanced smart grid," *IEEE Journal on Selected Areas in Communications*, vol. 32, no. 7, pp. 1344–1360, Aug. 2014.

[25] Z. Luo, Z. Hu, Y. Song, Z. Xu, and H. Lu, "Optimal coordination of plug-in electric vehicles in power grids with cost-benefit analysis —part I: Enabling techniques," *IEEE Transactions on Power Systems*, vol. 28, no. 4, pp. 3546–3555, 2013.

[26] Z. Ma, D. S. Callaway, I. Hiskens *et al.*, "Decentralized charging control of large populations of plug-in electric vehicles," *IEEE Transactions on Control Systems Technology*, vol. 21, no. 1, pp. 67–78, Jan. 2013.

[27] J. Hu, S. You, M. Lind, and J. Ostergaard, "Coordinated charging of electric vehicles for congestion prevention in the distribution grid," *IEEE Transactions on Smart Grid*, vol. 5, no. 2, pp. 703–711, Feb. 2014.

[28] Z. Li, Q. Guo, H. Sun, Y. Wang, and S. Xin, "Emission-concerned wind-EV coordination on the transmission grid side with network constraints: Concept and case study," *IEEE Transactions on Smart Grid*, vol. 4, no. 3, pp. 1692–1704, Sept. 2013.

[29] J. de Hoog, T. Alpcan, M. Brazil, D. A. Thomas, and I. Mareels, "Optimal charging of electric vehicles taking distribution network constraints into account," *IEEE Transactions on Power Systems*, vol. 30, no. 1, pp. 365–375, Jan. 2015.

[30] M. E. Khodayar, L. Wu, and Z. Li, "Electric vehicle mobility in transmission-constrained hourly power generation scheduling," *IEEE Transactions on Smart Grid*, vol. 4, no. 2, pp. 779–788, 2013.

[31] R. Li, Q. Wu, and S. S. Oren, "Distribution locational marginal pricing for optimal electric vehicle charging management," *IEEE Transactions on Power Systems*, vol. 29, no. 1, pp. 203–211, Jan. 2014.

[32] W. Yao, J. Zhao, F. Wen, Y. Xue, and G. Ledwich, "A hierarchical decomposition approach for coordinated dispatch of plug-in electric vehicles," *IEEE Transactions on Power Systems*, vol. 28, no. 3, pp. 2768–2778, Aug. 2013.

[33] S. Dempe, *Foundations of Bilevel Programming*. Springer Science & Business Media, 2002.

[34] R. R. Pakala, "A study on applications of Stackelberg game strategies in concurrent design models," Ph.D. dissertation, University of Houston, May 1994.

[35] R. Deng, Z. Yang, J. Chen, N. R. Asr, and M.-Y. Chow, "Residential energy consumption scheduling: A coupled-constraint game approach," *IEEE Transactions on Smart Grid*, vol. 5, no. 3, pp. 1340–1350, Apr. 2014.

[36] M. J. Neely, A. S. Tehrani, and A. G. Dimakis, "Efficient algorithms for renewable energy allocation to delay tolerant consumers," in *Proceedings of First IEEE International Conference on Smart Grid Communications (SmartGridComm)*, Oct. 2010.

[37] Y. Guo, M. Pan, and Y. Fang, "Optimal power management of residential customers in the smart grid," *IEEE Transactions on Parallel and Distributed Systems*, vol. 23, no. 9, pp. 1593–1606, Jan. 2012.

[38] Y. Guo, M. Pan, Y. Fang, and P. P. Khargonekar, "Decentralized coordination of energy utilization for residential households in the smart grid," *IEEE Transactions on Smart Grid*, vol. 4, no. 3, pp. 1341–1350, Aug. 2013.

[39] Y. Huang, S. Mao, and R. M. Nelms, "Adaptive electricity scheduling in microgrids," in *Proceedings of IEEE INFOCOM'13*, Apr. 2013.

[40] D. O. Neill, M. Levorato, A. Goldsmith, and U. Mitra, "Residential demand response using reinforcement learning," in *Proceedings of First IEEE International Conference on Smart Grid Communications (SmartGridComm)*, Oct. 2010.

[41] A. J. Conejo, J. M. Morales, and L. Baringo, "Real-time demand response model," *IEEE Transactions on Smart Grid*, vol. 1, no. 3, pp. 236–242, Oct. 2010.

[42] C. De Jonghe, B. F. Hobbs, and R. Belmans, "Optimal generation mix with short-term demand response and wind penetration," *IEEE Transactions on Power Systems*, vol. 27, no. 2, pp. 830–839, Jan. 2012.

[43] R. Yu, W. Yang, and S. Rahardja, "A statistical demand-price model with its application in optimal real-time price," *IEEE Transactions on Smart Grid*, vol. 3, no. 4, pp. 1734–1742, Dec. 2012.

[44] S.-E. Fleten and E. Pettersen, "Constructing bidding curves for a price-taking retailer in the Norwegian electricity market," *IEEE Transactions on Power Systems*, vol. 20, no. 2, pp. 701–708, May 2005.

[45] N. Lu, D. P. Chassin, and S. E. Widergren, "Modeling uncertainties in aggregated thermostatically controlled loads using a state queueing model," *IEEE Transactions on Power Systems*, vol. 20, no. 2, pp. 725–733, May 2005.

[46] E. Kara, M. Berges, and G. Hug, "Impact of disturbances on modeling of thermostatically controlled loads for demand response," *IEEE Transactions on Smart Grid*, vol. 6, no. 5, pp. 2560–2568, Sept. 2015.

[47] J. L. Mathieu, S. Koch, and D. S. Callaway, "State estimation and control of electric loads to manage real-time energy imbalance," *IEEE Transactions on Power Systems*, vol. 28, no. 1, pp. 430–440, Jan. 2013.

[48] D. Ban, G. Michailidis, and M. Devetsikiotis, "Demand response control for PHEV charging stations by dynamic price adjustments," in *Proceedings of IEEE Innovative Smart Grid Technologies (ISGT)*, Jan. 2012.

[49] "Website of Ontario's independent electricity system operator," Available online: https://www.ieso.ca, Jan. 2016.

[50] J. Widén and E. Wäckelgård, "A high-resolution stochastic model of domestic activity patterns and electricity demand," *Applied Energy*, vol. 87, no. 6, pp. 1880–1892, June 2010.

[51] P. Du and N. Lu, "Appliance commitment for household load scheduling," *IEEE Transactions on Smart Grid*, vol. 2, no. 2, pp. 411–419, May 2011.

[52] J. Atlason, M. A. Epelman, and S. G. Henderson, "Call center staffing with simulation and cutting plane methods," *Annals of Operations Research*, vol. 127, no. 1-4, pp. 333–358, 2004.

[53] P. E. Fishback, *Linear and nonlinear programming with Maple: an interactive, applications-based approach.* CRC Press, 2009.

[54] J. Kelly and W. Knottenbelt, "UK-DALE: A dataset recording UK Domestic Appliance-Level Electricity demand and whole-house demand," *ArXiv e-prints*, vol. 59, June 2014.

[55] I. Dincer, "Environmental impacts of energy," *Energy Policy*, vol. 27, no. 14, pp. 845–854, Dec. 1999.

[56] K. Neuhoff, "Large-scale deployment of renewables for electricity generation," *Oxford Review of Economic Policy*, vol. 21, no. 1, pp. 88–110, 2005.

[57] J. von Appen, M. Braun, T. Stetz, K. Diwold, and D. Geibel, "Time in the sun: the challenge of high PV penetration in the German electric grid," *IEEE Power and Energy magazine*, vol. 11, no. 2, pp. 55–64, 2013.

[58] M. Liserre, T. Sauter, and J. Y. Hung, "Future energy systems: Integrating renewable energy sources into the smart power grid through industrial electronics," *IEEE industrial electronics magazine*, vol. 4, no. 1, pp. 18–37, 2010.

[59] F. Katiraei and J. R. Aguero, "Solar PV integration challenges," *IEEE Power and Energy Magazine*, vol. 9, no. 3, pp. 62–71, 2011.

[60] E. Ela and M. O'Malley, "Studying the variability and uncertainty impacts of variable generation at multiple timescales," *IEEE Transactions on Power Systems*, vol. 27, no. 3, pp. 1324–1333, 2012.

[61] N. Navid and G. Rosenwald, "Market solutions for managing ramp flexibility with high penetration of renewable resource," *IEEE Transactions on Sustainable Energy*, vol. 3, no. 4, pp. 784–790, 2012.

[62] E. Ela, B. Kirby, E. Lannoye, M. Milligan, D. Flynn, B. Zavadil, and M. O'Malley, "Evolution of operating reserve determination in wind power integration studies," in *Power and Energy Society General Meeting, 2010 IEEE*. IEEE, 2010, pp. 1–8.

[63] E. Lannoye, D. Flynn, and M. O'Malley, "Evaluation of power system flexibility," *IEEE Transactions on Power Systems*, vol. 27, no. 2, pp. 922–931, 2012.

[64] M. Ghofrani, A. Arabali, M. Etezadi-Amoli, and M. Fadali, "Energy storage application for performance enhancement of wind integration," *IEEE Transactions on Power Systems*, vol. 28, no. 4, pp. 4803–4811, 2013.

[65] B. Hartmann and A. Dan, "Methodologies for storage size determination for the integration of wind power," *IEEE Transactions on Sustainable Energy*, vol. 5, no. 1, pp. 182–189, 2014.

[66] T. Kousksou, P. Bruel, A. Jamil, T. El Rhafiki, and Y. Zeraouli, "Energy storage: Applications and challenges," *Solar Energy Materials and Solar Cells*, vol. 120, pp. 59–80, 2014.

[67] "Grid energy storage," *US Department of Energy*, Dec. 2013.

[68] B. Zakeri and S. Syri, "Electrical energy storage systems: A comparative life cycle cost analysis," *Renewable and Sustainable Energy Reviews*, vol. 42, pp. 569–596, Feb 2015.

[69] Z. Tan, P. Yang, and A. Nehorai, "An optimal and distributed demand response strategy with electric vehicles in the smart grid," *IEEE Transactions on Smart Grid*, vol. 5, no. 2, pp. 861–869, 2014.

[70] G. Wang, J. Zhao, F. Wen, Y. Xue, and G. Ledwich, "Dispatch strategy of PHEVs to mitigate selected patterns of seasonally varying outputs from renewable generation," *IEEE Transactions on Smart Grid*, vol. 6, no. 2, pp. 627–639, 2015.

[71] P. Yang, P. Chavali, E. Gilboa, and A. Nehorai, "Parallel load schedule optimization with renewable distributed generators in smart grids," *IEEE Transactions on Smart Grid*, vol. 4, no. 3, pp. 1431–1441, Aug. 2013.

[72] Z. Zhu, S. Lambotharan, W. H. Chin, and Z. Fan, "A game theoretic optimization framework for home demand management incorporating local energy resources," *IEEE Transactions on Industrial Informatics*, vol. 11, no. 2, pp. 353–362, Apr. 2015.

[73] M. J. Neely, "Energy optimal control for time-varying wireless networks," *IEEE transactions on Information Theory*, vol. 52, no. 7, pp. 2915–2934, Jul. 2006.

[74] ——, "Stochastic network optimization with application to communication and queueing systems," *Synthesis Lectures on Communication Networks*, vol. 3, no. 1, pp. 1–211, 2010.

[75] "Website of national renewable energy laboratory," Available online: http://http://www.nrel.gov/, Jan. 2016.

[76] "Gaia-wind 133-11kW data sheet," Available online: http://www.wind-power-program.com/Library/Turbine%20leaflets/Gaia/Gaia-Wind_Datasheet_UK[1].pdf, Jan. 2017.

[77] "An examination of electric vehicle technology, infrastructure requirements and market developments," *The Office of Climate Change and Energy Efficiency, the Government of Newfoundland and Labrador*, Nov 2015.

[78] J. W. Brennan and T. E. Barder, "Battery electric vehicles vs. internal combustion engine vehicles: A united states-based comprehensive assessment," *Arthur D. Little*, 2016.

[79] T. Trigg, P. Telleen, R. Boyd, F. Cuenot, D. DAmbrosio, R. Gaghen, J. Gagné, A. Hardcastle, D. Houssin, A. Jones *et al.*, "Global EV outlook: understanding the electric vehicle landscape to 2020," *Int. Energy Agency*, pp. 1–40, Apr. 2013.

[80] "Electric vehicles in Europe: gearing up for a new phase?" *Amsterdam Roundtable Foundation*, 2014.

[81] "Multi-state ZEV action plan," *ZEV Program Implementation Task Force*, 2014.

[82] G. Pistoia, *Lithium-ion batteries: advances and applications.* Newnes, 2013.

[83] M. Yilmaz and P. T. Krein, "Review of battery charger topologies, charging power levels, and infrastructure for plug-in electric and hybrid vehicles," *IEEE Transactions on Power Electronics*, vol. 28, no. 5, pp. 2151–2169, May 2013.

[84] F. Bullo, E. Frazzoli, M. Pavone, K. Savla, and S. L. Smith, "Dynamic vehicle routing for robotic systems," *Proceedings of the IEEE*, vol. 99, no. 9, pp. 1482–1504, 2011.

[85] F. Hausler, E. Crisostomi, A. Schlote, I. Radusch, and R. Shorten, "Stochastic park-and-charge balancing for fully electric and plug-in hybrid vehicles," *IEEE Transactions on Intelligent Transportation Systems*, vol. 15, no. 2, pp. 895–901, 2014.

[86] I. S. Bayram, G. Michailidis, and M. Devetsikiotis, "Unsplittable load balancing in a network of charging stations under QoS guarantees," *IEEE Transactions on Smart Grid*, vol. 6, no. 3, pp. 1292–1302, 2015.

[87] M. L. Puterman, "Markov Decision Processes: Discrete Stochastic Dynamic Programming (Wiley Series in Probability and Statistics)," 2005.

[88] E. Brochu, V. M. Cora, and N. De Freitas, "A tutorial on Bayesian optimization of expensive cost functions, with application to active user modeling and hierarchical reinforcement learning," *arXiv preprint arXiv:1012.2599*, 2010.

Appendix A

Demand Diversity

We provide the data used in Chapter 4 to diversify the demand of residential consumers, given the appliances' parameters of the reference consumer which were also discussed in Chapter 4. The first reason for demand diversity is that consumers can occupy different states at the same time. The transition probabilities of the three different states (1='abs-cent', 2='inactive', 3='active') are given listed in Table A.1.

  We diversify appliance parameters for different consumers as follows:

1) For non-controllable appliances: the appliance' power level and turn-on probability is distributed uniformly within ±10% of the reference value. The mean turn-on duration changes within ±1 time slot.

2) For deferrable appliances: Turn-on probability is distributed uniformly within ±10% of the reference value.

3) For TCL appliances: Both thermal resistance and capacitance are distributed within ±10% of their reference value.

Table A.1: Consumer state transition probabilities

t	p_{11}	p_{12}	p_{13}	p_{21}	p_{22}	p_{23}	p_{31}	p_{32}	p_{33}
1	0.882	0.118	0	0.067	0.927	0.005	0	0.25	0.75
2	0.837	0.163	0	0.064	0.922	0.014	0	0.273	0.727
3	0.87	0.13	0	0.023	0.977	0	0	0.231	0.769
4	0.747	0.253	0	0.062	0.938	0	0	0.7	0.3
5	0.839	0.161	0	0.06	0.937	0.003	0	0.333	0.667
6	0.83	0.17	0	0.07	0.921	0.008	0	0.667	0.333
7	0.861	0.139	0	0.046	0.948	0.006	0	0	1
8	0.761	0.239	0	0.064	0.933	0.003	0	0.167	0.833
9	0.857	0.143	0	0.074	0.923	0.003	0	0.167	0.833
10	0.888	0.112	0	0.065	0.935	0	0.167	0.667	0.167
11	0.865	0.135	0	0.036	0.961	0.003	0	0	1
12	0.694	0.306	0	0.042	0.955	0.003	0	0.5	0.5
13	0.786	0.214	0	0.072	0.925	0.003	0	0.5	0.5
14	0.864	0.136	0	0.11	0.89	0	0	0	1
15	0.836	0.164	0	0.073	0.927	0	0	0.5	0.5
16	0.824	0.176	0	0.058	0.942	0	1	0	0
17	0.867	0.133	0	0.079	0.921	0	-	-	-
18	0.81	0.19	0	0.075	0.925	0	-	-	-
19	0.83	0.17	0	0.083	0.917	0	-	-	-
20	0.827	0.173	0	0.047	0.953	0	-	-	-
21	0.831	0.169	0	0.079	0.918	0.003	-	-	-
22	0.828	0.172	0	0.052	0.95	0.003	0	0	1
23	0.813	0.188	0	0.067	0.93	0.003	0	0	1
24	0.778	0.222	0	0.039	0.958	0.003	0	0.667	0.333
25	0.838	0.162	0	0.089	0.911	0	0	0.5	0.5
26	0.758	0.242	0	0.093	0.907	0	0	0	1
27	0.84	0.16	0	0.066	0.934	0	0	1	0
28	0.819	0.181	0	0.078	0.922	0	-	-	-
29	0.869	0.131	0	0.046	0.954	0	-	-	-
30	0.883	0.117	0	0.063	0.937	0	-	-	-
31	0.828	0.172	0	0.08	0.92	0	-	-	-
32	0.839	0.161	0	0.053	0.947	0	-	-	-
33	0.803	0.197	0	0.07	0.93	0	-	-	-
34	0.907	0.093	0	0.063	0.937	0	-	-	-

35	0.841	0.159	0	0.068	0.929	0.003	-	-	-
36	0.768	0.232	0	0.047	0.953	0	0	0	1
37	0.835	0.165	0	0.115	0.885	0	0	0	1
38	0.85	0.15	0	0.091	0.909	0	0	0	1
39	0.831	0.169	0	0.071	0.929	0	0	1	0
40	0.8	0.2	0	0.054	0.946	0	-	-	-
41	0.872	0.128	0	0.092	0.908	0	-	-	-
42	0.884	0.116	0	0.092	0.908	0	-	-	-
43	0.867	0.133	0	0.083	0.917	0	-	-	-
44	0.846	0.154	0	0.084	0.916	0	-	-	-
45	0.784	0.216	0	0.05	0.95	0	-	-	-
46	0.789	0.211	0	0.069	0.931	0	-	-	-
47	0.828	0.172	0	0.064	0.936	0	-	-	-
48	0.841	0.159	0	0.085	0.915	0	-	-	-
49	0.827	0.173	0	0.065	0.935	0	-	-	-
50	0.846	0.154	0	0.0734	0.926	0	-	-	-
51	0.813	0.187	0	0.1	0.9	0	-	-	-
52	0.869	0.131	0	0.086	0.914	0	-	-	-
53	0.882	0.118	0	0.072	0.928	0	-	-	-
54	0.777	0.223	0	0.083	0.917	0	-	-	-
55	0.85	0.15	0	0.042	0.955	0.003	-	-	-
56	0.862	0.138	0	0.088	0.913	0	0	1	0
57	0.837	0.163	0	0.058	0.942	0	-	-	-
58	0.858	0.142	0	0.047	0.953	0	-	-	-
59	0.809	0.191	0	0.071	0.929	0	-	-	-
60	0.805	0.195	0	0.064	0.936	0	-	-	-
61	0.805	0.195	0	0.096	0.904	0	-	-	-
62	0.837	0.163	0	0.098	0.902	0	-	-	-
63	0.793	0.207	0	0.07	0.93	0	-	-	-
64	0.818	0.182	0	0.065	0.935	0	-	-	-
65	0.842	0.158	0	0.064	0.933	0.003	-	-	-
66	0.812	0.188	0	0.061	0.939	0	0	1	0
67	0.859	0.141	0	0.054	0.94	0.006	-	-	-
68	0.836	0.164	0	0.079	0.921	0	0	1	0
69	0.737	0.263	0	0.052	0.948	0	-	-	-
70	0.73	0.27	0	0.055	0.942	0.003	-	-	-

71	0.728	0.272	0	0.042	0.955	0.003	0	1	0
72	0.644	0.356	0	0.033	0.967	0	0	1	0
73	0.8289	0.171	0	0.11	0.877	0.013	-	-	-
74	0.792	0.198	0.01	0.068	0.932	0	0	0.6	0.4
75	0.788	0.212	0	0.054	0.934	0.011	0	0.667	0.333
76	0.782	0.218	0	0.068	0.923	0.009	0	0.4	0.6
77	0.786	0.214	0	0.086	0.908	0.006	0	0.667	0.333
78	0.721	0.279	0	0.07	0.922	0.009	0	1	0
79	0.788	0.212	0	0.051	0.926	0.023	0	1	0
80	0.79	0.21	0	0.054	0.931	0.014	0	0.875	0.125
81	0.653	0.347	0	0.042	0.935	0.023	0	0.833	0.167
82	0.785	0.215	0	0.035	0.932	0.032	0	1	0
83	0.667	0.307	0.027	0.03	0.96	0.011	0	0.833	0.167
84	0.787	0.213	0	0.013	0.954	0.033	0	0.5	0.5
85	0.698	0.283	0.019	0.044	0.923	0.034	0.059	0.824	0.118
86	0.745	0.255	0	0.052	0.907	0.04	0	0.875	0.125
87	0.77	0.23	0	0.045	0.916	0.04	0	0.667	0.333
88	0.734	0.266	0	0.038	0.928	0.035	0	0.762	0.238
89	0.738	0.262	0	0.024	0.953	0.024	0	0.444	0.556
90	0.704	0.296	0	0.052	0.919	0.029	0	0.579	0.421
91	0.534	0.466	0	0.024	0.942	0.034	0	0.632	0.368
92	0.6	0.4	0	0.06	0.917	0.023	0	0.55	0.45
93	0.792	0.208	0	0.046	0.91	0.043	0	0.944	0.056
94	0.732	0.25	0.018	0.026	0.919	0.055	0	0.667	0.333
95	0.667	0.333	0	0.024	0.921	0.056	0	0.714	0.286
96	0.628	0.372	0	0.034	0.922	0.044	0.034	0.655	0.31
97	0.805	0.195	0	0.038	0.913	0.049	0	0.769	0.231
98	0.708	0.292	0	0.021	0.927	0.052	0	0.76	0.24
99	0.619	0.357	0.024	0.031	0.925	0.044	0	0.808	0.192
100	0.789	0.211	0	0.025	0.924	0.051	0	0.652	0.348
101	0.675	0.3	0.025	0.041	0.938	0.021	0	0.536	0.464
102	0.605	0.372	0.023	0.013	0.946	0.041	0	0.591	0.409
103	0.71	0.29	0	0.023	0.932	0.045	0.038	0.577	0.385
104	0.75	0.25	0	0.008	0.965	0.028	0	0.536	0.464
105	0.778	0.222	0	0.03	0.953	0.017	0	0.667	0.333
106	0.727	0.273	0	0.012	0.946	0.042	0	0.667	0.333

107	0.759	0.241	0	0.025	0.935	0.04	0	0.455	0.545
108	0.531	0.469	0	0.015	0.96	0.025	0	0.536	0.464
109	0.783	0.217	0	0.032	0.939	0.029	0	0.348	0.652
110	0.774	0.226	0	0.023	0.97	0.008	0	0.407	0.593
111	0.848	0.152	0	0.022	0.963	0.015	0	0.556	0.444
112	0.757	0.243	0	0.02	0.965	0.015	0	0.286	0.714
113	0.667	0.333	0	0.017	0.96	0.022	0	0.5	0.5
114	0.71	0.29	0	0.022	0.958	0.02	0	0.294	0.706
115	0.774	0.226	0	0.015	0.973	0.012	0	0.35	0.65
116	0.767	0.233	0	0.007	0.963	0.03	0	0.333	0.667
117	0.731	0.269	0	0.02	0.968	0.013	0	0.417	0.583
118	0.778	0.222	0	0.015	0.983	0.002	0	0.421	0.579
119	0.667	0.333	0	0.017	0.954	0.029	0	0.417	0.583
120	0.6	0.4	0	0.012	0.97	0.017	0	0.368	0.632
121	0.65	0.35	0	0.024	0.956	0.02	0	0.421	0.579
122	0.522	0.478	0	0.022	0.951	0.027	0	0.263	0.737
123	0.667	0.333	0	0.005	0.983	0.012	0	0.32	0.68
124	0.75	0.25	0	0.012	0.981	0.007	0	0.455	0.545
125	0.824	0.176	0	0.007	0.967	0.026	0	0.533	0.467
126	0.765	0.235	0	0.029	0.962	0.01	0	0.389	0.611
127	0.72	0.28	0	0.015	0.956	0.029	0	0.2	0.8
128	0.667	0.333	0	0.017	0.968	0.015	0	0.333	0.667
129	0.826	0.174	0	0.005	0.975	0.02	0	0.364	0.636
130	0.571	0.429	0	0.017	0.956	0.027	0	0.318	0.682
131	0.684	0.316	0	0.007	0.983	0.01	0	0.385	0.615
132	0.75	0.25	0	0.002	0.978	0.019	0.05	0.55	0.4
133	0.786	0.214	0	0.012	0.974	0.014	0	0.625	0.375
134	0.813	0.188	0	0.007	0.976	0.017	0	0.583	0.417
135	0.688	0.313	0	0.012	0.955	0.033	0	0.364	0.636
136	0.625	0.375	0	0.015	0.976	0.01	0	0.429	0.571
137	0.813	0.188	0	0.017	0.964	0.019	0	0.375	0.625
138	0.8	0.2	0	0.01	0.983	0.007	0	0.5	0.5
139	0.75	0.25	0	0.005	0.957	0.038	0	0.667	0.333
140	0.706	0.294	0	0.01	0.968	0.022	0	0.55	0.45
141	0.875	0.125	0	0.007	0.964	0.029	0	0.5	0.5
142	0.588	0.412	0	0.002	0.971	0.027	0	0.667	0.333

143	0.545	0.455	0	0.014	0.948	0.038	0	0.5	0.5
144	0.667	0.333	0	0.005	0.964	0.031	0	0.4	0.6
145	0.7	0.3	0	0.02	0.969	0.012	0	0.464	0.536
146	0.867	0.133	0	0.002	0.959	0.038	0	0.526	0.474
147	0.929	0.071	0	0.007	0.954	0.039	0	0.6	0.4
148	0.875	0.125	0	0.01	0.963	0.027	0	0.577	0.423
149	0.667	0.333	0	0.007	0.964	0.029	0	0.5	0.5
150	0.667	0.333	0	0.007	0.969	0.024	0	0.609	0.391
151	0.846	0.154	0	0.012	0.969	0.019	0	0.421	0.579
152	0.75	0.25	0	0.014	0.947	0.039	0	0.684	0.316
153	0.611	0.389	0	0.015	0.961	0.024	0	0.5	0.5
154	0.824	0.176	0	0.015	0.954	0.031	0	0.524	0.476
155	0.7	0.3	0	0.017	0.956	0.027	0	0.348	0.652
156	0.714	0.286	0	0.025	0.968	0.007	0	0.556	0.444
157	0.8	0.2	0	0.015	0.956	0.029	0	0.267	0.733
158	0.731	0.269	0	0.015	0.965	0.02	0	0.435	0.565
159	0.8	0.2	0	0.01	0.963	0.027	0	0.333	0.667
160	0.792	0.208	0	0.012	0.968	0.02	0	0.4	0.6
161	0.667	0.333	0	0.03	0.936	0.035	0	0.261	0.739
162	0.714	0.286	0	0.023	0.946	0.031	0	0.323	0.677
163	0.793	0.207	0	0.018	0.972	0.01	0	0.382	0.618
164	0.667	0.333	0	0.023	0.965	0.013	0	0.24	0.76
165	0.862	0.138	0	0.015	0.97	0.015	0	0.5	0.5
166	0.871	0.129	0	0.017	0.96	0.022	0	0.353	0.647
167	0.647	0.353	0	0.03	0.958	0.013	0	0.4	0.6
168	0.647	0.353	0	0.022	0.963	0.015	0	0.278	0.722
169	0.806	0.194	0	0.03	0.955	0.015	0	0.158	0.842
170	0.622	0.351	0.027	0.03	0.957	0.013	0	0.273	0.727
171	0.714	0.286	0	0.02	0.965	0.015	0	0.318	0.682
172	0.758	0.242	0	0.025	0.957	0.018	0	0.286	0.714
173	0.714	0.286	0	0.038	0.944	0.018	0	0.318	0.682
174	0.6	0.4	0	0.021	0.961	0.018	0	0.455	0.545
175	0.656	0.344	0	0.023	0.958	0.02	0	0.368	0.632
176	0.6	0.4	0	0.02	0.963	0.017	0	0.35	0.65
177	0.769	0.231	0	0.022	0.963	0.015	0	0.2	0.8
178	0.724	0.276	0	0.028	0.96	0.013	0	0.455	0.545

179	0.781	0.219	0	0.02	0.973	0.007	0	0.353	0.647
180	0.727	0.273	0	0.025	0.97	0.005	0	0.4	0.6
181	0.559	0.441	0	0.03	0.966	0.005	0	0.545	0.455
182	0.774	0.226	0	0.031	0.961	0.007	0	0.143	0.857
183	0.73	0.27	0	0.025	0.963	0.012	0	0.333	0.667
184	0.73	0.27	0	0.017	0.975	0.007	0	0.364	0.636
185	0.529	0.471	0	0.015	0.973	0.012	0	0.2	0.8
186	0.667	0.333	0	0.034	0.964	0.002	0	0.462	0.538
187	0.633	0.367	0	0.015	0.971	0.015	0	0.25	0.75
188	0.72	0.28	0	0.014	0.973	0.012	0	0.583	0.417
189	0.792	0.208	0	0.029	0.962	0.01	0	0.4	0.6
190	0.806	0.194	0	0.024	0.966	0.01	0	0.3	0.7
191	0.714	0.286	0	0.015	0.968	0.017	0	0.545	0.455
192	0.774	0.226	0	0.015	0.976	0.01	0	0.5	0.5
193	0.667	0.333	0	0.029	0.944	0.027	0	0.5	0.5
194	0.688	0.313	0	0.022	0.968	0.01	0	0.5	0.5
195	0.613	0.387	0	0.025	0.956	0.02	0	0.25	0.75
196	0.724	0.276	0	0.022	0.966	0.012	0	0.294	0.706
197	0.767	0.2	0.033	0.037	0.948	0.015	0	0.412	0.588
198	0.763	0.237	0	0.023	0.967	0.01	0	0.529	0.471
199	0.763	0.237	0	0.012	0.965	0.022	0	0.333	0.667
200	0.647	0.353	0	0.015	0.965	0.02	0	0.471	0.529
201	0.821	0.179	0	0.027	0.963	0.01	0	0.471	0.529
202	0.676	0.324	0	0.03	0.946	0.025	0	0.538	0.462
203	0.686	0.314	0	0.017	0.963	0.02	0	0.688	0.313
204	0.645	0.355	0	0.02	0.961	0.02	0	0.615	0.385
205	0.643	0.321	0.036	0.027	0.934	0.039	0	0.615	0.385
206	0.69	0.31	0	0.035	0.945	0.02	0	0.636	0.364
207	0.676	0.324	0	0.037	0.938	0.025	0	0.5	0.5
208	0.579	0.421	0	0.015	0.952	0.033	0.056	0.611	0.333
209	0.517	0.448	0.034	0.032	0.943	0.025	0	0.579	0.4201
210	0.714	0.286	0	0.027	0.943	0.03	0	0.421	0.579
211	0.774	0.226	0	0.035	0.94	0.025	0	0.609	0.391
212	0.711	0.289	0	0.015	0.957	0.028	0	0.421	0.579
213	0.606	0.394	0	0.013	0.967	0.02	0	0.364	0.636
214	0.84	0.16	0	0.022	0.958	0.02	0	0.409	0.591

215	0.767	0.233	0	0.02	0.96	0.02	0	0.381	0.619
216	0.613	0.387	0	0.025	0.945	0.03	0	0.429	0.571
217	0.69	0.31	0	0.017	0.96	0.022	0	0.375	0.625
218	0.815	0.185	0	0.012	0.96	0.027	0	0.458	0.542
219	0.63	0.37	0	0.032	0.935	0.032	0	0.5	0.5
220	0.633	0.367	0	0.015	0.95	0.035	0	0.44	0.56
221	0.8	0.2	0	0.045	0.928	0.027	0	0.464	0.536
222	0.763	0.237	0	0.018	0.954	0.028	0	0.462	0.538
223	0.722	0.278	0	0.003	0.972	0.025	0	0.48	0.52
224	0.593	0.407	0	0.025	0.948	0.027	0	0.391	0.609
225	0.692	0.308	0	0.01	0.965	0.025	0	0.44	0.56
226	0.727	0.227	0.045	0.012	0.968	0.02	0	0.458	0.542
227	0.524	0.476	0	0.01	0.973	0.017	0	0.364	0.636
228	0.6	0.4	0	0.012	0.971	0.017	0	0.238	0.762
229	0.786	0.214	0	0.019	0.964	0.017	0	0.261	0.739
230	0.789	0.211	0	0.012	0.973	0.014	0	0.292	0.708
231	0.8	0.2	0	0.007	0.978	0.014	0	0.217	0.783
232	0.895	0.105	0	0.014	0.978	0.007	0	0.417	0.583
233	0.87	0.13	0	0	0.981	0.019	0	0.353	0.647
234	0.6	0.4	0	0.014	0.969	0.017	0	0.316	0.684
235	0.611	0.389	0	0.01	0.974	0.017	0	0.5	0.5
236	0.667	0.333	0	0.007	0.976	0.017	0	0.471	0.529
237	0.846	0.154	0	0.021	0.96	0.019	0	0.563	0.438
238	0.8	0.2	0	0.002	0.981	0.017	0	0.2670	0.733
239	0.765	0.235	0	0.014	0.964	0.021	0	0.556	0.444
240	0.526	0.474	0	0.002	0.988	0.01	0	0.176	0.824
241	0.727	0.273	0	0.026	0.956	0.019	0	0.167	0.833
242	0.789	0.211	0	0.005	0.981	0.015	0	0.348	0.652
243	0.824	0.176	0	0.005	0.988	0.007	0	0.333	0.667
244	0.75	0.25	0	0.005	0.976	0.019	0	0.235	0.765
245	0.857	0.071	0.071	0.01	0.962	0.029	0	0.381	0.619
246	0.875	0.125	0	0.017	0.973	0.01	0	0.346	0.654
247	0.667	0.333	0	0.012	0.976	0.012	0	0.381	0.619
248	0.842	0.158	0	0.005	0.9860	0.01	0	0.167	0.833
249	0.778	0.222	0	0.01	0.969	0.021	0	0.421	0.579
250	0.833	0.167	0	0.005	0.988	0.007	0	0.65	0.35

251	0.412	0.588	0	0.005	0.984	0.012	0	0.3	0.7
252	0.556	0.444	0	0.005	0.986	0.009	0	0.333	0.667
253	1	0	0	0.009	0.973	0.018	0	0.5	0.5
254	1	0	0	0.012	0.975	0.014	0	0.571	0.429
255	0.813	0.188	0	0.007	0.986	0.007	0	0.75	0.25
256	0.938	0.063	0	0.011	0.975	0.014	0	0.5	0.5
257	0.65	0.35	0	0.009	0.979	0.012	0	0.333	0.667
258	0.647	0.353	0	0.014	0.965	0.021	0	0.5	0.5
259	0.824	0.176	0	0.009	0.976	0.014	0	0.571	0.429
260	0.833	0.167	0	0.009	0.967	0.023	0	0.417	0.583
261	0.789	0.211	0	0.005	0.979	0.017	0	0.529	0.471
262	0.824	0.176	0	0.014	0.962	0.024	0	0.333	0.667
263	0.85	0.15	0	0.012	0.966	0.022	0	0.65	0.35
264	0.409	0.591	0	0.007	0.979	0.014	0	0.438	0.563
265	0.917	0.083	0	0.019	0.968	0.014	0	0.333	0.667
266	0.737	0.263	0	0.028	0.962	0.009	0	0.563	0.438
267	0.808	0.192	0	0.012	0.976	0.012	0	0.364	0.636
268	0.808	0.192	0	0.014	0.97	0.007	0	0.667	0.333
269	0.667	0.333	0	0.009	0.969	0.023	0	0.7134	0.286
270	0.727	0.273	0	0.03	0.958	0.012	0	0.25	0.75
271	0.862	0.138	0	0.017	0.969	0.014	0	0.385	0.615
272	0.875	0.125	0	0.031	0.952	0.017	0	0.429	0.571
273	0.78	0.22	0	0.022	0.963	0.015	0	0.4	0.6
274	0.707	0.293	0	0.037	0.953	0.01	0	0.267	0.733
275	0.773	0.227	0	0.042	0.938	0.02	0	0.467	0.533
276	0.784	0.216	0	0.02	0.962	0.018	0.063	0.313	0.625
277	0.776	0.224	0	0.043	0.934	0.023	0	0.294	0.706
278	0.818	0.182	0	0.034	0.961	0.005	0	0.524	0.476
279	0.845	0.155	0	0.033	0.959	0.008	0	0.417	0.583
280	0.806	0.194	0	0.044	0.943	0.013	0	0.6	0.4
281	0.806	0.194	0	0.042	0.943	0.016	0	0.111	0.889
282	0.871	0.129	0	0.029	0.949	0.021	0	0.429	0.571
283	0.75	0.25	0	0.043	0.949	0.008	0.063	0.25	0.688
284	0.789	0.211	0	0.037	0.952	0.011	0	0.357	0.643
285	0.743	0.257	0	0.037	0.958	0.005	0	0.308	0.692
286	0.803	0.197	0	0.034	0.953	0.013	0	0.545	0.455

287	0.788	0.212	0	0.078	0.917	0.005	0	0.4	0.6
288	0.768	0.232	0	0.035	0.949	0.016	0	0.25	0.75

Appendix B

Proof of Theorem 4.1

The proof is based on the following two lemmas:

Lemma B.1.

$$\bar{h}_i(\mathbf{x}, \infty) \triangleq \lim_{m \to \infty} \bar{h}_i(\mathbf{x}, m) = h_i(\mathbf{x}), \ almost\ surely \tag{B.1}$$

Proof. Since both sequences S_j^i and N_j^i where index $j = 1, 2, \ldots, m$ are i.i.d., then using SLLN:

$$\lim_{m \to \infty} \frac{1}{m} \sum_{j=1}^{m} S_j^i = \mathbb{E}[S^i], \ almost\ surely$$
$$\lim_{m \to \infty} \frac{1}{m} \sum_{j=1}^{m} N_j^i = \mathbb{E}[N^i], \ almost\ surely \tag{B.2}$$

From the definition of S^i, it can be written as

$$S^i = \sum_{k=1}^{N^i} \mathbb{1}_{\{W_i \leqslant D_i\}}, \tag{B.3}$$

where $\mathbb{1}_{\{.\}}$ is the indicator random variable which takes the value of one if the condition between the braces is satisfied and zero otherwise. The expectation of S^i can be given by:

$$\mathbb{E}[S^i] = \sum_{n^i=1}^{\infty} \mathbb{E}\left\{\sum_{k=1}^{N^i} \mathbb{1}_{\{W_i \leqslant D_i\}} | N^i = n^i\right\} \mathbf{Pr}(N^i = n^i)$$

$$= \sum_{n^i=1}^{\infty} n^i \mathbf{Pr}(W_i \leqslant D_i) \mathbf{Pr}(N^i = n^i) \qquad \text{(B.4)}$$

$$= \mathbf{Pr}(W_i \leqslant D_i) \mathbb{E}[N^i]$$

$$= [h_i(\mathbf{x}) + \delta] \, \mathbb{E}[N^i]$$

We attempt to find the probability that $\bar{h}_i(\mathbf{x}, m) = h_i(\mathbf{x})$ as m goes to infinity:

$$\mathbf{Pr}\left\{\bar{h}_i(\mathbf{x}, m) = h_i(\mathbf{x})\right\} = \mathbf{Pr}\left\{\frac{\sum_{j=1}^{m} S_j^i}{\sum_{j=1}^{m} N_j^i} = \frac{\mathbb{E}[S^i]}{\mathbb{E}[N^i]}\right\} \geqslant$$

$$\mathbf{Pr}\left\{\sum_{j=1}^{m} S_j^i = \mathbb{E}[S^i] \text{ and } \sum_{j=1}^{m} N_j^i = \mathbb{E}[N^i]\right\} \qquad \text{(B.5)}$$

$$= \mathbf{Pr}\left\{\sum_{j=1}^{m} S_j^i = \mathbb{E}[S^i]\right\} + \mathbf{Pr}\left\{\sum_{j=1}^{m} N_j^i = \mathbb{E}[N^i]\right\}$$

$$- \mathbf{Pr}\left\{\sum_{j=1}^{m} S_j^i = \mathbb{E}[S^i] \text{ or } \sum_{j=1}^{m} N_j^i = \mathbb{E}[N^i]\right\}$$

By combining equations (B.2) and (B.5) and taking the limit as $m \to \infty$ we can deduce:

$$\mathbf{Pr}\left\{\bar{h}_i(\mathbf{x}, \infty) = h_i(\mathbf{x})\right\} = 1 \qquad \text{(B.6)}$$

which proves the lemma. $\square$

Lemma B.2. *Given* Γ *a finite subset of the feasible solution set* X, *then:*

$$\boldsymbol{Pr}\left\{\bigcap_{i,\mathbf{x}} \bar{h}_i(\mathbf{x}, \infty) = h_i(\mathbf{x}), \forall i \in \mathcal{Q}, \mathbf{x} \in \Gamma\right\} = 1 \qquad \text{(B.7)}$$

Proof. From De Morgan's rule:

$$\mathbf{Pr}\left\{\bigcap_{i,\mathbf{x}}\bar{h}_i(\mathbf{x},\infty)=h_i(\mathbf{x}),\forall i\in\mathcal{Q},\mathbf{x}\in\Gamma\right\}$$

$$=1-\mathbf{Pr}\left\{\bigcup_{i,\mathbf{x}}\bar{h}_i(\mathbf{x},\infty)\neq h_i(\mathbf{x}),\forall i\in\mathcal{Q},\mathbf{x}\in\Gamma\right\} \tag{B.8}$$

$$\geqslant 1-\sum_{i,\mathbf{x}}\mathbf{Pr}\left\{\bar{h}_i(\mathbf{x},\infty)\neq h_i(\mathbf{x})\right\}=1$$

$\square$

We define the set $X_1=\{\mathbf{x}\in X:h(\mathbf{x})\not\geqslant 0\}$. X_1 represents the set of solutions violating the QoS constraints. If we guarantee that $\mathbf{x}_m\notin X_1$, then $\mathbf{x}_m$ is a feasible solution. By applying lemma B.2 for each point $\mathbf{x}\in X_1$, then $\bar{h}(\mathbf{x},\infty)=h(\mathbf{x}),\forall\mathbf{x}\in X_1$, almost surely. Let $\epsilon=-\min_{x\in X_1}\min_i\{h_i(\mathbf{x})\}$, then $|h_i(\mathbf{x})|>\epsilon>0,\forall\mathbf{x}\in X_1,i\in\mathcal{Q}$. If we define:

$$M_1=\inf\left\{m_1:\max_x\max_i|\bar{h}_i(\mathbf{x},m)-h_i(\mathbf{x})|<\epsilon,\forall m\geqslant m_1\right\}$$

then $M_1<\infty$, since ϵ is positive and $\bar{h}(\mathbf{x},\infty)-h(\mathbf{x})=0$, almost surely. For an arbitrary point $\mathbf{x}_m\in X_m^*$, we know that $\bar{h}_i(\mathbf{x}_0,m)\geqslant 0$. Then we guarantee that after a finite number of simulation runs the event $\{h_i(\mathbf{x}_0)>-\epsilon,\forall i\in\mathcal{Q}\}$ will occur and persist, which also means that $\mathbf{x}_m\notin X_1$. As a consequence, $X_m^*\not\subseteq X_1$ as $m\to\infty$ almost surely, which proves the first part of the theorem.

Similarly, we define the set $X_2=\{\mathbf{x}\in X^*:h(\mathbf{x})>0\}$. By applying lemma B.2 for each point $\mathbf{x}\in X_2$, then $\bar{h}(\mathbf{x},\infty)=h(\mathbf{x}),\forall\mathbf{x}\in X_2$, almost surely. Let $\epsilon=\min_{x\in X_2}\min_i\{h_i(\mathbf{x})\}$, then $h_i(\mathbf{x})>\epsilon>0,\forall\mathbf{x}\in X_2,i\in\mathcal{Q}$. If we define:

$$M_2=\inf\left\{m_2:\max_x\max_i|\bar{h}_i(\mathbf{x},m)-h_i(\mathbf{x})|<\epsilon,\forall m\geqslant m_2\right\}$$

then $M_2<\infty$, since ϵ is positive and $\bar{h}(\mathbf{x},\infty)-h(\mathbf{x})=0$, almost surely. Similarly, we guarantee that after a finite number of simulation runs the event $\{h_i(\mathbf{x}_m)>-\epsilon,\forall i\in\mathcal{Q}\}$ will occur and persist. Since the elements of X_2 require that $h_i(\mathbf{x})>\epsilon$, then $X_2\subseteq X_m^*$ as $m\to\infty$ almost surely. If X_2 is non-empty, then $\mathbf{x}_m$ is guaranteed to be optimal, as all the members of X_m^* correspond to the same value of the objective function.

It might be useful to mention that the condition of X_2 being non-empty is easy to be satisfied practically, since it requires a good coincidence for an integer solution to hit exactly one of the pre-specified QoS levels. Even if this coincidence happens, the QoS levels can be perturbed by an infinitesimal amount to make sure that no integer solution can perfectly hit them, while practically not changing the original problem.

Appendix C

Proof of Theorem 5.1

We begin with characterizing c^* using the following lemma:

Lemma C.1. *Assuming that the optimization problem (**P1**) is feasible and that the system inputs, $\boldsymbol{\omega}(t) \triangleq \{a_i(t), r(t)\}$, are independent and identically distributed (i.i.d.) processes, then there exist an $\boldsymbol{\omega}$-only policy which can achieve c^*. Under such policy, the following set of inequalities hold:*

$$\mathbb{E}\{x_i(t)\} \geqslant \mathbb{E}\{a_i(t)\}, \forall i \in \mathcal{Q} \tag{C.1}$$

Proof. See Appendix 4.A of [74].

$\square$

The importance of Lemma C.1 is that it let us focus on $\boldsymbol{\omega}$-only policies, i.e., policies that observe only the current state of the system and not the entire system history. Thus, if we find a policy that is optimal among $\boldsymbol{\omega}$-only policies, it will be optimal among all other policies as well.

We proceed to use Lyapunov optimization which is supposed to provide different limits on all queues (real and virtual), in addition to minimizing the objective function in **P1**. Lyapunov optimization avoids dynamic programming by developing a greedy algorithm (that will become Algorithm 3) which minimizes both the objective function and the queueing cost. First, we introduce a measure of queueing congestion, referred to as Lyapunov function: $L(\boldsymbol{\Theta}(t)) \triangleq \frac{1}{2} \sum_i w_i [Q_i^2(t) + Z_i^2(t)]$, where $\boldsymbol{\Theta}(t)$ is the state of all queues

$\{Q_i(t), Z_i(t)\}$ and $\{w_i\}$ are proper weights to treat queues differently according to their classes. The queueing cost we aim to minimize is the conditional Lyapunov drift given by:

$$\Delta(\Theta(t)) \triangleq \mathbb{E}\{L(\Theta(t+1)) - L(\Theta(t))|\Theta(t)\}. \tag{C.2}$$

The following lemma provides an upper bound on $\Delta(\Theta(t))$:

Lemma C.2. *Assuming that scheduling decisions are bounded, i.e., $0 \leqslant x_i(t) \leqslant x_i^{max}$, then Lyapunov drift at any time slot t is upper-bounded by the following expression:*

$$\Delta(\Theta(t)) \leqslant B + \sum_{i=1}^{N_q} w_i \left[Q_i(t)\mathbb{E}\{a_i(t) - x_i(t)\} + Z_i(t)\mathbb{E}\{\epsilon_i - x_i(t)\}|\Theta(t) \right] \tag{C.3}$$

Proof. From eq. (5.2):

$$Z_i(t+1) \leqslant [Z_i(t) - x_i(t) + \epsilon_i]^+$$

and hence:

$$w_i Z_i^2(t+1) \leqslant w_i[Z_i(t) - x_i(t) + \epsilon_i]^2$$

Thus:

$$w_i[Z_i^2(t+1) - Z_i^2(t)] \leqslant$$
$$w_i[\epsilon_i - x_i(t)]^2 + 2w_i Z_i(t)[\epsilon_i - x_i(t)] \leqslant$$
$$w_i \max\left[\epsilon_i^2, (x_i^{max})^2\right] + 2w_i Z_i(t)[\epsilon_i - x_i(t)]$$

Similarly from eq. (5.1):

$$w_i[Q_i^2(t+1) - Q_i^2(t)] \leqslant$$
$$w_i[x_i^2(t) + a_i^2(t) - 2x_i(t)a_i(t)] + 2w_i Q_i(t)[a_i(t) - x_i(t)] \leqslant$$
$$w_i[(x_i^{max})^2 + (a_i^{max})^2] + 2w_i Q_i(t)[a_i(t) - x_i(t)]$$

Substituting these bounds in the definition of Lyapunov drift (eq.(C.2)) proves the lemma.

$\square$

The greedy algorithm is composed of minimizing both the drift bound defined in (C.3) and the second moment of the total power consumption weighted by a tradeoff parameter V. Thus, for each time slot t we need to solve the following problem:

$$\textbf{P3}: \quad \min_{x_i, \forall i \in Q} V\mathbb{E}\left\{\left(r(t) + \sum_{i=1}^{N_q} x_i(t)\right)^2\right\} - \\ \sum_{i=1}^{N_q} w_i\left[Q_i(t) + Z_i(t)\right]\mathbb{E}\{x_i(t)\} \tag{C.4}$$

Problem **P3** can simply be solved by setting the gradient of the objective function to zero, which yields eq.(5.4) of Algorithm 3.

We now focus on proving the part 1 of the theorem. Since all queues were initially empty then $Q_i(0) \leqslant Q_i^{max}$. Assume, at an arbitrary time t_0, that $Q_i(t_0) \leqslant Q_i^{max}$. If we attempt to prove that $Q_i(t_0 + 1) \leqslant Q_i^{max}$ then $Q_i(t) \leqslant Q_i^{max}$ for all t by induction. We divide our solution into two complementary cases: 1) when $Q_i(t_0) \leqslant Q_i^{max} - a_i^{max}$, and 2) when $Q_i^{max} - a_i^{max} < Q_i(t_0) \leqslant Q_i^{max}$, where Q_i^{max} is defined in theorem 5.1. For the first case, it is obvious that $Q_i(t_0 + 1) \leqslant Q_i^{max}$, since $Q_i(t)$ can be incremented by at most a_i^{max}. For the second case:

$$w_i Q_i(t_0) > 2N_q V\left\{N_q a_i^{max} + r^{max}\right\}$$

and hence by using the result in (5.4):

$$x_i(t_0) = \frac{\sum_{i=1}^{N_q} w_i\left[Q_i(t_0) + Z_i(t_0)\right]}{2N_q^2 V} - \frac{r(t_0)}{N_q} \geqslant \\ \frac{w_i Q_i(t_0)}{2N_q^2 V} - \frac{r(t_0)}{N_q} > a_i^{max}.$$

We then divide the second case into two complementary sub-cases: 1) when $Q_i(t_0) \leqslant x_i(t_0)$, and 2) when $Q_i(t_0) > x_i(t_0)$. For the first sub-case $Q_i(t_0 + 1) = a_i(t_0 + 1) \leqslant a_i^{max} \leqslant Q_i^{max}$. For the second sub-case $Q_i(t_0)$ will be decremented by at least $a_i^{max} - a_i(t_0 + 1)$ and hence $Q_i(t_0 + 1) \leqslant Q_i(t_0) \leqslant Q_i^{max}$. Hence, under all circumstances $Q_i(t_0 + 1) \leqslant Q_i^{max}$. Similar argument can be made for Z_i^{max}.

The second part of the theorem can be proved as follows. According to the i.i.d. assumptions, the results in Lemma C.1 can be applied. We refer to the decisions of the

optimal $\boldsymbol{\omega}$-only policy as $x_i^{\boldsymbol{\omega}}$. Our greedy algorithm is not an $\boldsymbol{\omega}$-only policy, as the scheduling decisions depends on $\boldsymbol{\Theta}(t)$ as well, however it minimizes the objective function in **P3** among all policies including the optimal $\boldsymbol{\omega}$-only policy, thus:

$$\Delta(\boldsymbol{\Theta}(t)) + V\mathbb{E}\left\{\left(r(t) + \sum_{i=1}^{N_q} x_i(t)\right)^2\right\} \leqslant$$

$$B + V\mathbb{E}\left\{\left(r(t) + \sum_{i=1}^{N_q} x_i^{\boldsymbol{\omega}}(t)\right)^2\right\} + \sum_{i=1}^{N_q} w_i\left[Q_i(t)\mathbb{E}\{a_i(t) - x_i^{\boldsymbol{\omega}}(t)\} + Z_i(t)\mathbb{E}\{\epsilon_i - x_i^{\boldsymbol{\omega}}(t)\}|\boldsymbol{\Theta}(t)\right]$$

By applying Lemma C.1 results:

$$\Delta(\boldsymbol{\Theta}(t)) + V\mathbb{E}\left\{\left(r(t) + \sum_{i=1}^{N_q} x_i(t)\right)^2\right\} \leqslant B + Vc^*. \tag{C.5}$$

By taking the expectation on both sides:

$$\mathbb{E}\{L(\boldsymbol{\Theta}(t+1)\} - \mathbb{E}\{L(\boldsymbol{\Theta}(t)\} + V\mathbb{E}\left\{\left(r(t) + \sum_{i=1}^{N_q} x_i(t)\right)^2\right\} \leqslant B + Vc^*. \tag{C.6}$$

By summing from $t = 0$ to $t = T - 1$ then:

$$\mathbb{E}\{L(\boldsymbol{\Theta}(T)\} - \mathbb{E}\{L(\boldsymbol{\Theta}(0)\} + V\sum_{t=0}^{T}\mathbb{E}\left\{\left(r(t) + \sum_{i=1}^{N_q} x_i(t)\right)^2\right\} \leqslant \tag{C.7}$$
$$BT + VTc^*.$$

However, $L(\boldsymbol{\Theta}(0) = 0$ (since queues are initially empty) and $L(\boldsymbol{\Theta}(t) \geqslant 0$ for any time slot, and hence:

$$V\sum_{t=0}^{T-1}\mathbb{E}\left\{\left(r(t) + \sum_{i=1}^{N_q} x_i(t)\right)^2\right\} \leqslant BT + VTc^*. \tag{C.8}$$

Dividing by VT completes the proof.

Appendix D

Proof of Theorem 5.2

We define the T-slot sample-path drift as follows:

$$\Delta_T(\mathbf{\Theta}(t)) \triangleq L(\mathbf{\Theta}(t+T)) - L(\mathbf{\Theta}(t))$$

which can be re-written as:

$$\Delta_T(\mathbf{\Theta}(t)) = \sum_{j=t}^{t+T-1} L(\mathbf{\Theta}(j+1)) - L(\mathbf{\Theta}(j)).$$

From the proof provided in lemma C.2:

$$
\begin{aligned}
\Delta_T(\mathbf{\Theta}(t)) &\leqslant \sum_{j=t}^{t+T-1} \left\{ B + \sum_{i=1}^{N_q} w_i \left[Q_i(j)\{a_i(j) - x_i(j)\} + Z_i(j)\{\epsilon_i - x_i(j)\} \right] \right\} \\
&= BT + \sum_{j=t}^{t+T-1} \left\{ \sum_{i=1}^{N_q} w_i \left[Q_i(j)\{a_i(j) - x_i(j)\} + Z_i(j)\{\epsilon_i - x_i(j)\} \right] \right\}.
\end{aligned}
\tag{D.1}
$$

We attempt to provide an upper bound for the future values of various random variables. Since the maximum increment for any queue is its maximum arrival rate, then:

$$
\begin{aligned}
Q_i(j)\{a_i(j) - x_i(j)\} &\leqslant \{Q_i(t) + (j-t)a_i^{max}\}\{a_i(j) - x_i(j)\} \\
&\leqslant Q_i(t)\{a_i(j) - x_i(j)\} + (j-t)(a_i^{max})^2
\end{aligned}
$$

and

$$Z_i(j)\{\epsilon_i - x_i(j)\} \leqslant \{Z_i(t) + (j-t)\epsilon_i\}\{\epsilon_i - x_i(j)\} \leqslant Z_i(t)\{\epsilon_i - x_i(j)\} + (j-t)\epsilon_i^2$$

By substituting into inequality (D.1):

$$
\begin{aligned}
\Delta_T(\boldsymbol{\Theta}(t)) \leqslant \; & BT + \sum_i^{N_q} w_i \frac{(\epsilon_i^2 + (a_i^{max})^2)T(T-1)}{2} \\
& + \sum_{j=t}^{t+T-1} \left\{ \sum_{i=1}^{N_q} w_i \left[Q_i(t)\{a_i(j) - x_i(j)\} + Z_i(t)\{\epsilon_i - x_i(j)\} \right] \right\}.
\end{aligned}
\tag{D.2}
$$

However, from the definition of B given in theorem 5.1:

$$\sum_i^{N_q} w_i \frac{(\epsilon_i^2 + (a_i^{max})^2)}{2} \leqslant B$$

then:

$$\Delta_T(\boldsymbol{\Theta}(t)) \leqslant BT^2 + \sum_{j=t}^{t+T-1} \left\{ \sum_{i=1}^{N_q} w_i \left[Q_i(t)\{a_i(j) - x_i(j)\} + Z_i(t)\{\epsilon_i - x_i(j)\} \right] \right\}. \tag{D.3}$$

Starting from inequality (D.3) and after adding the cost term $V \sum_{j=t}^{t+T-1} \left(r(t) + \sum_{i=1}^{N_q} x_i(t) \right)^2$, we can follow the same procedure used for proving theorem 5.1. The rest of the proof is eliminated for brevity.

Appendix E

List of Publications

Accepted papers

1) F. Elghitani, W. Zhuang, "Aggregating a Large Number of Residential Appliances for Demand Response Applications," *IEEE Transactions on Smart Grid*, 2017.

Submitted papers (still under review to the date of writing this thesis)

1) F. Elghitani, E. El-Saadany, "Optimal Assignment of Electric Vehicles to Charging Stations," *IEEE Transactions on Smart Grid*, Submit date: December 2017.

2) F. Elghitani, E. El-Saadany, "Smoothing Power Variations Using Residential Demand Response," *IEEE Transactions on Industrial Informatics*, Submit date: January 2018.